

# Stress detection using a Field Kelvin Probe

Daniel Timothy Thorgersen Solvang  
Cedric Liam Landsmeer

Bachelor's thesis in General Mechanical  
Engineering

Bergen, Norway 2022





# Stress detection using a Field Kelvin Probe

Daniel Timothy Thorgersen Solvang

Cedric Liam Landsmeer

Department of Mechanical- and Marine Engineering

Western Norway University of Applied Sciences

NO-5063 Bergen, Norway

Høgskulen på Vestlandet  
Fakultet for Ingeniør- og Naturvitskap  
Institutt for maskin- og marinfag  
Inndalsveien 28  
NO-5063 Bergen, Norge

Cover and backside images © Norbert Lümmen

*Norsk tittel:* Deteksjon av spenning med en Field Kelvin Probe

Author(s), student number: Daniel Solvang, 581294  
Cedric Landsmeer, 585080

Study program: General Mechanical Engineering

Date: May 2022

Report number: IMM 2022-M10

Supervisor at HHVL: Richard John Grant

Assigned by: Norwegian Research Centre AS

Contact person: Eugen Florin Turcu

Antall filer levert digitalt: 1

## Preface

The work and research of this thesis was carried out at the Department of Mechanical and Marine Engineering at Western Norway University of Applied Sciences (WNUAS), under the programme of General Mechanical Engineering. The project was supervised by Professor Richard John Grant, whose academic competence, constant availability for offering advice and guidance, as well as positive attitude greatly facilitated the project. The research was conducted in collaboration with Norwegian Research Centre AS (Norce), who offered access to their facilities. The external supervisor was Dr. Eugen Florin Turcu, who has been invaluable through his extensive knowledge, great reliability, thoughtfulness, and frequent encouragements.

An additional word of gratitude goes to those who have made this project possible through their practical contributions.

First, we want to thank all the lab engineers at the university for their relentless support. We also wish to direct a special thanks to Harald Moen, who provided us with the opportunity of using the Instron and guided us through its operation.

We want to express our gratitude to Bergen Construction Services AS, who kindly donated some materials for our samples.

We would like to thank Professor Lars Arne Jordanger for his input on data analysis and providing us with his notes.



## Abstract

Being able to quantify the stress state of a mechanical component in situ by use of a field instrument would be of great utility for mechanical engineers. Even more so when the measurement technique in question is non-destructive and can work on painted components. The Field Kelvin Probe (FKP) – a compact, mobile Kelvin probe invented at the Max Plank Institute and developed by Norce – may hold a potential of acting as an instrument of this kind. The literature suggests that a link exists between the stress state of a metal and its electronic work function (EWF). In this report investigates whether an FKP can detect changes in the EWF of various metal samples as they are exposed to tensile stress.

Pieces of mild steel, stainless steel, aluminium, and brass, some paint-coated and some polished, were exposed to stress in the elastic regime using a tensile testing machine. Simultaneously, the EWF was measured with an FKP. A linear regression analysis was performed on the data and a hypothesis test was conducted on the slope of the regression line to investigate whether a significant relationship between stress and EWF could be detected.

It was found that for some samples, the response of the EWF was different during the first exposure to tensile stress than during subsequent tests. Also, a strong dependence of the EWF on the sample-probe distance was observed which as a source of error partially overshadowed the more direct influence of stress on the EWF. Attempts at quantifying the influence of and effectively controlling the sample-probe distance failed. As the results cannot be viewed without regards to this, no direct statement about the level of interconnection between stress and EWF as measured by an FKP could be made.





## Sammendrag

Å kunne kvantifisere spenningstilstanden til en mekanisk komponent i montert tilstand ved bruk av et portabelt måleinstrument kunne være til stor nytte for maskiningeniører. Dette gjelder spesielt dersom måleteknikken var ikke-destruktiv og kunne virke på malte komponenter. En Field Kelvin Probe (FKP) – en kompakt, mobil Kelvin probe oppfunnet i Max Plank instituttet og utviklet av Norce – har muligens potensialet til å fungere som et slikt instrument. Resultater fra litteraturen tyder på en sammenheng mellom spenningstilstanden og løsrivningsarbeidet. Denne rapporten undersøker om en FKP kan registrere forandringer i løsrivningsarbeid for ulike metallprøver mens de er utsatt for strekkspenning.

Metallprøver av lavkarbon stål, rustfritt stål, aluminium og messing, noen av prøvene har blitt malt og andre har blitt polert, har blitt utsatt for strekkspenning i det elastiske området ved bruk av en servohydraulisk strekkmaskin. Samtidig har løsrivningsarbeidet blitt målt med en FKP. En lineær regresjonsanalyse har blitt gjennomført på dataen og en hypotesetest har blitt anvendt på stigningstallet til regresjonslinjen for å undersøke om det eksisterer et signifikant forhold mellom spenning og løsrivningsarbeid.

For noen metallprøver ble det funnet at responsen til det målte løsrivningsarbeidet var ulik under den første strekkbelastningen enn under påfølgende belastninger. I tillegg ble det registrert en sterk avhengighet av løsrivningsarbeidet på avstanden mellom FKP'en og metallprøven. Som feilkilde har den overskygget den direkte påvirkningen av spenningen på løsrivningsarbeidet. Forsøk på å kvantifisere innflytelsen til avstanden og kontrollere den effektivt lyktes ikke. Siden det ikke er mulig å betrakte resultatene uten å ta hensyn til dette, kunne det ikke gjøres et direkte utsagn om forholdet mellom løsrivningsarbeid og spenning.



## Table of contents

Preface.....	V
Abstract .....	VII
Sammendrag.....	IX
Nomenclature .....	XV
1. INTRODUCTION.....	1
1.1 HISTORY OF THE KELVIN PROBE.....	1
1.2 THE FIELD KELVIN PROBE .....	1
1.3 AIM STATEMENT .....	1
1.4 THE OBJECTIVES.....	2
1.5 NOVELTY .....	2
1.6 STRUCTURE OF THIS THESIS .....	2
2. LITERATURE AND UNDERLYING THEORY .....	3
2.1 THE KELVIN PROBING TECHNIQUE.....	3
2.1.1 Underlying theory – electric potential energy .....	3
2.1.2 Underlying theory – removing electrons from a metal sample .....	5
2.1.3 Underlying theory – connecting two dissimilar metals.....	6
2.1.4 The Kelvin probing technique in general .....	9
2.1.5 The Scanning Kelvin Probe (SKP) and Field Kelvin Probe (FKP).....	10
2.1.6 Factors influencing measurements with an FKP .....	11
2.1.7 Summary and conclusions concerning the Kelvin probing technique.....	13
2.2 CONNECTION BETWEEN EWF AND MECHANICAL STRESS .....	14
2.2.1 Observations – experimental results.....	14
2.2.2 Observations – theoretical results.....	16
2.2.3 Tabular overview.....	17
2.2.4 Interpretations – elastic range.....	18
2.2.5 Interpretations – plastic range .....	19
2.2.6 Conclusions drawn from the literature review .....	21

3.	DEVELOPING METHODOLOGY AND PRELIMINARY RESULTS .....	23
3.1	BEORE FIRST LAB VISIT .....	23
3.2	EARLY LAB WORK .....	23
3.3	DECIDING ON A TEST SET-UP .....	23
3.4	VICE TESTING .....	24
3.4.1	Materials:.....	24
3.4.2	Equipment: .....	25
3.4.3	General procedure for testing in the vice.....	25
3.4.4	Results and conclusion .....	26
3.4.5	Sources of error .....	26
3.5	WAY FORWARD .....	26
3.6	INSTRON TESTING .....	27
3.6.1	Materials:.....	27
3.6.2	General procedure for Instron tests .....	29
3.6.3	Data .....	29
3.6.4	Sources of errors.....	30
3.7	DISTANCE TESTING.....	30
3.8	NEW INSTRON TEST .....	31
3.9	DATA TREATMENT.....	32
4.	RESULTS, DISCUSSION, AND OUTLOOK .....	34
4.1	RESULTS AND DISCUSSION .....	34
4.1.1	Overarching line of argument.....	34
4.1.2	Patter: Drift.....	36
4.1.3	Pattern: Deviant first tests .....	39
4.1.4	Invertibility: Going from EWF to stress.....	41
4.1.5	Likely mechanisms connecting EWF and stress .....	43
4.1.6	Summary .....	54
4.2	OUTLOOK.....	54

---

4.2.1	FKP for evaluating corrosion resistance.....	54
4.2.2	FKP for detecting overload .....	55
4.2.3	FKP for early detection of fatigue .....	55
5.	CONCLUSIONS AND FURTHER WORK.....	56
	Referances .....	57
	List of figures .....	59
	Appendix A1 .....	61

Use the word processor to generate Table of Contents. Then chances are the best that it will be right. Use the style templates for chapters as done in this sample report. The page reference should of course be given in the listing. Attachments must also be included. Keep in mind that only the report's main sections from introduction to conclusion should be numbered. Attachments can be numbered as shown in the list above. It is optional to have a list of Figures and Tables as well as Nomenclature and Attachments.

The table of contents is also placed on odd page numbers.

You can choose if you want to place the beginning of the main sections 1, 2, 3, 4 and 5 on odd page numbers, as is typical for chapters in books. This is not done in this report.



## Nomenclature

$A$	=	area of the plates of a parallel plate capacitor [mm <sup>2</sup> ]
$C$	=	capacitance [F]
$d$	=	distance between capacitor plates
$E_{vac}$	=	energy at the local vacuum level [eV]
$E_{vac}^*$	=	energy at the vacuum level at infinity [eV]
$E_{ref}$	=	energy at the chosen reference level [eV]
$g$	=	acceleration due to gravity [m/s <sup>2</sup> ]
$h$	=	height above reference level [m]
$m$	=	mass [kg]
$n$	=	number of EWF measurements needed
$PE$	=	potential energy [J]
$Q$	=	electric charge [C]
$V$	=	voltage [V]
$z_{0.05}$	=	5% quantile of the standard normal distribution
$\beta$	=	slope of linear regression line
$\hat{\beta}$	=	empirical estimate of regression line slope
$\epsilon$	=	permeability of medium in between capacitor plates [F/m]
$\Delta\Psi$	=	Volta potential difference [V]
$\mu_e$	=	chemical potential [eV]
$\bar{\mu}_e$	=	electrochemical potential [eV]
$\sigma$	=	in a mechanical context: stress [MPa], in a statistical context: standard deviation
$\Phi$	=	electronic work function [eV].
$\chi$	=	potential drop across the surface dipole layer [V]
$\Psi$	=	Volta potential [V]





## **1. INTRODUCTION**

### **1.1 HISTORY OF THE KELVIN PROBE**

Before going into the technical details, lets first review the history of electrochemistry which led to the invention of an incredible device.

The journey starts with Alessandro Volta. He was an Italian scientist who lived in the 18<sup>th</sup> to the early 19<sup>th</sup> century. His most known invention was the voltaic pile which led to the modern battery, but that was far from his only contribution to science. One of these contributions is the condenser electroscope, a device that is highly sensitive to electric charge [1]. And this device would be crucial in the research of the electromotive force that occurs when two dissimilar metals are connected.

Lord Kelvin, also known as William Thompson, was an esteemed scientist from Great Britain. He was active within many branches of science, and one of these branches was electrochemistry. He referred to the work of Volta and conducted experiments, building upon his research. His parallel plate capacitor experiments were performed with a Volta-condenser [2], and it was these experiments that explored the contact potential difference of metals (CPD), or the Volta Potential.

The effects discovered by Lord Kelvin would later be used by William Zisman to develop an instrument capable of measuring CPD. The advancement that led to this was the integration of a vibrating condenser [3], and this instrument was termed the Kelvin Probe.

The technology continued to evolve, and in the 90s the instrument was introduced to the field of corrosion science by Martin Stratmann [3]. This became a driving force for further development.

The most recent evolution of the Kelvin Probe is the FKP (Field Kelvin Probe) which is being developed by Norce. This approach to the Kelvin Probe technology led to a device which is more robust and well suited for use outside of a laboratory environment.

### **1.2 THE FIELD KELVIN PROBE**

The Field Kelvin Probe is a completely new approach to the kelvin probe technology.

One of the things that set it apart from its earlier cousins is the internal reference. This allows the probe to compare the readings from the surface of interest to the readings from the reference and thereby verify the integrity of the data.

The internal reference is made possible by a major change in design and operating principle compared to other probes. Instead of the conventional vibrating tip, the FKP operates by having a rotating tip that continuously alternate between the scanning surface and the reference.

It is also significantly smaller in size than its counterparts and it is wireless. These factors combined makes it an ideal instrument for field work.

### **1.3 AIM STATEMENT**

The KP technology could have a variety of different uses in determining the condition of metal surfaces. And while there are several different phenomena that possibly could be observed with a kelvin probe, time does limit the extent of this project. Therefore, a clear objective has been set and formed into the following aim statement:

*“Evaluate the possibility of employing the current version of the FKP as an instrument for detecting applied tensile stress with a view to practical contexts”*

## **1.4 THE OBJECTIVES**

To achieve this, there has been set a number of sub goals. These goals will lead towards fulfilling the objective and reaching a conclusion.

- i. Change the applied load on a sample and look for a response in the EWF at one point measured by the FKP
- ii. Ideally: Establish inverse relationship that allows deducing changes of tensile stress from changes in the EWF
- iii. Evaluate relevance of the above finding (if present). Statistical significance, sources of error, overlapping effects

## **1.5 NOVELTY**

The current state of the art Kelvin probes is predominately laboratory equipment designed for small samples and precise measurements over a small area [4]. The purpose of the Field Kelvin Probe is quite different, and as the name suggest, it is intended for field use.

Therefore, the approach of this project is to investigate whether it is practically possible to detect stress under realistic circumstances instead of just theoretically possible under ideal conditions.

While SKPs work on microscopic levels, the FKP is working on macroscopic levels. Which is a natural effect of the dimensions of the “tip” which is considerably larger than on other probes. This makes it possible to scan large areas without regards to different phases in the metal, tiny imperfections, small local variations in height and several other factors that would affect the reading of any other Kelvin Probe.

## **1.6 STRUCTURE OF THIS THESIS**

The reader has now been introduced to the FKP and next up is a review of the existing literature on the subject and how this may be linked to the research in this project. Following that is an in-depth walkthrough of the experiments that have been performed and the reasoning behind them, and thereafter the results of the conducted tests and a discussion on how these data can be interpreted.

## 2. LITERATURE AND UNDERLYING THEORY

A great deal has been written about the Kelvin probing technique and its applications. The literature and the underlying theories on which it builds can help the reader understand the working principles of this instrument in greater detail (reference section 2.1) as well as aid in evaluating the relevance of this method for investigations of mechanical stress states (reference section 2.2). Conclusion drawn from this chapter provide important starting points for the scope of the current work.

### 2.1 THE KELVIN PROBING TECHNIQUE

It may be helpful to first present the Kelvin probing technique in detail. The rest of this work depends upon the understanding of its working principles. This concerns the experimental approach – what one can hope to measure with a Kelvin probe – as well as the interpretation of the results – evaluating what they may mean and pointing out possible sources of error. At the risk of providing superfluous explanation, this section aims to introduce the underlying theory and the basics of its technical implementation in such a way that no previous knowledge of Kelvin probes is required.

The first three subsections (2.1.1: Electric potential energy, 2.1.2: Removing electrons from a metal, 2.1.3: Connecting two dissimilar metals) are meant to describe relevant concepts and phenomena, which lead over naturally to the basic working principle of any Kelvin probe (2.1.4: The Kelvin probing technique in general). More detail is then provided on some of the modern branches of this technology (2.1.5: The Scanning- and the Field Kelvin Probe). This information is used to evaluate what may influence the measurements made with the device used in the current work, an FKP, (2.1.6: Factors influencing measurements with an FKP). Finally, important results are summarized for later referencing (2.1.7: Summary and Conclusions).

#### 2.1.1 Underlying theory – electric potential energy

A Kelvin probe measures the “work function” of a material surface, also known as its “electronic work function” (EWF) for short<sup>1</sup>. This quantity may provide a great amount of useful information about a material and its surface condition. To obtain a clearer picture of what it means, it may be worth taking several steps back. The strategy taken in this and the following two subsections is to begin by introducing concepts on a very superficial level of analysis and then go into greater detail as the picture develops. Hence, terms such as *electric potential energy* will at first be used broadly without adhering to a rigorous definition in order to then be replaced by more precise and appropriate terminology later.

For the purposes of the current subsection, one may take *electric potential energy* to simply be a quantity that is higher at the location from which electrons move and lower at the location to which they move, given that movement is possible; between locations of equal potential energy, there is no net electric current, even if electron motion is allowed. This concept is used preliminarily as a capacious term encompassing any number of factors that cause electrons to move from location A to B, if given the chance<sup>2</sup>. A comparison to mechanics may provide accompanying intuition: for instance, an object at rest

---

<sup>1</sup> The term “electronic” is added to make sure no confusion arises with the *work function* as it is sometimes used in thermodynamics, referring to the Helmholtz energy. EWF and Helmholtz energy are not the same [15].

<sup>2</sup> A misconception that is perhaps not uncommon among those without a background in electrostatics, is that electrons only move because like charges repel and unlike charges attract. However, one need only consider the immersed electrodes of a Galvanic cell to realise that more than just electrostatic repulsion / attraction is important. At the at the negative anode, for instance, metal oxidises and cations go into solution, spontaneously moving away from the anode despite its opposing charge [16] (Chemistry textbook Sandtorv)

in a gravitational potential field will move from a point of higher potential energy to a point of lower potential energy, if allowed to do so. The analogy to gravitational potential energy points to a concept that needs to be considered when making statements about potential energy: the reference level.

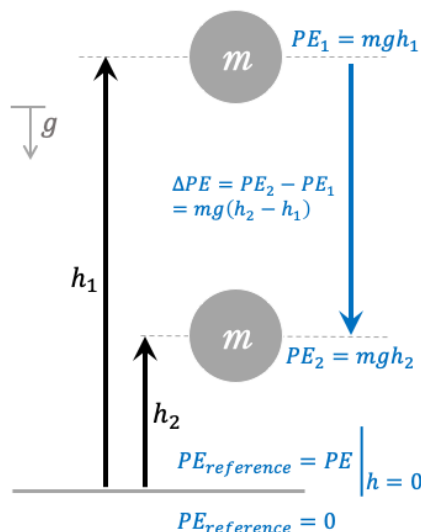


Figure 2.1 Illustration potential energy

*An object with mass, unconstrained in a gravitational potential field. The field exerts a force on the object. Once the object moves towards a region of lower potential (be it due to the influence of the force) work is done to the object as its potential energy is reduced. Also: The difference in potential energy between two states can be found by use of a reference level. In the illustration, everything relating to the potential energy of the object is coloured in blue.*

For comparing the potential energy possessed by different objects, a common reference level is required. For objects in earth's gravitational field, this may, for example, be mean sea level. For the potential energy possessed by an electron, several references are commonly used: local vacuum level,  $E_{vac}^*$ , vacuum level at infinity,  $E_{vac}$ , and the standard hydrogen electrode  $E_{SHE}$  [3]. The choice of reference does not matter as long as it is consistent. In the current work, the local vacuum level is taken to be the reference. At the reference, the potential energy is by definition equal to zero. The utility of this concept lies in the fact that the electric potential energy at any location can now be found by considering how much work would have to be done by or to the electron to move it from that location to the reference<sup>3</sup>. One could also imagine a neutral metal sample in a vacuum, set the reference for the electric potential energy to be just above the surface and imagine extracting an electron from within the metal and move it to the reference (Figure 2.2, page 5). If note is taken of all the energy expended in that process, and since the potential energy at the reference is zero, the electric potential energy which the electron has inside the metal can be calculated.

<sup>3</sup> All that must be asserted is that all the forces acting on the electron are conservative.

### 2.1.2 Underlying theory – removing electrons from a metal sample

A special name is given to the energy expended in the extraction process just described (Figure 2.2): Electronic work function, EWF, usually given the Greek symbol  $\Phi$ . One would not expect the metal to spontaneously eject electrons, hence it is reasonable to assume that in most cases the EWF stands for a quantity of work that must be expended to extract the electron. By convention, work done to a system is considered positive. If work is done to the electron to elevate it to a potential energy of zero, it must have rested at a negative potential energy while still inside the metal. This will be reflected in the proceeding equations. Should the sign on some of the variables appear confusing, it is helpful to consider which variables refer to an energetic state, and which refer to the difference in between states. The electronic work function, EWF, may be formally defined as:

*The work needed to extract an electron from the Fermi level to a position just outside the sample, far enough to eliminate contributions from image forces [3] [5].*

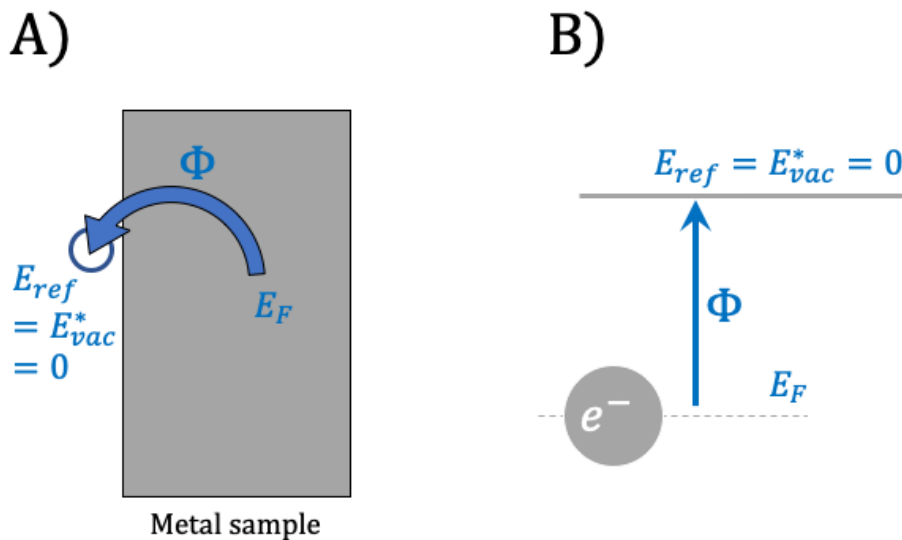


Figure 2.2 Extracting one electron from an electrostatically neutral sample in a vacuum

*A) Extracting an electron from within the sample, moving it to a reference location just outside the surface B) Diagram representing the potential energy of the extracted electron in the vertical direction*

This is a convenient point for making some of the concepts introduced thus far more detailed. In a real metal sample, not all electrons rest at the same energy level [6]. Some are more tightly bound to the nucleus, while others are freely shared between the ions within the metal. Electrons at the *Fermi level*,  $E_F$  are a certain group of electrons, free electrons in the case of a metal, with a comparatively high energy. More information on the definition of this term may be found in several sources [6] [7]. For the purposes of the current work, the electrons to be extracted from the metal sample are at the Fermi level. The term also lends a more appropriate description of what was meant by the *electric potential energy* of an electron resting inside the metal. Another term, the *electrochemical potential*,  $\bar{\mu}_e$ , is sometimes used synonymously when discussing metal samples [3].

Thus, given what was stated about the *Fermi level* and the *EFW* earlier, the following equation can be given in accordance with [3] and [5].

$$\Phi = -E_F = -\bar{\mu}_e \quad (2.1)$$

$\Phi$  is the EWF and  $E_F$  is the energy at the Fermi level. Note that this equation only applies if <sup>4</sup> the metal sample is electrostatically neutral and / or if the reference is chosen at  $E_{vac}^*$ . The sign convention here is as described earlier: Positive work is invested,  $\Phi$ , to move one electron from its negative potential in the metal,  $E_F$ , to the zero-reference  $E_{vac}^*$ . One could also say that  $\Phi$  is the energy difference between two energetic states: the energy at the Fermi level,  $E_F$ , and the energy at the reference,  $E_{vac}^*$ . The latter is equal to zero under the conditions given at the beginning of this paragraph.

By convention, the work function is often given as the sum of two contributions:  $\mu_e$  and  $e\chi$  (see equation 2.2). The *chemical potential*<sup>5</sup>,  $\mu_e$ , influenced by properties of the bulk [5], such as the sample material, its temperature, etc. It is thought to be a contribution to the energy at the Fermi level / the electrochemical potential. A greater  $\mu_e$  is associated with easier electron extraction and thus a lower  $\Phi$ . The surface dipole potential,  $\chi$ , is an electrostatic potential; multiplied by the elementary charge  $e$  it gives the energy needed for one electron to traverse an electrostatic dipole<sup>6</sup>. Why it is common to model the surface of a metal sample as a dipole in the context of electron extraction is beyond the scope of the current work. The product  $e\chi$  may be taken to simply model contributions to the EWF due to the idiosyncrasies of the sample's surface: the crystalline orientation of the exposed pane, its charge density, its topography and more may play a role [5]. A greater  $\chi$  will make electron extraction more difficult and is thusly associated with a greater  $\Phi$ . Hence, drawing on sources [3] and [5], the work function may be expressed as:

$$\Phi = -\mu_e + e\chi \quad (2.2)$$

Equation 2.2 implies an electrostatically neutral sample or a definition of the reference at the local vacuum level when no regard is taken to the electrostatic charge. The reason will become apparent when considering the following thought experiment.

### 2.1.3 Underlying theory – connecting two dissimilar metals

Two metal samples, 1 and 2, made of dissimilar materials and both electrostatically neutral are placed in a vacuum. Reference points for the local vacuum level are set: point A for sample 1 and point B for sample 2 (see Figure 2.3, page 7). It is known from some previous experiment that sample 1 has a higher EWF with respect to its local vacuum reference than sample 2 compared to its respective reference:  $\Phi_1 > \Phi_2$ . Several simple observations can now be made. Note that neither sample is electrostatically charged, so no electric field is present, and every point of the vacuum is electrically equipotential: A so-called *flat vacuum condition* [5]. Thus, for this case<sup>7</sup>:  $E_{vac A}^* = E_{vac B}^*$ . As was lined out in section 2.1.1, it is the *common* reference level that allows the comparisons of potential energy at different locations.

<sup>4</sup> This condition is to say that  $E_{vac}^* = 0$ . Should this not be the case, for example because another reference level was chosen to be the zero level, making  $E_{vac}^* \neq 0$ , then this can be accounted for by defining the EWF as  $\Phi = E_{vac}^* - \bar{\mu}_e$ . More on why the zero / reference level is sometimes chosen to be something other than  $E_{vac}^*$  will follow in the next subsection.

<sup>5</sup> not to be confused with the *electrochemical potential*  $\bar{\mu}_e$

<sup>6</sup> Recall that it takes energy for a negative charge to traverse an electric dipole from the negative side to the positive side. Going the other way, the charge can do work. The potential is hence higher on the positive side than on the negative side. Here, this potential difference is denoted as  $\chi$ .

<sup>7</sup> As will become apparent later in this subsection, the equality of the flat vacuum condition also includes the vacuum level at infinity:  $E_{vac A}^* = E_{vac B}^* = E_{vac}^*$ .

It justifies the alignment of  $\Phi_1$  and  $\Phi_2$  around  $E_{vac A}^* = E_{vac B}^*$  in Figure 2.3 and hence the statement that the Fermi level is higher in sample 2 than in sample 1 (see equation 2.1).

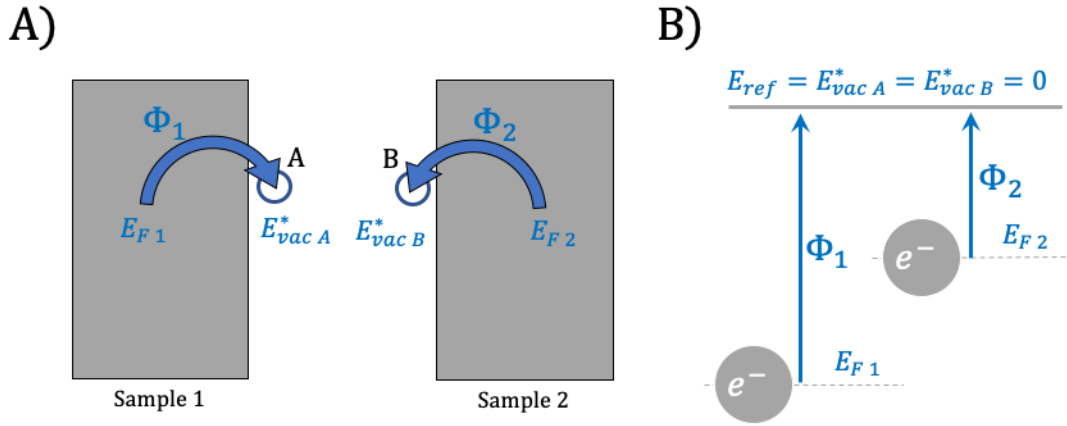


Figure 2.3 Two metals, not yet connected

**A)** Two metal samples with different EWF in a vacuum, electrically isolated. **B)** Schematic illustration where Energy is given in the vertical direction and the Fermi levels of the two samples is compared.

Now suppose the two metals are connected by a conductor (see Figure 2.4, page 8). To make what happens next easier to understand and gain an intuition for the process, the concept of *electric potential energy* will be invoked again. The correct terminology will be reapplied once the complete picture has been presented. In the given scenario, the potential energy is higher in the second sample than in the first. The conductor now provides a passageway and electrons flow from the second to the first. As they do so, another effect sets in; namely electrostatic charging [3] [5]. Where the electrons accumulate because of the locally low electric potential energy, their presence in greater numbers will lead to a new contribution to the potential energy at said point: an electrostatic potential term. The potential energy increases locally until it is the same as in the surrounding and the influx of more charge is thusly stopped. One can observe that this process will necessarily continue until all initial differences in potential energy are perfectly compensated by electrostatic charge accumulation. Before describing this process formally and presenting important equations, some points need to be addressed.

Firstly, note that the addition of an electrostatic potential makes it very important to be aware of where the reference is set. The vacuum condition is now no longer flat [5], meaning that  $E_{vac A}^* \neq E_{vac B}^*$ . An arbitrary point, e.g. A, needs to be chosen as a global reference for the entire two-metal system and that choice must be consistent. Here, it may also be natural to pick the vacuum level at infinity,  $E_{vac}$ , as the global reference for the entire two-sample system. This has the advantage of guaranteeing that no electric field is present at the reference.

Secondly, the Fermi level / electrochemical potential of different conductors will equalise when they are in electric contact. In the literature, this is referred to as *Fermi level alignment* [3] [5]. This allows the conclusions drawn in the preceding thought experiment to still be valid once *electric potential energy* has been replaced with the correct terminology.

Thirdly, the Fermi level / electrochemical potential is dependent on the electrostatic potential. This electrostatic potential can be thought of as the energy required to move one electron from the local

reference to the global reference through the electric field that may exist between the two (see Figure 2.4). Where this intermediate local reference is located does not matter since regardless of where in the two-metal system the electron is extracted and which path it takes, once it arrives at the global reference the net work done on it will be the same [3]. This follows from the fact of Fermi level alignment across the system and the condition that all forces acting on the electron are conservative.

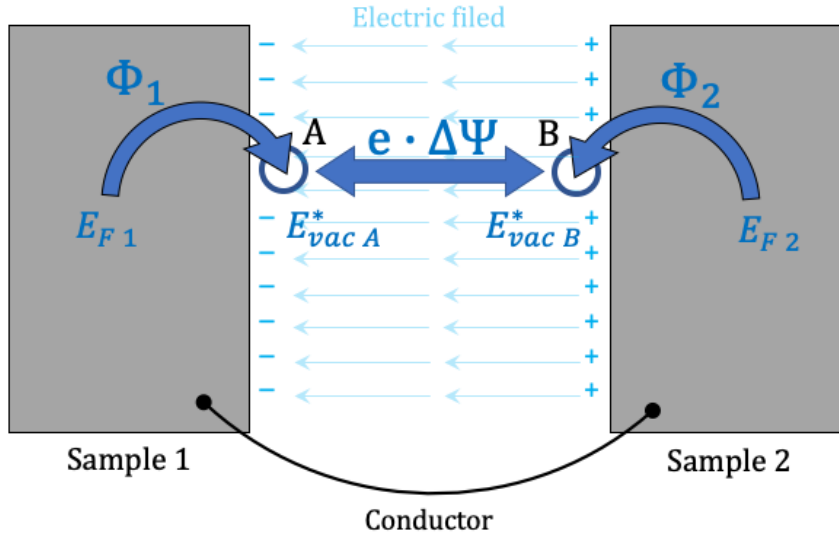


Figure 2.4 Two connected metals with dissimilar EWF

*Upon connection, an electric current flows and the initially neutral metals become electrostatically polarised so as to reach thermodynamic equilibrium and a common Fermi level.*

With these conceptual tools in place, the process ensuing upon connection of the two samples can be described as simply the Fermi level alignment of the samples and the build-up of the accompanying electric fields and electrostatic potentials. The following equation taken from [3] casts this process in the following equations:

$$\bar{\mu}_{e1} = -\Phi_1 + e\Psi_A = \bar{\mu}_{e2} = -\Phi_2 + e\Psi_B \quad (2.3)$$

$$\Phi_1 - \Phi_2 = e(\Psi_A - \Psi_B) \quad (2.4)$$

$$\Phi_1 - \Phi_2 = e\Delta\Psi \quad (2.5)$$

$\Psi$  denotes a *Volta potential* and  $\Delta\Psi$  is the difference in Volta potential between the samples, which may also be referred to as the *contact potential difference* [5]. Note that  $e\Delta\Psi$  is a positive number.  $e$ , the electron charge, is a negative number and the difference  $\Phi_1 - \Phi_2$  is a positive number since it was established that  $\Phi_1 > \Phi_2$ .



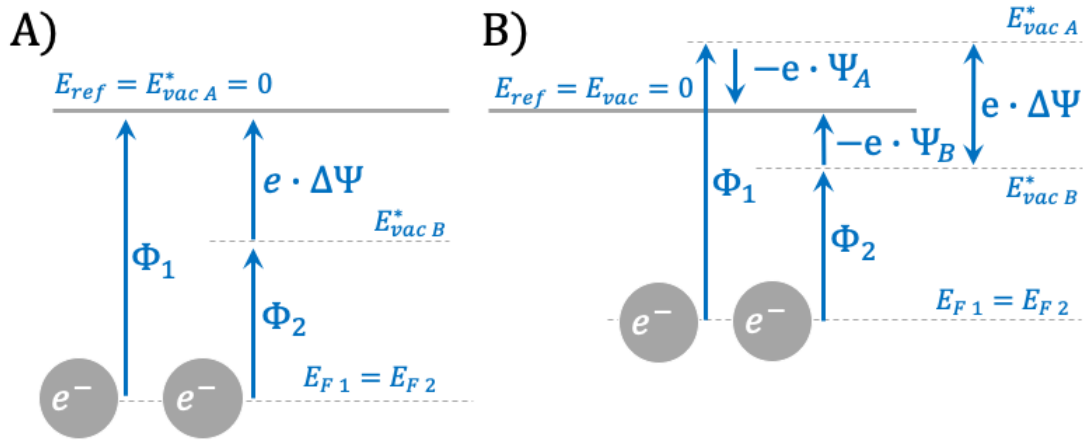


Figure 2.5 Illustration showing skew vacuum condition

Due to Fermi level alignment, an electric field has developed between the metal samples, introducing the Volta potential  $\Delta\Psi$  (see Figure 2.4, page 8). **A)** Global zero reference is set at the local vacuum level at A. Hence, for an electron to move from point B to that reference point it must traverse the electric field between the samples, gaining the potential energy  $e\Delta\Psi$  after already having gained  $\Phi$  to get to the local vacuum level at B. **B)** The global zero reference is set to be the vacuum level at infinity. Hence, the local vacuum level at A lies  $e\Psi_A$  higher than the vacuum level at infinity and the local vacuum level at B lies  $e\Psi_B$  lower than the vacuum level at infinity.  $e\Psi_A$  is positive and  $e\Psi_B$  is a negative number. Moving from A outwards to the reference at infinity,  $e\Psi_A$  work can be done by the electron, whereas an electron situated at point B would require work to be done on it equal to the absolute value of  $e\Psi_B$ . Regardless of how the global zero-reference is defined, equation 2.5 applies.

From the above one may conclude that an electric field builds up between points of locally different work function, in this case: The two samples. This phenomenon is exploited by a Kelvin probe to make measurements of the local EWF.

### 2.1.4 The Kelvin probing technique in general

Consider again Figure 2.4 on page 8. The distance between them can be changed. The electric potential difference between the samples is not affected by this, as it only depends on the work function (see equation 2.5). Hence, a certain amount of charge must be transferred between the samples to sustain the Volta potential difference at  $\Delta\Psi$ . This follows from looking at the two samples as a parallel plate capacitor and asserting that:

$$Q = CV \quad (2.6)$$

Where C, the capacitance, changes with the distance as given by [8]:

$$C = \frac{\epsilon A}{d} \quad (2.7)$$

$d$  is the distance between the plates,  $A$  is their area.  $\epsilon$  is the permeability of the medium in between the plates. This term may change depending on, for instance, the humidity.

William Thomson realised that this phenomenon could be used a measuring device for the EWF [2]. The set-up need only be altered in a few points. Firstly, one of the metal samples becomes the probe, the other becomes the sample. The EWF of the probe is known by calibration or definition. As the distance between the two is changed, the ensuing displacement current is recorded. Several variations of the technique exist, but in the original experiment as well as many modern Scanning Kelvin Probes (SKP's) the *nulling method* is used [2] [3]: An additional voltage is applied between the probe and the sample such that no more displacement current can be measured upon change in the probe-sample distance. The applied voltage is then equal to the Volta potential between the probe and the sample. From this and the known EWF of the probe, the local EWF of the sample can be calculated according to equation 2.5. As the probe is moved along the surface of the sample, any variation of the EWF – hence any variation of either  $\mu_e$  or  $e\chi$  – will be registered by the Kelvin probe as a change in the local Volta potential difference.

### 2.1.5 The Scanning Kelvin Probe (SKP) and Field Kelvin Probe (FKP)

The SKP is a modern instrument, widely used to make EWF measurements; in all the articles referred to concerning the interconnection of stress and EWF (see section 2.2) an SKP was used. In this design, the probe is typically in the form of a needle mounted on a vibrating cantilever [3]. Traditionally, the nulling-method is used to attain measurements of the Volta potential. The pointy tip allows for high resolutions up to 100nm and has made it possible to combine this device with atomic force microscopy, hence using the same tip to attain both the EWF and the topography of the sample [3]. However, since the needle shape deviates far from the geometry an ideal plate capacitor, the device is sensitive to stray capacitances introducing noise and must work very close to the surface of the sample [3].

The FKP represents a new branch of the Kelvin probing technology. Its name is suggestive for its design: High scanning speeds, a resilient mechanism featuring several technological innovations, all enclosed in a casing of compact dimensions. It differs from an SKP in several regards. Firstly, the tip of the probe does not oscillate up and down but instead it rotates. To still be able to attain precise measurements, it is shielded from outside electric fields except for a small window on the underside, where the sample is placed. Secondly, the FKP features an internal reference sample. Since this sample is made from an inert material, is fully shielded from the outside and does not move relative to the axis of the rotor it can be relied upon to produce a steady signal. This signal can in turn be used verify the validity of the EWF measurements taken of the actual sample below the probe. Thirdly, the FKP uses the so-called *off-nulling method* to measure Volta potential. As it is of practical relevance for interpreting the precision of measurement results, it will briefly be explained:

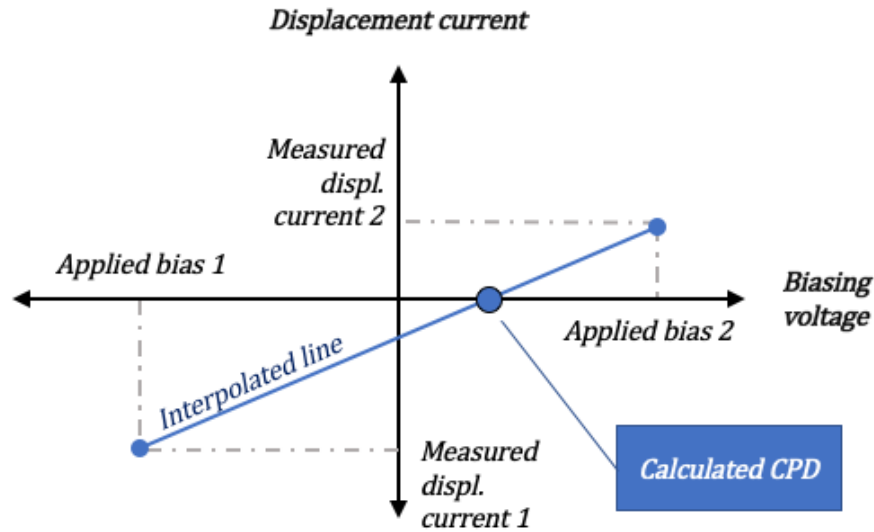


Figure 2.6 Illustration off-nulling method

*The Contact Potential Difference (CPD), ie the difference in Volta potential between sample and probe, can be calculated when the displacement current is measured during the application of two different biasing voltages applied between the probe and the sample.*

The method works by taking two measurements of the displacement current while the capacitance changes, for each a biasing voltage is applied between the sample and the probe. The applied voltage is of opposite polarity for the two measurements. The bias will be added to the pre-existing Volta potential difference between the probe and the sample, increasing it when the polarities match and decreasing it when the polarities are opposite. A displacement current is measured for this sum of bias and Volta potential and the result can be visualised as two data points in a Cartesian coordinate system (see Figure 2.6). The Volta potential is recovered as the x-intercept of the line connecting these two points. This method gives accurate results since the displacement current is not as small as with the nulling method, making it easier to register. Moreover, this method is per se well-suited to minimize the effect that sample-probe distance has on the results. At a closer distance, the absolute value of the displacement current will increase since the capacitance is greater. However, since the current is positive for one measurement point and negative for the other, the Volta potential does, in theory, not change. As will be addressed in the subsequent subsection, situations may arise when distance, despite of the use of the off-nulling method, is a factor that needs to be accounted for.

### 2.1.6 Factors influencing measurements with an FKP

Given the FKP's working principle and the underlying theory it is possible to attain an indication of how the properties of this device as an instrument for measuring EWF arise. A more detailed discussion of the specific experiments conducted for the current work (see chapter 3) will draw on what is presented here to evaluate possible sources of error.

First, it may be worth addressing a caveat: The scientific literature does not yet provide a complete account of how different material properties and states influence the EWF precisely [9]. Studies analysing EWF changes from an analytic perspective may only hope to give correct order-of-magnitude estimates [9], while the results of empirical research on the topic are partially contradictory [10]. A reason for this may be the great number of factors relating to the EWF of a metal sample; attaining consistent empirical results as well as a precise match of theoretical predictions with in situ

measurements is very difficult to do [9]. It is of course possible to gain a broad overview by inspecting equations such as (2.2) and reasoning what may change the parameters as was done in subsection 2.1.2. Ranking these factors in terms of their relative influence on the measured EWF, however, is very challenging. Drawing only on estimations and lacking precise knowledge of the causal relationships, experiments performed to investigate the connection between EWF and a given factor, stress in the case of the current work, would need to be well-controlled. Several factors in particular have the potential to change the EWF suddenly and without regards to the current stress state:

The presence of surrounding electric fields is such a factor. As was discussed in subsection 2.1.4, a Kelvin probe may be regarded as a device measuring Volta potential, i.e. probing the electric field between the tip and the sample. Should any other electric fields be present in that space, then they will influence the reading. Such field may come in the form of electromagnetic noise in the surrounding or as a consequence of electrostatic charge accumulation. Grounding both probe and sample will help to address the latter cause, while other measures can be taken in relation to the former. Probe and sample may, for example, be shielded by a Faraday cage, though this is often impractical. The FKP also offers the use of the reference-sample to detect electromagnetic disturbances; whenever the reference-sample changes significantly in its EWF, the data collected for the actual sample below may be inaccurate. Lastly, reducing the distance between the probe and the sample can also be expected to mitigate the influence of electromagnetic noise as well as stray capacitances.

The sample-probe distance matters in another regard too. Despite the use of the *off-nulling method* in an FKP, distance can have a direct influence on the EWF readings<sup>8</sup>. **Footnote:** The reason is technical rather than physical. In an FKP, the EWF of both the internal reference-sample and the external sample are measured with the same rotating sensor. The distance to the internal reference is fixed; the distance to the external sample can vary. If the external sample is moved very close to the rotating sensor, the ensuing displacement currents will be very strong compared to the displacement currents associated with the internal reference. Unless the electronics in the FKP are specifically calibrated for this dissonance, faulty measurements can occur.

Another group of factors influences the EWF of a metal sample, but their control is not as crucial as the control of the aforementioned factors in the context of the current work. These are factors that are mainly relevant when comparing different samples in terms of absolute EWF but are not as likely to impact changes of EWF with changes of stress dramatically. These are temperature, humidity of the air and local contaminations of the sample. As will be discussed in further detail in chapter 3, part of the wish with the experiments conducted for the current work was to evaluate the capabilities of the FKP outside a strictly controlled lab-environment. Care is still taken to mitigate the influence of detrimental sources of error, but were a device like this to be employed in the field then it should also be able to show a certain amount of resilience.

Lastly, there are some factors that may prove to play a particularly important role in the interconnection between stress and EWF investigated by the current work. The next section, section 2.2: Connection between EWF and mechanical stress, show which factors these may be and why they may be relevant.

---

<sup>8</sup> EWF measurements with an FKP were not known to vary strongly with probe-sample distance at the time the experiments for the current work were commenced. Towards the end of the process, it was found that a strong variation with distance exists in some situations (see chapter 3). Further, it was noted that distance variations in the experimental set-up used were more drastic than anticipated. This called the validity of the data already collected into question. More on the issue will be presented in chapter 4.

### 2.1.7 Summary and conclusions concerning the Kelvin probing technique

- 1) The Kelvin probing method allows detection of changes in electronic work function (EWF) in space and time: from one place on a sample to another, from one sample to another, on the same sample from one time to another
- 2) This is done by probing an electric field between the sample and the probe ( $\Delta\Psi$ ). All sources of error implied in that are implied in the measurements
- 3) The EWF can be taken as information about the energetic state of electrons in the sample due to:
  - a) The properties of the metal bulk:  $\mu_e$
  - b) The properties of the local surface interface of the sample:  $\chi$
- 4) EWF measurement on a metal sample may be impacted by a great number of factors relating to the sample, the probe and the environment; an exhaustive analysis of the mechanisms involved is extremely challenging both analytically and empirically

## 2.2 CONNECTION BETWEEN EWF AND MECHANICAL STRESS

The current work rests on the assumption that the EWF of a piece of metal, as measured by an FKP, is influenced by its stress state. The following literature review should clarify whether this is a reasonable assumption. Additionally, the previous work presented allows the selection of the most promising experimental approaches.

This section will be structured as follows: Observations are presented, first experimental results, then theoretical ones. Subsequently, interpretations for these are presented and evaluated. Relevant conclusions for the present work are drawn in the ensuing section.

### 2.2.1 Observations – experimental results

The Kelvin probing technique has found numerous applications in surface physics and more recently corrosion science [3]. Some researchers employ it to better understand the electronic and mechanical behaviour of nanomaterials [10] [11]. Others mean to use the close connection between the EWF measurements of a Kelvin Probe and the local corrosion potential [3] to investigate effects such as stress-corrosion cracking and pitting [12]. Some are also convinced the Kelvin probe will prove to be a useful tool in investigations into mechanical phenomena in general [10].

Due to their varying intentions, researchers have also tested a variety of metals. Stainless steel was of particular importance in studies with a focus on corrosion science: [13] [12] [14]. Wang et al. conducted research on 2205 Duplex stainless steel. They found that samples deformed elastically by a tensile load increased in their EWF by about 100 meV. When continuing to increase the strain into the plastic range, the EWF eventually dropped very significantly. The observed effects applied to both the austenitic and ferritic phases. Casales et. al conducted a similar experiment with 301LN stainless steel. Their samples portrayed a positive change of about 30 to 70 meV between the unstressed state and the yield point. Here too, the potential decreased by some 150 meV upon plastic deformation of the material.

Other metals have been tested as well. Pieces of pure (>99.95%), rolled Al and Cu were the subject of an investigation by Zhou et al. In contrast to what was observed for stainless steel [13] [14], the EWF of these metals appeared to decrease for increasing tensile strain in the elastic regime. Further increasing the strain into the plastic regime led to a steep drop in EWF (see Figure 2.7, page 15). It is noteworthy that in this study, the samples were also tested for a response to compressive loads. In the elastic range, the response of the FKP readings to compressive loads was contrary to what it had been for tension; the EWF increased. In the plastic domain, the response did not change when compared to tension; the EWF strongly decreased in either case. Several explanations were offered, and details will be discussed in subsection 2.2.4 and 2.2.5. Many of these explanations refer to the reversible nature of the elastic deformation mechanism and the irreversible nature of its plastic counterpart. In another experiment described in said paper, a planar stress state was induced in a copper sample, where compression in the x-direction was combined with tension in the y-direction. In the elastic range, the contrary effects on the EWF appeared to cancel; the EWF stayed roughly constant with strain. Beyond the yield point, a notable decrease in EWF was observed. Lastly, it was shown that in the plastic deformation regime, the strain rate had an influence on the EWF for both Al and Cu, where higher strain rates produced a lower EWF.

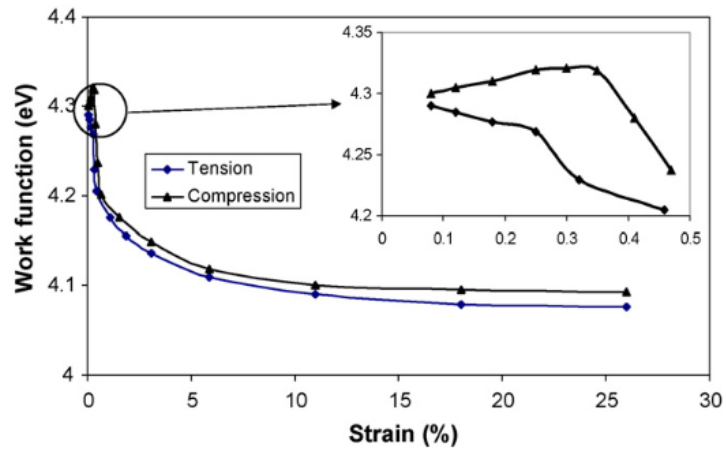


Figure 2.7 Variation in EWF of Al; from Zhou et al.

Figure 1 from [10]. EWF of Al with respect to strain under the bending condition. The inset shows variations in the EWF with respect to elastic strain.

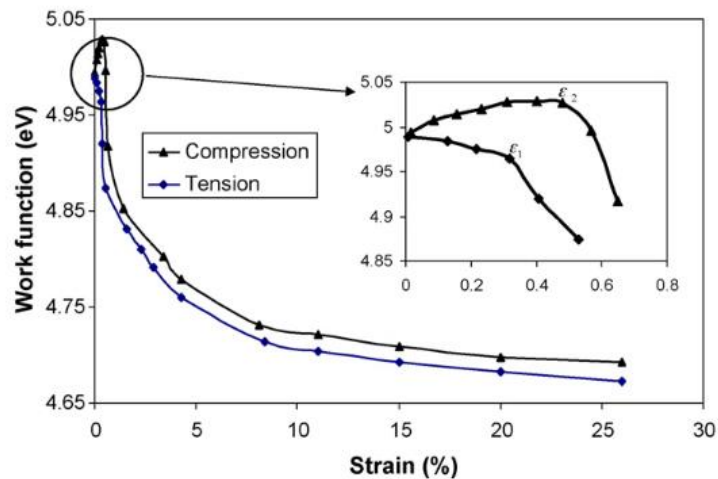


Figure 2.8 Variations in the EWF of Cu; from Zhou et al.

Figure 2 from [10]. EWF of Cu with respect to plastic strain under the bending condition. The inset shows variations in the EWF with respect to elastic strain

Zhou et al. also refer to the earlier work done by Levitin et al., a group that worked with samples made of Al, Ti, Fe and Ni alloys. Levitin et al. too found that the EWF of the materials they tested decreased when a tensile load within the elastic range of the material was applied. They underpinned their experimental observations with theoretical predictions.

## 2.2.2 Observations – theoretical results

Several researchers have analysed the connection of mechanical loads and the EWF of a piece of metal from a theoretical perspective. Two studies will be presented here [11] and [9]. They both build on what is referred to as the “stabilised jellium model”. In very broad terms, the motivating thoughts behind this model are as follows: On a microscopic level, numerous complicated interactions occur within the crystal lattice of a metal. Describing all of these in detail to find their cumulative effect is tedious and requires heavy numerical calculation. A much simpler approach is to ignore the discrete nature of the crystal lattice as well as its possible anisotropies. Roughly, this is what is entailed by the term “jellium model” [11]. The issue is that in some situations, such a model may not yield sufficiently accurate results. Then a “stabilised jellium model” may be more appropriate. Here, discrete interparticle interactions are taken account of, but only in the form of an average effect per primitive unit cell of the lattice [11]. The equations produced by this model are solved by employing the so-called “self-consistent Kohn-Sham method”.

Kiejna and Pogosov [11] have adapted this model for the description of elastically deformed metals. To apply it, they considered a single, uniform crystal of the chosen material in the shape of a rectangular prism. The changes in EWF they report refer to the upper face of the prism. Given a crystallographic orientation of the face, the desired EWF can be calculated. The crystallographic orientation matters since dependent on how the plane cuts the crystal lattice, the properties of said plane will vary. For polycrystalline samples, the results for the different orientations would have to be averaged to obtain an indication of how the polycrystal would behave. The authors are aware of these and other simplifying procedures and assumptions limiting the accuracy of their findings. Additionally, and as mentioned earlier (see subsection 2.2.1) the EWF of a surface is dependent on a wide range of factors, which renders accurate predictions inherently difficult to produce. Nevertheless, Kiejna and Pogosov are able to show alignment of their predictions with empirical observations.

Concerning this, it may be worth discussing one more caveat pointed out by Kiejna and Pogosov, relating to the comparison of theoretical and empirical results. In their paper [11], the authors state that strictly speaking, the Kelvin probing technique cannot be used to infer the EWF of a surface. Instead, the CPD causing the displacement current in a Kelvin probe is more directly related to something the authors refer to as the “effective potential” of the surfaces, rather than the EWF. However, these two quantities, effective potential and EWF, are closely interlinked. The distinction is made to the end of showing that situations may arise when theoretical considerations would predict a slight decrease in EWF, while a Kelvin probe would indicate a small increase<sup>9</sup>. Taking account of this effect when matching measurements and predictions should lead to a closer fit between the two.

Kiejna and Pogosov draw several relevant conclusions from their work: Firstly, the EWF varies linearly with strain in the elastic region, for both tensile and compressive loads. The range of strain under consideration in their study is  $-0.03$  to  $0.03$ . The fact that this relationship is linear has previously been shown experimentally by sources Kiejna and Pogosov reference and it was part of the motivation for developing this theoretical model. Secondly, Kiejna and Pogosov show that the amount of change in the effective potential of a surface due to strain is heavily dependent on the crystallographic orientation of that surface. For example, straining the Al single crystal by  $0.03$  will lead to a change of  $-0.103$  eV in effective potential when measuring on the surface (111),<sup>10</sup> while it will change said potential by only  $-0.064$  eV when considering the crystallographic plane (100). A noteworthy finding for Al is that irrespective of planar orientation (face (111) or (100)), the effective potential decreases for tensile strain and increases for compressive strain. This agrees with the empirical results by Zhou et al.

More recently, V.V. Pogosov partnered with A.V. Babich in another investigation on the effects of elastic deformation on the properties of metal surfaces [9]. This time, the focus lay on single crystals of

---

<sup>9</sup> In [11] this is shown to occur for crystallographic orientation of Li.

<sup>10</sup> This notation refers to a vector in the crystal system normal to the plane that is to be described [17]



Al, Au, Cu, and Zn covered by a dielectric insulator. It was concluded that under these conditions too, there exists a linear relationship between the effective potential and the elastic strain. Again, the authors deem it more appropriate to talk about effective potential than to talk about EWF. Both the Al and Cu crystals do, in this model and under these circumstances, behave similarly to the samples observed by Zhou et al: Compressive loads increase the effective potential and tensile loads decrease it. The strong dependence on crystallographic orientation remains. On the effect of the dielectric coating itself it is remarked that this feature decreases the EWF and increases the CPD [9].

### 2.2.3 Tabular overview

Material	Response of EWF upon tensile,				Reference
	elastic deformation		plastic deformation		
	sign	magnitude <sup>(1)(4)</sup>	sign	magnitude <sup>(2)(4)</sup>	
2205 Duplex stainless steel	+	100	–	150	[13]
301LN stainless steel	+	30...70	–	150	[14]
Al, purity >99.95%	–	25	–	175 <sup>(3)</sup>	[10]
Al, idealized single crystal	–	103 <sup>(5)</sup> , 64 <sup>(6)</sup>			[11]
Cu, purity >99.95%	–	30	–	270 <sup>(3)</sup>	[10]
Cu, idealized single crystal, dielectric coating	–	45 <sup>(5)</sup> , 23 <sup>(6)</sup>			[9]

#### NOTES:

- (1) *Units in meV. Change of EWF between unstressed state and yield point*
- (2) *Units in meV. Change of EWF between yield point and the limit approached by the EWF as plastic strain increases (see for example Fig (insert fig. Reference to figure from Zhou et al.) for illustration)*
- (3) *Zhou et al. show the strain-rate dependence of this value. This applies for a strain rate of  $1.45 \cdot 10^{-4} \frac{1}{s}$*
- (4) *For the study by Kiejna and Pogosov changes in effective potential will be presented instead of changes in EWF*
- (5) *For face (111)*
- (6) *For face (100)*

Considering the table above, several trends are observable:

1. There is a dichotomy between the response of the EWF in the plastic regime and its response in the elastic regime.
2. During plastic deformation, the EWF decreases and levels out at least 150 meV below its value at yield.
3. During elastic deformation, the change in EWF upon tension loading depends on the material, where it is positive with some (2205 Duplex- and 301LN stainless steel) and negative with

others (Al and Cu)<sup>11</sup>. However, in terms of absolute value, the change in the elastic regime is always smaller than the change in the plastic deformation regime.

## 2.2.4 Interpretations – elastic range

The observations presented above clearly indicate that the EWF can be expected to vary with the mechanical load applied to the sample. However, it has not yet been discussed what kind of connection this may be and where its causes may lie. In fact, the literature does not provide a universally accepted, consistent theory explaining all the results. A range of different interpretations are offered to match the given data and it is suggested that different, independent effects may really be present simultaneously. The dichotomy between elastic and plastic behaviour of metals offers the starting point for many such explanations, which often seek to describe the mechanisms of EWF change during plastic deformation as separate from those mechanisms which are dominant during elastic deformation. It is for this reason that the current subsection presents plausible explanations for the phenomena in the elastic range. The plastic range will be the focus of the next subsection.

Pogosov, Kienja and Babich [11] [9] rest their theoretical predictions of the EWF variation on a change of the crystal lattice geometry due to elastic strain. The shape of the primitive unit cell of the crystal changes and with it the distribution and energy states of the electrons within. The latter is detectable with a Kelvin Probe. Furthermore, real metals have a Poisson's ratio smaller than 0.5, meaning that they change volume when undergoing elastic deformation. This effect additionally changes the average electron density, which also affects the EWF and the effective potential [9] [11].

An entirely different approach is taken by Wang et al. [13]. They seek to explain why the EWF of 2205 Duplex stainless steel increases with tensile stress and offer a model based on surface roughness. The samples used in this study were polished with 0.5 $\mu\text{m}$  diamond paste, the residual roughness was hence on the nanoscale, with very small and sharp peaks and troughs. Upon elastic deformation, these features became smoother in their topography. The overall surface roughness increases but the edges on that surface, Wang et al. claim, are actually less sharp. Figure 2.9 is included in their article to demonstrate this. However, it is on sharp edges that electrons are bound less strongly by surrounding atoms and can thus escape more easily. As the surface roughness increases, and hence the sharpness of the microscopic topography decreases, the electrons are more tightly bound, corresponding to an increase in EWF.

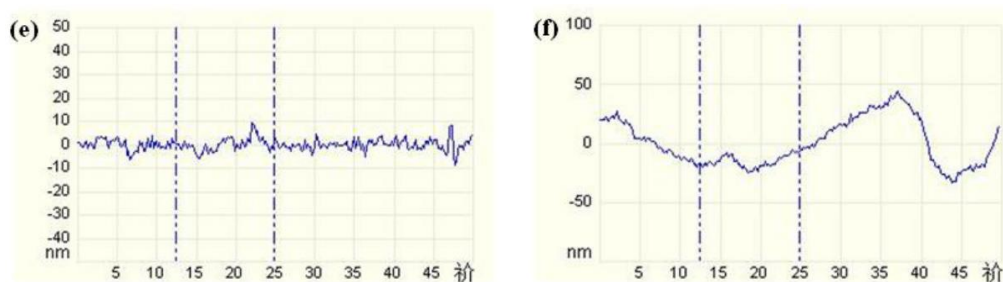


Figure 2.9 Surface topography along scan line; from Wang et al.

Figure 1 from [13]; surface topography along the same scan-line **e)** before deformation **f)** at 4.5% strain

<sup>11</sup> From the data presented in the table above, it may seem as though the alloys react negatively, while the pure metals react positively. The reader is referred to a paper by Levitin et al. not discussed in the current work, where negative changes were observed for several metallic alloys. V.V. Levitin, O.L. Grin, V.K. Yatsenko, Vacuum 63 (2001) 367.

### 2.2.5 Interpretations – plastic range

In the plastic range, deformation occurs by a different mechanism than in the elastic range: motion of dislocations, rather than the change of interatomic distance. It is this feature that all consulted sources analysing plastic deformation refer to when explaining the decrease of EWF in this domain [14] [13] [10].

Dislocations represent a break in the otherwise regular crystal geometry. These regions are associated with higher energy electrons, which can escape more easily [13]. Hence, the EWF is decreased locally. As these dislocations begin to emerge at the surface of the metal in the form of slip bands [13], the EWF of the surface will be reduced. Wang et al. also illustrate this by showing that the locations of slip bands, as detected by scanning the surface topography, precisely match regions of low EWF (see Figure 2.10). Zhou et al. further underpin the important role of dislocations for EWF change by an experiment where they plastically deformed Al and Cu samples at different rates. Higher rates of strain are associated with greater dislocation density [10]. Accordingly, lower EWF values were observed at a given level of strain when a higher strain rate was used [10].

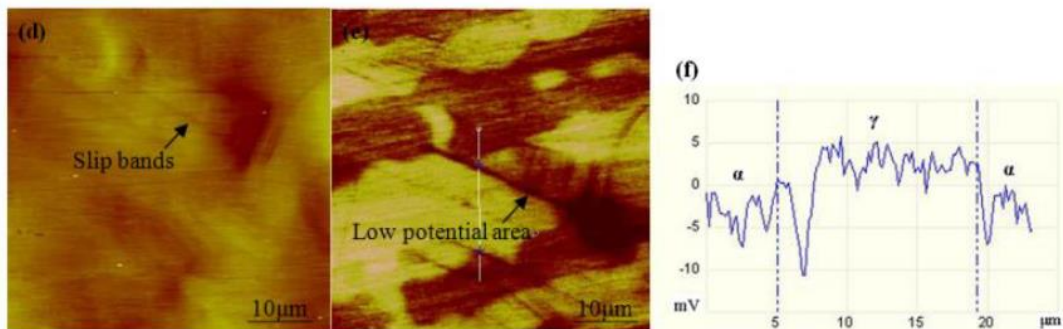


Figure 2.10 Surface topography, surface potential for stainless steel 9% elongated; from Wang et al.

*Figure 2 from [13]; These are from a deformed (9% elongation) piece of 2205 Duplex stainless steel. d) surface topography e) surface potential image f) Surface potential along the white scan line in c. The two different phases of the material are also marked and you can see two clear drops at the locations of the slip bands (about 10 mV). "Surface potential" can be taken to mean the EWF per the unit charge e.*

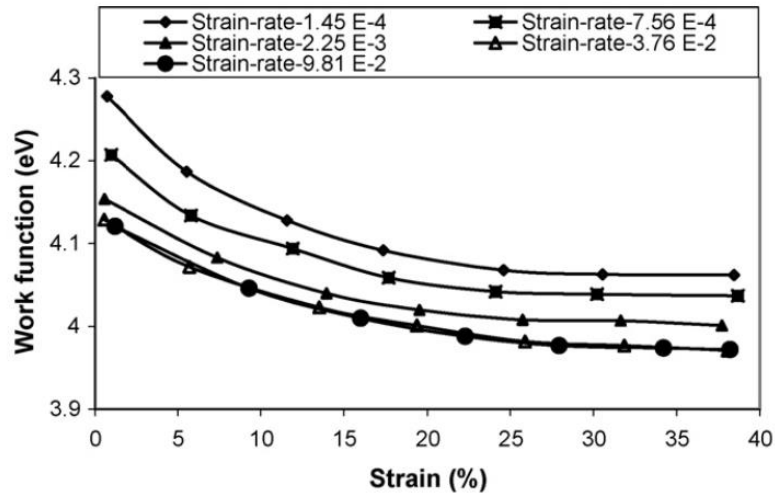


Figure 2.11 EWF of Al, plastic region, various strain rates; from Zhou et al.

*Figure 3 from [10]. Variations of the EWF of Al with respect to strain at various strain rates under tension*

When dislocations appear on the surface of stainless steel samples, they also rupture the passive film [14]. It was observed that plastic deformation will lead to a greater drop in EWF when the passive film of the metal is thick [14]. This is because the EWF of a stainless-steel surface has a strong positive dependency on the thickness of the passive film: a thicker film leads to a higher EWF and a thinner film to a lower EWF [14]. As the film ruptures entirely and unoxidised metal is exposed, the EWF will drop significantly.

Aside from explanations focusing on the role of dislocations, models based on surface roughness have also been applied to the plastic domain as well. Both Wang et al. and Casales et al. observed that roughness increases during plastic deformation of stainless steel. However, the latter group conducted a control experiment with unstressed metal samples of varying roughness and concluded that changes in topology cannot be expected to contribute much more than 20 meV to the changes in EWF during plastic deformation [14]. It is not clear to what extent these results contradict the roughness-based explanation for changes of EWF in the elastic domain proposed by Wang et al., since the samples used by Wang et al. were of lower surface roughness than the ones used by Casales et al. It is, however, an indication suggesting that surface roughness might not be playing as dominant a role as other factors.

Finally, it may be worth mentioning yet another model that was brought to bear on the plastic behaviour of 301LN stainless steel. This material belongs to a group of austenitic stainless steels referred to as “metastable”. The austenite phase will in case of cold working transform into alpha-martensite. The plastic deformation experiments performed by Casales et al. caused the martensite content in the microstructure of 301LN stainless steel to increase from about 50 to 100%. With reference to other articles, said authors state that martensite formation can cause ruptures of the passive film, hence further supporting the decrease of the EWF during this stage of deformation.

## 2.2.6 Conclusions drawn from the literature review

The first section of this chapter presents relationships that form the basis of interpreting measurements made with the Kelvin probing technique. The subsequent section tries to summarise important findings and draw conclusions from the presented literature. A particular focus lies on how this information may be used in an experimental setup.

The literature does not present one universally accepted theory. Instead, several likely mechanisms are suggested and the challenge lies in discerning which of them is most dominant at any given time. For instance, an effect active during elastic deformation should not cease to be active because yield occurred, but rather, it may cease to be relevant since another phenomenon has started to dominate the response of the EWF. This creates the dichotomy of EWF responses in these two areas, plastic and elastic, and the literature is unanimous on the point that effects associated to dislocations have a particularly strong influence on the EWF [10] [12] [13] [14].

Concerning the elastic deformation of metals, there is an argument to be made that surface roughness influences the EWF during deformation [13], though this influence is likely not exceedingly big [14]. One could investigate this in the following way: Polishing a tensile sample with rectangular cross section, one could take care to control the direction in which the SiC paper or polishing paste is moved across the surface. On the one side of the sample, the direction is chosen to be parallel to the direction of strain, on the other side, it is chosen to be transverse to the strain. The peaks and troughs on the two surfaces should now be predominantly oriented in the chosen direction. When a tensile load is applied, one should expect the topography to change differently on each side. On the side with the transverse polishing direction, a deformation analogous to that of an accordion may be expected; the peaks will become less sharp and it should be harder for electrons to escape. Hence, the EWF should increase there. On the opposite side, this effect should not be as pronounced.

Assessing the relative dominance of the microscopic mechanism relied upon by Kienja and Pogosov as well as Babich and Pogosov does not appear to be possible within the scope of this work. However, said authors make the testable prediction that the relationship between strain and the measurements of the FKP should be linear in the elastic region. If the data collected for the current work shows a relationship and it is clearly not linear, it may be concluded that the explanation offered by Pogosov, Kienja and Babich is at least not exhaustive.

Casales et al. underline the importance of passive film rupture and the exposure of unoxidised metal as a factor leading to EWF change in the plastic domain. This provides several interesting suggestions for possible experiments: Metals known to form very compact oxide layers, such as stainless steel or aluminium, might show the onset of plastic deformation very clearly. Furthermore, if oxidation of newly exposed metal occurs after the local rupture of the passive film, then the availability of oxygen would play an important role. A simple layer of paint on the metal surface may already reduce the speed at which this reaction can occur. Exposing painted and unpainted samples to stresses close to their yield point while simultaneously measuring the EWF, one would expect a different reactions from the two groups.

In bullet points, the relevant conclusions for the progress of this work are:

1. Mechanical stress and EWF are connected
2. Expect small and linear changes of EWF in the elastic range
3. Expect bigger, irreversible, negative changes in EWF in the plastic range
4. Experiment with surface roughness: The polishing direction may influence the EWF response under an elastic tensile load
5. Closely observe the EWF changes at the onset of plastic deformation for metals that form passive films (e.g. stainless steel and aluminium)
6. The availability of oxygen may influence the change in EWF at the start of and during plastic deformation. Consider comparing painted and unpainted samples.

### **3. DEVELOPING METHODOLOGY AND PRELIMINARY RESULTS**

#### **3.1 BEFORE FIRST LAB VISIT**

At the start of the project, before the work in the lab started, the time was spent on preparations. Some time went into researching how kelvin probes work and understanding the physics behind. Time was also spent searching for literature that could be related to the project. This information would aid in evaluating different testing methods and determine how to approach the project.

The bachelor thesis of a previous group that worked with the FKP was acquired and read through. Some of the sections there would provide valuable insight to what methods worked well and what issues that could occur.

#### **3.2 EARLY LAB WORK**

Early in the project there was conducted some tests with the kelvin probe on plain metals. This served as a way to get to know the probe and the associated software and get some experience with interpreting the probe readings. Different metals were tested and different areas on the same surface was scanned, this was done to get a feeling for what values to expect for different metals and how the values might change locally. During this testing “drift” was sometimes observed, this is when the reading would gradually move in one direction even though no changes was made to the test setup. In addition, a varying level of noise in the readings was observed.

#### **3.3 DECIDING ON A TEST SET-UP**

It was clear that a testing rig would be needed to progress the project. Work started on deciding which properties that was desired from the rig, before looking into the mechanics.

From the report from the earlier group, it was noted that bending of the metal as a form of stress induction would result in uneven changes in the distance between the sample and the probe. This would make it hard to distinguish between the contributors to any measured change. From this it was decided that a form of stressing that induces minimal geometric change was to be preferred.

A conclusion was made that when compared to the other possible stressing methods tension stress would allow for the most factors to be controlled and would therefore be the most suitable type of stressing. It would also ensure an even level of stress throughout the measured area.

Another point from this report was sample size, where the load applied was not sufficient to reach wanted stress levels due to the thickness of the sample plate. With this in mind it was decided that small samples would yield the best results since they could be stressed to the end of their elastic limit. This would also have the benefit of samples being cheaper and easier to obtain, giving a great amount of freedom in how to conduct the tests.

It was also decided that changes in the readings while in the elastic area of the metal would be of greatest interest. The objective was to explore the practical use of the instrument, and since a metal that has undergone plastic deformation is usually regarded as broken, the effects in the plastic area would be of less interest.

With these factors in consideration work began on developing a test setup. The possibility of constructing a rig was investigated, but it was decided that using an existing rig would be more time efficient. Some discussion led to the idea of using a device constructed and used by the university, a vice modified to stretch thin metal sheets. Using this device would allow testing to start sooner, and despite being a quite simple device it would be adequate for conducting some preliminary tests. The device was then borrowed from the university and relocated to Norce's lab.

### 3.4 VICE TESTING

The following tests were conducted as preliminary tests to help decide how to design the final test setup and to decide which metals would be worth investigating further. The tests were conducted in a lab environment using the modified vice with the FKP resting on a separate stand. And for some tests additional instruments were used to control various factors.

The data from these tests was not statistically analysed and is not presented in this report, it was only used to aid in determining the further approach of the project.

#### 3.4.1 Materials:

The materials looked at during this stage of testing were primarily aluminium, steel, and brass.

The aluminium was in the form of thin strips cut from a large, rolled sheet with cut direction perpendicular to the roll direction. It was cold rolled to 99% work hardening, some of the samples had been heat treated and normalized.

The brass and steel were acquired from a local workshop, it was then cut into strips in the same way as the aluminium.

Copper tape was used for a single test. This piece had been carefully cut into the shape of a dog bone to avoid stress concentrations. The piece of "paper" that protects the adhesives was not removed prior to testing to prevent the tape from sticking to the setup. This should not affect the measurements.

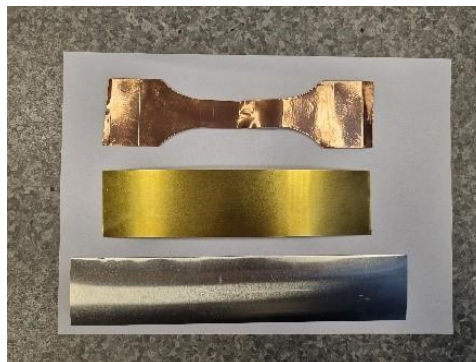


Figure 3.1 Three materials tested in the vice. Descending order: Cu, brass, Al



### 3.4.2 Equipment:

The device used to apply tension to the samples was a modified machine vice. The modification is the addition of two pieces of steel, one on top of each part of the jaw, which can be clamped down on the jaw by tightening two bolts. This construction allows for a thin metal sheet to be inserted and clamped to the two vice jaws, such that when the screw is turned counter-clockwise and the jaws are forced apart, the plate will be stretched longitudinally.



Figure 3.2 Test set-up with vice, FKP and camera microscope

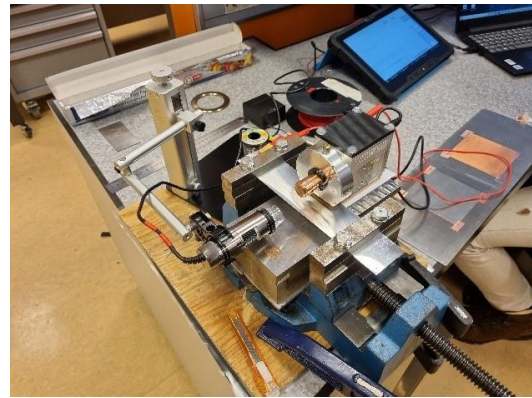


Figure 3.3 Test set-up vice from above

Several different devices were used to monitor factors that could influence the FKP reading. A camera microscope was used to record the movement of the vice jaw during tensioning. This data was used to calculate the stress on the sample. The camera microscope was also used to observe changes in distance between the probe and sample, later a laser distance sensor would be used for this purpose.

### 3.4.3 General procedure for testing in the vice

First the sample was cleaned with ethanol before being inserted into the clamping device, it would be carefully aligned with the direction of movement, then the bolts were tightened using a torque wrench. The screw was then turned until resistance was felt to get a slight pre-tension. The stand the probe was resting on was then adjusted to ensure optimal probe placement and the camera microscope was positioned. Then the system was connected to electrical ground.

The probe was started and left to run for a few minutes so that the measurements would be stable, and the condition of the setup could be evaluated. Logging was then started to record the probe data. The screw on the vice was then turned counterclockwise with a slow and continuous movement until a high level of resistance was reached (tests had been conducted to determine the breaking point of the samples so that near yield could be achieved during testing with the probe).

If the sample did not break under maximum load, the screw would be carefully turned clockwise to release the tension. The test was then concluded, and the data would be saved. Notes were taken during and after each test so that important details would get noted.

### **3.4.4 Results and conclusion**

From these tests it was concluded that any relation between work function and stress could not easily be observed. The limited control of several factors combined with issues in the setup and a low degree of repeatability made it evident that a new and more precise setup would be needed.

### **3.4.5 Sources of error**

The aluminium was work hardened and should experience minimal plastic deformation before breaking, but for the more malleable metals it was impossible to determine when the end of the elastic area was reached, and plastic deformation occurred. Since only the elastic area is of interest this made it difficult to draw conclusions from the tests.

Most of the samples had a slight bend to them (due to coming from a roll), this caused some variation in distance to the probe with increasing load. Attempts were made to monitor this change but the impact on the probe readings could not be reliably determined.

Another hindrance was that the vice would only move smoothly during tension, attempts were made to carefully unload the sample, but the vice would lock in place and make a sudden “jump” where all stress was released at once. This made it impossible to observe the effects of gradually lowering the stress.

All samples except the copper tape was in the form of rectangular sheets, this resulted in some samples breaking long before they should due to stress concentrations in the clamping area. An FEM analysis verified this and showed that the area under the probe would not reach the elastic limit before breakage occurred close to the jaws of the vice.

Repeatability of the tests was also an issue, with unknown elastic range, materials tending to snap and the vice unable to evenly unload the sample, it proved difficult to conduct repeated tests with the same initial conditions.

## **3.5 WAY FORWARD**

The time came to return the vice since the university had need for it, and a new setup was needed. With regards to all the uncontrolled factors in the first setup emphasis was put on designing a new setup where as many of these factors as possible could be controlled.

It was noted from the earlier tests that even the issues that should be negated by choosing tensile stress was still present. It was then concluded that tensile testing would still be the preferred method of stressing the sample, as any other method would be likely to result in more uncontrollable factors. Work then began on developing a new test setup.

It was proposed to construct a new device based on a vice where the issues of the previous version would be addressed. Some work went into researching strain gages as a method of measuring the stress during testing. Several of these were acquired from the university, but none were used during testing.

Even though bending was deemed unsuitable, it was proposed as a way of testing on spring steel. The large elastic area of spring steel would be ideal for conducting tests without exceeding yield.

A pulley system utilising gravity was also considered. Weights would be used, and the force would be used to calculate the stress on the sample. This would also allow for unloading the sample smoothly.

In the time during this deliberation correspondence was initiated with the university's lab engineer and the option of using their servo-hydraulic tensile testing machine was discussed. It was affirmed that the machine could be used, with some limitations to availability.

Out of the proposed options it was clear that the tensile testing machine would be the best choice and that the benefit of increased control over the test parameters would outweigh the drawback of limited availability. Arrangements was then made, and preparations commenced.

### **3.6 INSTRON TESTING**

The experiences from the preliminary testing led us to a test setup using the university's servo-hydraulic tensile testing machine, an Instron minitower 8801

#### **3.6.1 Materials:**

For the Instron more sophisticated samples were needed. After a visual inspection of the machine and a brief discussion with the lab engineer it was decided that a flat dog-bone design would be the best choice of sample shape. A 3D model was made and sent to the university's CNC operator, this became the template for all the samples with only thickness varying between the different metals.

The metals used were mild steel, stainless steel, aluminium and two different kinds of brass. The surface of the samples was not machined and was left untreated, with the exception of two pieces of mild steel where the surface was sanded down to a 2000 grit finish. Additionally, some samples of mild steel and aluminium was applied a coating of Bengalack.

The coating was applied to prevent a new layer of oxide from forming if the original layer cracked during the test, (looking at this as a possible reason for change in WF). And because the FKP is intended to be able to scan through paint in the field it was deemed worthwhile to investigate the effects under this condition.

The polishing was done to research the "accordion effect." During sanding care was taken to only sand lengthwise for one side of the sample and crosswise for the other side. This was intended to impact how the surface behaved under longitudinal extension, so that surface changes could be investigated as a source of change in the measurements.

The materials chosen were picked for distinct reasons, the mild steel because it is the most common construction material, aluminium because it is a common construction material, the brass because of corrosion resistance, and stainless steel to compare steel with a high content of alloying elements to mild steel, and to see if the passive film of the stainless steel differentiates it from the mild steel.

The mild steel and aluminium were in good availability and multiple samples was acquired of these metals. The brass and stainless-steel samples was made from surplus material from the university's workshop and were limited to one sample of each. During the course of the testing a different piece of brass was acquired, and two new samples were made from it.

Due to uncertainty in material type for several of the samples, tests have been performed to determine the yield strength of some metals prior to FKP testing.



Figure 3.4 Selection of tensile samples

Table 3.1 Overview of the used samples

Code name	Descriptive name	Width	Thickness
16_02_SST	Stainless Steel	15.1	5.05
16_02_BR	Brass	15.15	5
04_03_ST2	Steel, unpainted	15.2	3.01
18_03_ST1	Steel, unpainted	15.15	3.02
25_02_ST1	Steel, painted	15.2	3.01
25_03_ST1	Steel, painted	15.2	3
25_02_AL2	Aluminium, unpainted	14.95	2.02
16_02_AL1	Aluminium, painted	15.1	2.6
16_02_AL3	Aluminium, painted	15.05	2.6
25_02_AL1	Aluminium, painted	15.02	2.01
06_04_pST1	Steel, polished	15.5	3.1
16_02_AL2	Aluminium, unpainted	15.05	2.6
06_04_BR1	New brass	15.2	3.04

To attach the FKP to the Instron an improvised stand was constructed, this was deemed unsatisfactory after one testing session. Thereafter some work went into designing and constructing a rig that would allow for precise and repeatable probe placement. 3D-printing was utilised as a form of construction. The new rig proved to be successful and was used for all the subsequent tests.

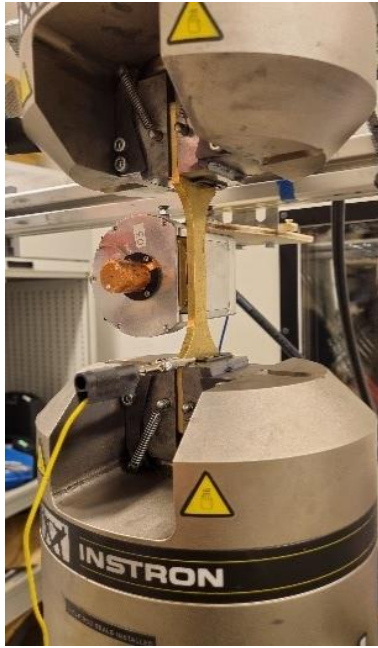


Figure 3.5 Brass sample in testing machine; FKP to the left, attached to improved rig

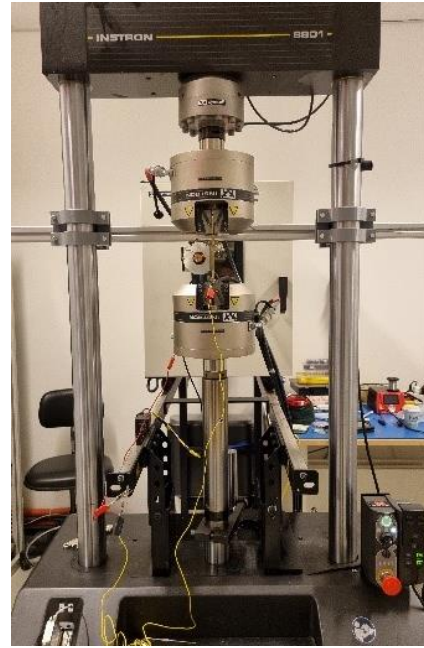


Figure 3.6 Instron tensile testing machine with inserted sample and mounted FKP

### 3.6.2 General procedure for Instron tests

The sample was held in place in the machine using the alignment tabs to ensure correct angle, and the lower jaw was closed. The measured parameters of the machine were then reset before the upper jaw was closed. The strain rate was then set in the Instron software. The probe was moved into position and ground was connected. The probe was started and left to run for a few minutes.

Logging was started, the Instron was started, and the timestamp was noted. The machine would be left to run at a constant strain rate until the applied load reached the maximum allowed for the material, the machine would then be stopped manually. The usual strain rate was 0,02 mm/s, but 0,04 mm/s and 0,08 mm/s were used for certain samples to shorten the test duration.

The machine would be left in loaded state for a short while before the machine was programmed to return to zero load over 100 seconds. The software would not allow decrease in load at a set rate, so this was used as an alternate solution. A new timestamp was noted at the start of the 100 seconds.

The loading and unloading procedure would then be repeated two additional times for most of the samples to gather sufficient amounts of data for statistical analysis, and to determine the repeatability of any observed effect.

The log file from the FKP would be saved, and in addition, the log file from the Instron would be saved.

### 3.6.3 Data

The Instron software logs the (machine)extension and load continuously for the duration of the test. Due to limitations in the software, no Instron log was generated for the unloading part of the tests.

### **3.6.4 Sources of errors**

While being a major improvement from the vice there are still several factors that could negatively affect the readings and cause uncertainty in determining the source of the measured changes.

There were some difficulties aligning the probe with the sample due to a small rotation in the clamp with reference to the pillars. This resulted in the probe not being completely parallel with the sample but rather at an angle to it. The effect of this is unknown, and the alignment changed between the testing days. The reason for this being that the entire rig had to be disassembled at the end of a session.

The fact that the timestamps are handwritten makes this a possible source of error. The timestamps are used to extract the test data from the FKP log since the software logs continuously before, during and after the test. A mistake here could lead to a situation where the data analysed is skewed from the actual data from the test.

For the later test, a distance gage was used to check the distance between the probe and sample prior to testing. Before this was acquired the initial distance was random and varied with each sample that was put in.

After the distance gage was acquired, it was discovered that between an unloaded and loaded sample a distance change in the area of 50 – 100 microns could be observed. This effect appeared to be completely reversible, and outside the range of contraction in the sample.

Different probes have been used on different testing days, and the condition of the probe might have changed between testing days since the probe is used for other purposes as well.

The Instron is also used by others between testing sessions, this have resulted in some parts being changed, and initial conditions being slightly different.

## **3.7 DISTANCE TESTING**

After the observation that small distance changes would result in large changes in the measured value it was decided that some tests were needed to evaluate the extent of the effect.

In the lab at Norce there was an FKP mounted on a frame consisting of three “linear translation stages” with integrated stepping motors. This gave the possibility of precisely changing the position of the probe while scanning. This setup was used to measure and observe the exact effect of distance change on all the different metal types that had been used in the Instron tests.

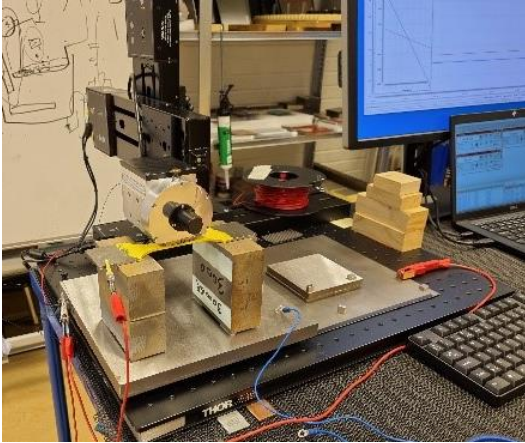


Figure 3.7 Rig used for distance testing; FKP suspended from computer-controlled frame; sample supported by steel blocks



Figure 3.8 Close-up FKP and brass sample; starting point for experiment 50  $\mu\text{m}$  initial distance

The test started with positioning of the probe; a distance gage was used to ensure a distance of 50 microns at the initial position. A program had been written to ensure that all the tests were equal, the program would raise the probe short distances in steps with pauses in between. This was done instead of a continuous movement to eliminate any potential influence from the electromotors.

From the results of these tests, it was observed that some metals displayed a “critical range” up to 150 microns where changes would lead to large variations in measurements, and higher above the only effect would be gradually increasing levels of noise. For the other samples, the only observed effect was increasing noise levels.

### 3.8 NEW INSTRON TEST

On the last day of testing the distance from probe to sample was carefully adjusted and monitored to prevent distance effects from affecting the results. But after a while it was discovered that the probe responded differently to the changes than expected, and manually pushing the probe away from the sample revealed that the effect of distance change would occur even at large distances and affect the readings with a magnitude that would overshadow any other effect.

At this point, a radical new approach was proposed. Pieces of post-it-notes would be cut into pieces and applied to the sample to function as an insulating layer while the probe was pushed against it and secured with a rubber band. The purpose of this was to ensure that minimal amounts of change would occur during the test.

This approach was not used earlier as direct connection between the probe and sample was undesired. Reason being that a non-perfect isolator could affect the readings negatively, and due to the nature of the rig holding the probe, movement in the sample could lead to a change in the angle between the probe and sample. The approach was still used in this case since the value of negating distance change was high enough to sacrifice some precision.

### 3.9 DATA TREATMENT

This last section deals with the last link in the chain between experiment and result: treatment of data. It relates specifically to the second objective of the current work (see chapter 1), that concerns characterising the relationship between EWF and stress. The data treatment will be discussed for the experiments on the tensile testing machine and for the experiments where sample-probe distance was investigated. For both, the intentions for the data treatment will be discussed and underlying concepts will be addressed, before indicating what was done to implement this practically.

The experiments on the “Instron” testing machine were designed in such a way that stress and EWF should be directly comparable. Hence, data from the FKP, the testing machine, and notes concerning the way the experiment was conducted would have to be unified. With corresponding EWF and stress measurements in place, it was deemed desirable to fit a regression model to the data. The choice fell on a linear model, since the prediction was made by two sources in the literature [9] [11] that the relationship between EWF and stress may be linear. After computing the regression model and estimating its parameters, a two-tailed hypothesis test can be performed on  $\hat{\beta}$ , the estimated slope of the regression line, to put claims of dependence between EWF and stress on a slightly more formal footing. The zero hypothesis is in this case that  $\hat{\beta} = 0$ . The level of significance was set at 2.5% for the purposes of the current work, though with all graphical representations of the results featuring p-values the reader is free to set higher standards independently. Another measure that was deemed useful and hence included in the graphs for the experiments is the correlation between EWF and stress, or rather the empirical estimate of the correlation squared. If it is low, that could be an indication that there is a lot of noise and not a strong linear relationship between EWF and stress. This can happen easily when the slope of the regression line connecting the two variables is small<sup>12</sup>. An adapted correlation measure can also be used to compare how well different models fit the data. Although it would be very interesting to compare different statistical models, a subsection of chapter four will do so without the aid of further statistical analysis, leaving further regression models as a welcome enhancement for further work.

Implementing this kind of data treatment implies to first integrate information from three different sources: The FKP, the tensile testing machine and the notes taken during the experiment. The process was partially manual and partially automated by code written for this purpose. There were three parts to it: Accessing the log files from the FKP, accessing the log files from the testing machine and integrating the relevant data using the notes so that one Excel sheet was produced where the data could be easily manipulated and visualised. The first part, accessing the FKP logs, was automated by a piece of code in Python written for this purpose. It changed the file type and removed unnecessary data columns. Another code was used for accessing the log files from the Instron. Great amounts of unnecessary information were removed, as the testing machine logged 100 data points per second, the FKP software just one. This, and all other codes written for the current work are presented in the appendix. The reader is encouraged to inspect them, given the great importance they have had in the data analysis process. The rest of the necessary operations for integrating and filing the data were carried out manually.

After the data had been stored in this way, it had to be analysed and the graphs shown throughout chapter four had to be created. The bulk of this work was executed in the Matrix Laboratory (MatLab) software by MathWorks. Again, codes were written specifically for this purpose (see appendix). Here, the approach was to automate as much of the work as possible, since the same kind of analysis would have to be applied to the data sets from a great number of experiments. Since there were variations in many parameters concerning the data, such as the number of tests within the given experiment, its duration, the type of graph that would be most useful etc., the code had to allow for a high level of flexibility. While it is always a challenge to code in this way, the strategy proved successful. With the appropriate input files<sup>13</sup> to the MatLab code prepared, it is easily done to run the code again and change single

---

<sup>12</sup>  $Corr(X, Y) = \frac{Cov(X, Y)}{\sigma_X \sigma_Y} = \beta \frac{\sigma_X}{\sigma_Y}$ , taken from [18]

<sup>13</sup> The input files carry the experimental data



parameters controlling the appearance or content of the output graph, the way it is saved, or which tests should enter in the analysis, and which should not<sup>14</sup>. By “tesst” is meant one continuous increase or decrease of stress. An “experiment” on one sample usually consists of two to eight tests.

---

<sup>14</sup> As will become apparent in the next section, it is sometimes of interest to exclude certain tests within one experiment from the regression analysis.

## 4. RESULTS, DISCUSSION, AND OUTLOOK

This chapter is divided into two sections. The first presents and discusses the results of the experiments conducted for the current work. The second is smaller in length and means to point to different implementations of the FKP technology which, considering the recent discussion, may appear promising. This will form the bridge to the final chapter of the report: conclusions and further work.

### 4.1 RESULTS AND DISCUSSION

As will become apparent during the course of the following pages, the results presented here do not appear to lend themselves to clear conclusions. To try to integrate their various facets into a single picture, they will be presented using an overarching argumentative structure that is presented in a couple of pages. Results and interpretations will be offered simultaneously.

Before doing so, however, a disclaimer is in order: No attempt is made at offering an exhaustive explanation of the observed phenomena. The appendix provides graphical data from all experiments underlying the current section, should the reader wish to form an independent opinion. Referring to the appendix is also encouraged to the end of viewing all the material referenced in the following discussion. Most of the experimental data is presented during various examples in the text itself, but the remainder is available in the appendix.

#### 4.1.1 Overarching line of argument

To develop a structure that will guide the reader through the collected results, it is worth taking some steps back first. It has been laid out in chapter two that the EWF as measured by an FKP may vary due to a multitude of factors. Some of these are connected to stress. The literature presented in section 2.2 draws out several mechanisms by which this may happen directly or indirectly. However, it has been stated repeatedly that the EWF also varies due to factors completely independent of applied tensile stress. Such factors include temperature, chemical reactions on the surface, contaminations etc. (see section 2.1). Additionally, the EWF also varies with certain factors that arise from the FKP's operating principle (see subsection 2.1.6). Electric fields, humidity of the air and distance between the probe and the sample, for instance. The last of these is a factor that was observed to be connected to the application of stress, but only by virtue of the experimental set-up that was used. These findings, detailed references are found in chapter 2, are called to mind again to make the following point: The EWF may well vary without a variation of the applied stress. All the current work hopes to investigate is: Whenever the applied tensile stress *does* vary, will the EWF as measured by an FKP vary as well?

Consider again the aim statement laid down in chapter one: *“Evaluate the possibility of employing the current version of the FKP as an instrument for detecting applied tensile stress with a view to practical contexts”*. It can be said that this possibility depends on an important prerequisite: when the stress state of a metal *does* vary, the response of the EWF as measured by the FKP must reflect this change. Inspecting the EWF during times of changing stress, it is *necessary* that *there be a significant relationship between EWF and stress, should the FKP in its current version be used as an instrument for detecting stress*. Hence, the experimental data can be inspected with the aim of finding an interconnection of EWF and stress during changes of applied stress.

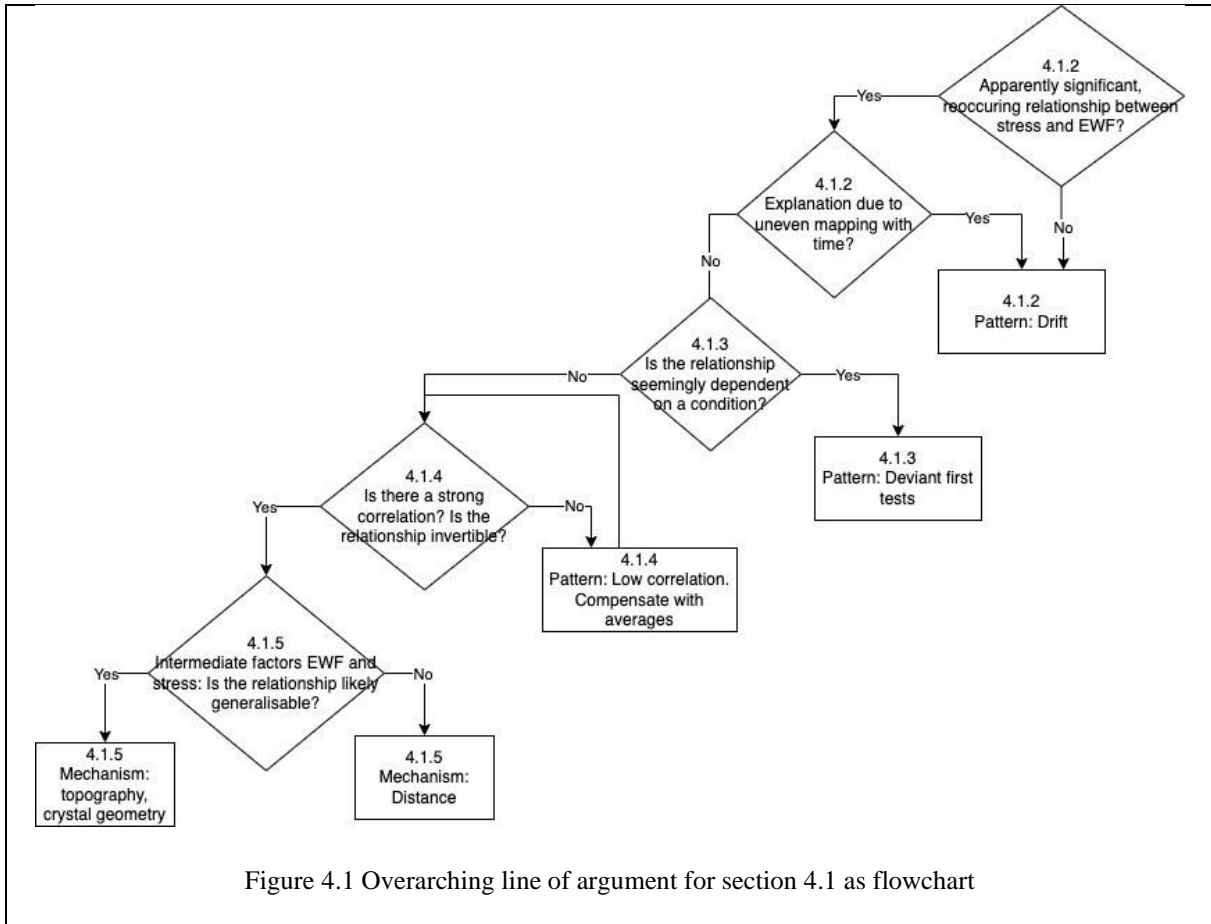
A natural objection at this point may be: Given the *necessary* condition above is met, this is not yet *sufficient* for stating that the FKP is well-suited for the tasks of a stress measuring device. Indeed, it is not. In a realistic situation, attempting to measure the stress state of a mechanical part, one would expect to receive clear information from such a device. One would expect of that the output reading to change if *and only if* the stress state of the sample changes. Here, the fact that the EWF of a sample can alter due to a variety of factors independent or only partially dependent on stress in the sample poses a real challenge. Whether this can be overcome is not certain. An approach suggested by Norce to bypassing the problem would be to always scan whole areas at once and then characterise the EWF values on this map. When the EWF changes in areas where a different stress may be expected, this change in stress may perhaps be quantified by use of the EWF. Further, the EWF patterns appearing on this map due to stress would have a different characteristic in terms of how they interact with the geometry of the part than the EWF contributions from local corrosion, for example. This is, however, not the focus of the current work. More important is the evaluation of the necessary condition stated earlier. This has several reasons, primary among them the fact that this condition is much easier to investigate than the technological feasibility of an actual, FKP-based stress-measuring device and how it may perform under different circumstances. Should the experiments performed for the current work indicate that at least a prerequisite for the development for such a device is met, then this would make further pursuits of such a technology appear justified. In case the results do not clearly support this application of the FKP technology, recommendations can perhaps be made on which fields or problems may hold greater promises for this device. The wording of the aim statement meant to reflect that the “*possibility* of employing the current version of the FKP...” is investigated and hence a necessary condition is considered, rather than for instance the “*technological feasibility and utility* of employing the current version of the FKP...”. That would be a second step beyond the scope of the current work.

Whether the necessary condition under investigation is fulfilled can be analysed by posing the following question that will make it easier to discuss the experimental results: How good of an explanatory variable is the applied tensile stress, to account for changes in the EWF under changing stress in the experiments performed? Note what is implied in this: The EWF is viewed as function of multiple (explanatory) variables. These variables will all vary to some extent within the bounds set by the degree of error control in the experiment. The experiments are performed by varying a certain subset of these factors. Ideally, this would be only the applied tensile stress, but due to the inherent imperfections of the experimental set-up and the physical interconnection of the variables, several factors will be changed with the stress. The surface topography of the sample, for example, changes because of a direct connection to the applied stress, while the sample-probe distance may change inadvertently due to the way the experiment is conducted. One may note that: *if it is shown that a significant relationship exists between the EWF and stress while stress is changed and this interconnection of stress and EWF is exploitable in contexts beyond this experiment<sup>15</sup>, the necessary condition may be deemed fulfilled.*

The purpose of the overarching line of argument alluded to before is to go about testing this in a systematic way. As it consists of a series of decision gates, it may best be visualised graphically (see Figure 4.1). In the ensuing sections, the experimental results for each tested sample will be put through this scheme and comments on the arising patterns will be made.

---

<sup>15</sup> : If the linking factor responsible for EWF changes with stress is, for instance, changes in crystal geometry, then this mechanism applies to more than just these experiments. If the link should prove to be changes in sample-probe distance, it does not



The numbers in the elements of the flow chart stand for the numbers of the sub-sections discussing this question or pattern. The idea is that each question represents a filter; starting with the data from all the experiments, only the results from few promising experiments will remain prior to the last decision gate (4.1.5). Each of the side-branches in the diagram represent a set of experiments that show some deviant pattern, not supporting a fulfilment of the necessary condition. In a final sub-section, 4.1.6, the findings will be summarised.

#### 4.1.2 Patter: Drift

As referred to earlier, data analysis was conducted by mapping each EWF measurement to the corresponding tensile stress and then fitting a simple linear regression model. Surprisingly, all experiments showed a significant linear relationship<sup>16</sup> between EWF and stress, when all tests were considered. However, as the rest of this section will show, the underlying patterns are very different from experiment to experiment. The first pattern to be discussed is, for the purposes of the current work, termed “drift”.

Recall that the EWF varies with factors independent of stress. These stress-independent factors again can be taken to vary with time. This is the reason that the EWF shifts to some extent with the passage

<sup>16</sup> Greatest value for p value of beta-hat: 0.013

of time, even when there is no obvious reason for this. Broadly, this text will speak of “drift” when variations with time start to form a visible pattern independent of the variation with stress. Such time-dependent patterns are particularly prominent when they cause divergence of individual tests within a single experiment

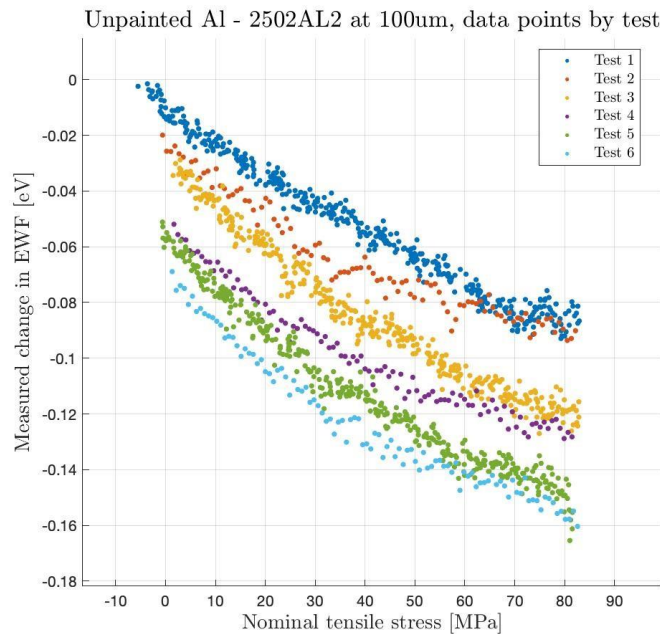


Figure 4.2 Graph showing divergence of individual tests

*Unpainted aluminium sample, 2502AL2, measured at 100  $\mu\text{m}$  of initial displacement between the probe and the sample*

In theory, one would expect all variables independent of stress to vary within a certain range. So, given the experiment is repeated often enough, only a mean contribution of these factors should be visible and time as a factor should no longer be of great importance. The same can occur when the stress-independent variables change very quickly, have little influence on the EWF or barely change at all. Some experiments show precise alignment of their individual tests right away (see some figure with aligning tests). In other experiments, it seems that no test is like the previous and it is not clear how many tests would have to be conducted before the dependence on time becomes negligible, if it ever will (see Figure 4.2).

The pattern “drift” has been identified within these samples / experiments. The code in the end specifies an individual sample:

- Painted aluminium 1602AL2 and 1602AL3
- Unpainted aluminium 2502AL2
- Painted steel 2502ST1 and 2503ST1

That the individual tests of an experiment diverge in their response to changing tensile stress implies that the time-dependent variables responsible for this divergence change within a similar time frame as the duration of an individual test, so anywhere between one and five minutes. It is noteworthy that 4 out of 5 samples showing drift were coated. A possible explanation might be that the application of stress ruptures the oxide layer of the metal underneath the paint. Since the coating restricts the flow of oxygen to areas of exposed metal, the oxidation reaction takes longer than usual and EWF changes are observable on the time scale of 10 to 20 minutes.

However, with just five samples, the data set and hence also the amount of trust that should be placed in the conclusions drawn from it is small. Consider, for instance, that only one sample of unpainted aluminium was properly tested for the current work<sup>17</sup> and that it shows drift. It is also imaginable that drift occurred due to a factor not related to the sample. Maybe the air conditioning happened to switch on during these experiments and the subtle change in room temperature was enough to cause drift.

Consider the graph in Figure 4.3. The individual tests lie close together but there is still a tendency to drift. It can be deemed significant that the slope of the linear regression is other than zero. With such a graph, it makes sense to guard against a particular objection relating to the validity of the linear relationship between EWF and stress: maybe this data is explainable by an EWF that decreases at a constant rate with time; the trend that low EWF values typically correspond to high values of stress is simply because more data has been collected while increasing the stress than while decreasing the stress.

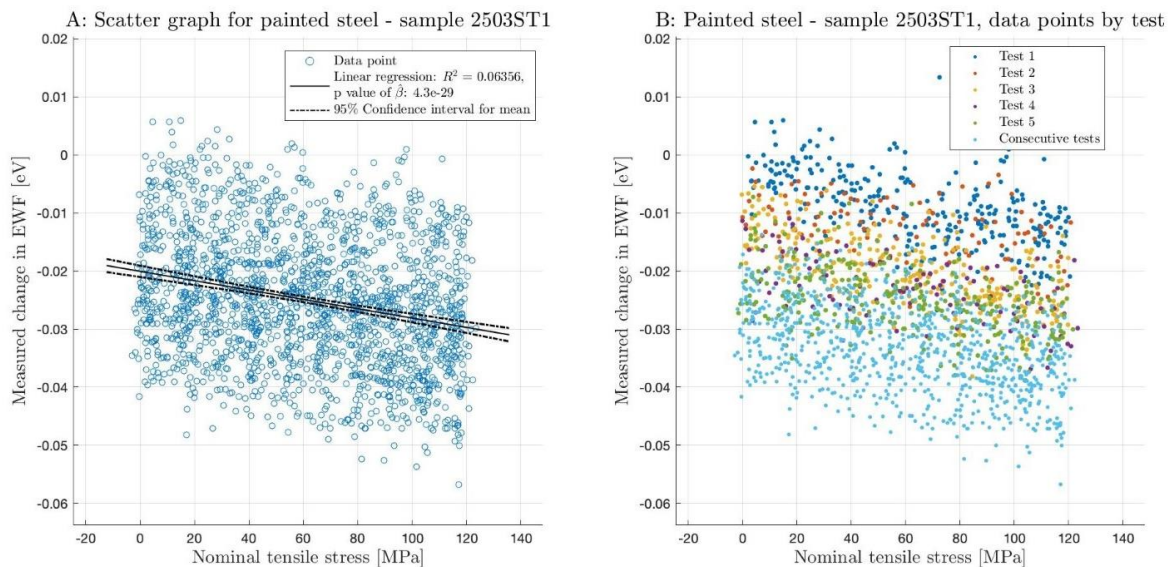


Figure 4.3 A sample of painted steel, 2503ST1, showing drift where tests still lie close together

The fact that time is not mapped evenly onto the stress-EWF plane is ultimately because of the idiosyncrasies of the used tensile testing machine (see subsection 3.6.2). Objections that build on this

<sup>17</sup> A second sample of unpainted aluminium was briefly tested on the last day at the lab, but since this experiment consisted of just one test, its results are not deemed reliable. Moreover, with both experiments involving unpainted aluminium, there were severe challenges controlling the influence of the sample-probe distance on the results. More on this will be presented in 4.1.5.

uneven mapping of time are what is being referred to by the decision gate with number 4.1.2 in the overarching line of argument (Figure 4.1). The validity of the objection is testable in so far as it predicts that there is in fact no relationship between the stress and the EWF. The value of the measured EWF is displayed in the time domain and the start- and end times of each test, hence of each period of stress variation, is marked. Red areas indicate tests in which the stress was raised, green areas indicate tests in which the stress was lowered.

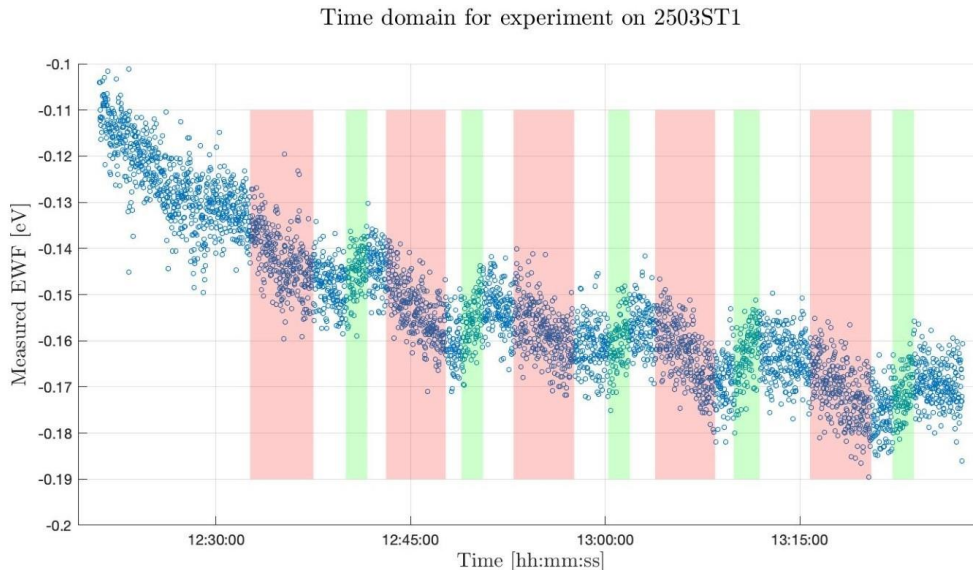


Figure 4.4 Time domain for experiment on 2503ST1

From the graph above it is clearly visible that at least some covariance between EWF and stress is exceedingly likely. Obviously, it is still a question of probability and any pattern that may suggest a connection between EWF and stress could be purely coincidental and due to factors independent of stress. However, while this objection is decently reasonable when supposing that the EWF simply decreases linearly with time, explaining far more complex patterns this way would not. The conjecture that the EWF decreases completely independently of the stress may be rejected based on the graph above (Figure 4.4). This kind of diagram has only been constructed for the sample 2503ST1; it is the only one where this seemed justified. With the remaining four samples displaying drift, at least some covariance of stress and EWF can be read off directly from the stress-EWF graphs containing all the tests.

#### 4.1.3 Pattern: Deviant first tests

Referring to diagram (Figure 4.1, page 36): Once ascertained that the apparent relationship between EWF and stress is not purely due to the uneven mapping of time, it can be discussed whether it is dependent on a condition. It was observed that with a certain subset of the experimental results, it is. The pattern they follow was freely termed “deviant first test”. Sets of experimental data portraying this pattern only show a significant linear relationship between EWF and stress when the first, and in some cases second, test is included. Removal will lead to a relationship that is no longer significant.

“Deviant first tests” were observed in the following experiments:

- Painted aluminium 1602AL1 and 2502AL1
- Painted steel 2502ST1
- Unpainted steel 0403ST2 and 1803ST1
- Brass 1602BR1, experiment 1

It may be noted that some of the samples mentioned above were already referred to in relation to “drift”. The reason is that once the first test is removed from the data set of these experiments, the linear relationship between EWF and stress seizes to be significant. At the same time, “drift” can be observed in the data that remains.

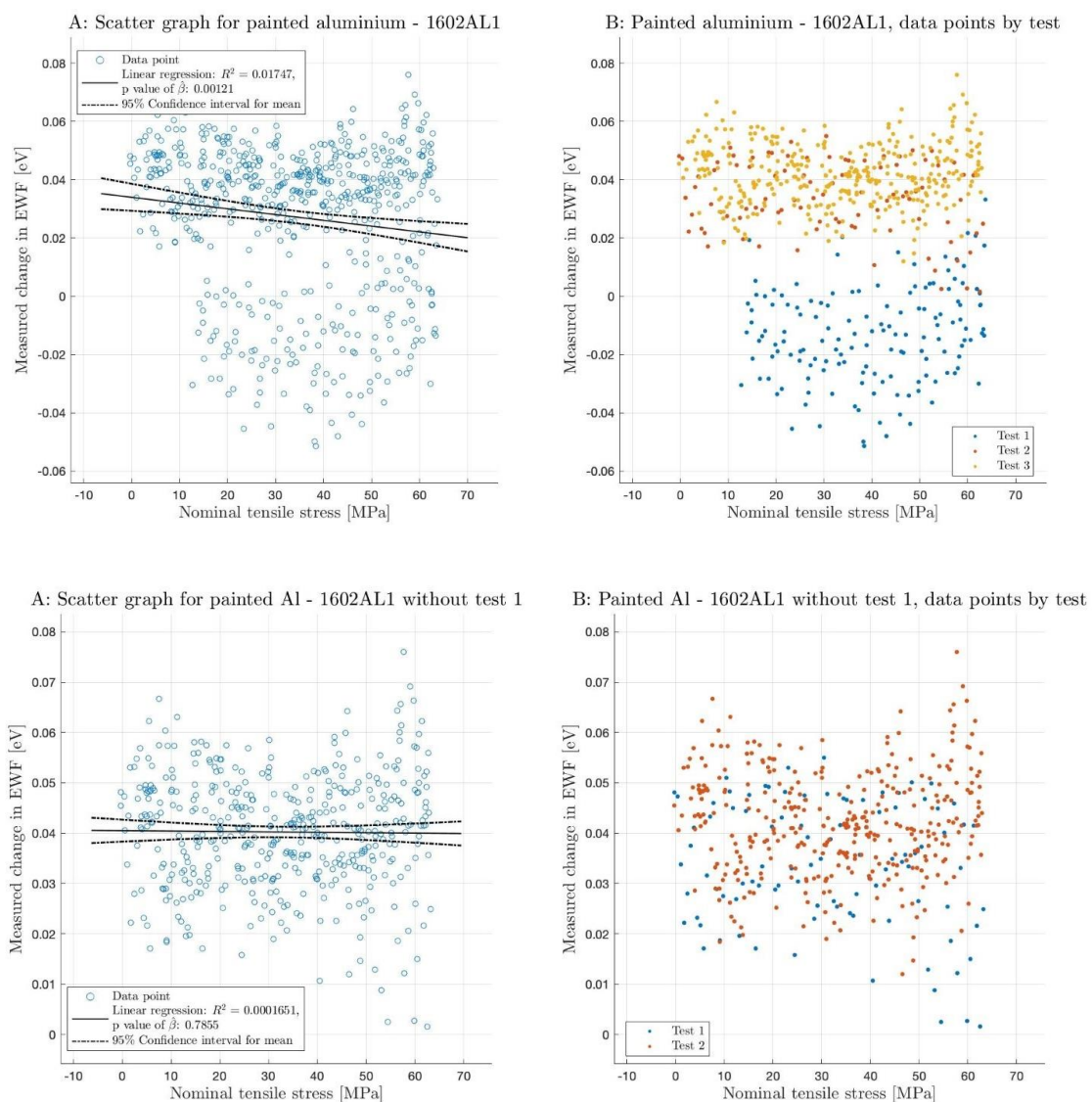


Figure 4.5 1602AL1 painted aluminium - example of a "deviant first test"



Whatever causes this behaviour is likely an irreversible process. Brass 1602BR1 shows an interesting example of where “deviant first tests” were observed for two tests, with the first test exposing the sample to a lower tensile stress than the second. A permanent offset in the EWF was observed during the first test and then again as the previous maximal stress was surpassed. When experimented on again a week later at the same stress level, no permanent offsets between the tests were observed. Another noteworthy observation is that the occurrence of this pattern is not strictly tied to the sample material; three different kinds of samples portray it. Also within sample types the response is not unanimous: two of the three samples of painted aluminium show it while one does not. Care must be taken to not take these trends as absolute. They are based on observations from a small number of samples and it cannot be guaranteed that samples of like type do not differ in some regard relevant to the experiment.

A plausible explanation taken from the literature review (section 2.2, page 14) again relates to the rupture of the oxide layer. This would fit with the fact that the first test takes a special position. Coated and uncoated samples have been included in the experiments performed here to investigate the extent to which oxidation after oxide layer rupture may occur. One may, with all due care, state that samples painted and unpainted steel tend to react slightly differently. With the unpainted steel, bigger deviations in between the first and consecutive tests have been observed. “Deviant first tests” occur in all samples of unpainted steel and only in one of two samples of painted steel. Also, the tendency for drift is not as pronounced for unpainted steel as it is for painted steel. Though again, the small sample size does not permit reliable conclusions to be drawn.

Taking up another inspiration from the literature (section 2.2, page 14), one may compare those samples with a passive film to those with a less compact oxide, such as steel. Here, no consistent pattern could be detected.

When supposing that oxide layer rupture is in fact responsible, it is very remarkable that the first test sometimes shows a permanent decrease in EWF, but just as often, it displays a permanent increase. According to what has been stated in the literature review, an increase in EWF cannot be explained by the exposure of unoxidised metal or even the onset of plastic deformation.

In the group of samples portraying “deviant first tests”, the linear relationship between EWF and stress can be shown to be conditional. After the first test, when exposed to the same change in load again, no change in EWF can be expected. These sets of experimental data can hence not be invoked in support of showing the necessary condition (see subsection 4.1.1, page 34) to be fulfilled.

#### **4.1.4 Invertibility: Going from EWF to stress**

Part of the aim for the current work is to view the stress-detection capabilities in a practical context. In any such context, what is available is sets of EWF measurements from which changes of stress need to be deduced.

To find out whether this is practically doable, the correlation between stress and EWF in the performed experiments needs to be considered. As was already stated in sub-section 3.9, this statistical measure can be used to quantify how much of the variance in the EWF measurements is explainable by the variance in stress. It is directly tied to the variance of the error-term in the linear regression model. Values of  $R^2$  close to 1, where  $R^2$  is the empirical estimator of the square of the correlation, indicate that

a good estimate of the stress can be obtained with only few measurements of the EWF at the unknown stress level<sup>18</sup>.

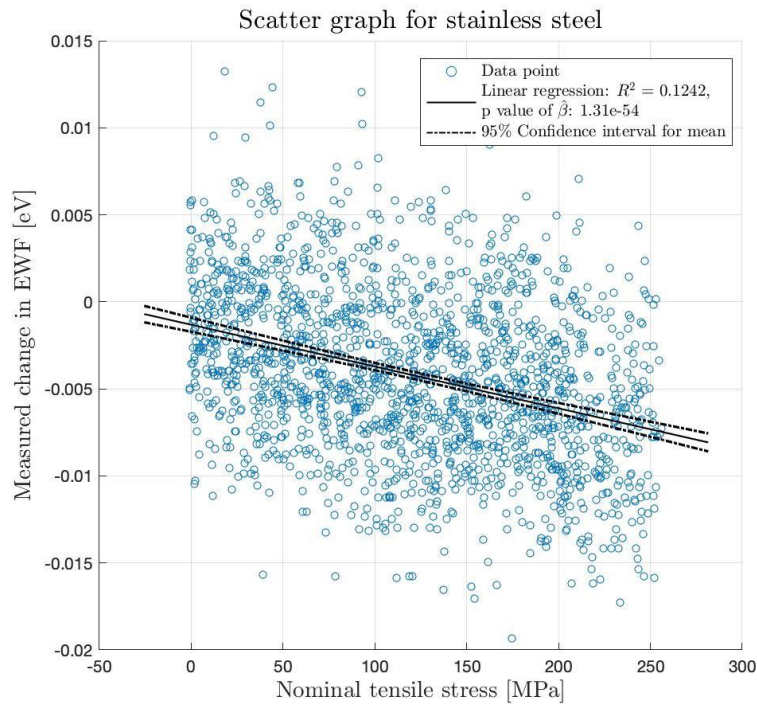


Figure 4.6 Scatter graphs for stainless steel showing significant linear relationship, but low correlation

Regrettably, correlation tends to be low for the experimental data. Some few experiments show a very high degree of correlation, but as will be discussed in the next sub-section, these tend to be associated with a problem compromising the data's reliability. It will be necessary to address the low correlation; imagine the following scenario: For a piece of metal, the difference in stress between two states is to be found. For state one and state two a set of EWF measurements is available. It is known that the correlation between EWF and stress is low. The question of whether a decently accurate estimation of the difference in stress between state one and state two is possible may be answered with yes. To do so, however, a large number of EWF measurements for both states is required.

The statistical reasoning behind this is that with many EWF measurements for each state, the chances are high that the respective averages of the two sets lie close to their responding population means. The EWF's population mean at a given stress is, due to the given model, linearly related to the stress. Given the number of EWF measurements is high enough, arbitrary accuracy in identifying the stress changes between the states is in theory attainable. Even when the correlation is low, one can be very confident about the value of the mean EWF at some given stress value, if only enough data is available. To visualise this, a 95% confidence interval for the mean has been placed around the regression line for all the sets of experimental data.

<sup>18</sup> Of course, what has been discussed in sub-section 4.1.1 still applies: All that is being considered for now are cases where the stress actually does change

Averaging can technically be used to compensate for low correlation. To show this, the following example calculation is presented. It uses the data from stainless steel shown above and assumes, for the sake of simplicity, the linear regression model to be accurate. Suppose two sets of EWF measurements are available: at 0 and at 100 MPa. How many measurements are needed, if in 90% of cases, the change in stress should be detected to be  $100 \pm 25$  MPa?

The appendix shows how the relevant formula can be derived. Information from [15] is used in the process.

$$n = \frac{2 z_{0.05}^2 \sigma^2}{\beta^2 a^2} \quad (4.1)$$

he standard deviation sigma is taken to be the root mean squared error of the linear regression model for stainless steel: 0.0045.  $z_{0.05}$  is the 5% quantile of the standard normal distribution, known to be 1.645 [15].  $\beta$ , for now assumed to be identical to  $\hat{\beta}$ , is  $-2.4106 \cdot 10^{-5}$ .  $a$  is half of the range which the detected stress is allowed, so 25 MPa.

The result is that 302 EWF measurements would be necessary for each state. The current version of the FKP logs one EWF measurement per second. Hence, it would take about 10 minutes in total to collect all the necessary EWF measurements for the two states. This is not impossible to do, but long measuring times reduce the practicality of such a stress measuring device. Further, they imply that quick fluctuations in stress cannot be registered accurately. One way of explaining why the calculation above calls for so many EWF measurements is that 100 MPa of difference in stress correspond to only  $100 \text{ MPa} \cdot \beta = 100 \text{ MPa} \cdot 2.4106 \cdot 10^{-5} \frac{\text{eV}}{\text{MPa}} \cong 2.41 \text{ meV}$  of difference in work function, according to the experiment shown above. To register changes in EWF this small, the EWF readings of the probe must either be very accurate or many measurements must be made. It is feasible to optimise the FKP for the task of stress measurement in such a way that maximum accuracy is attained, which may lie lower than the 4.5 meV of standard deviation shown in the experiment with stainless steel. However, use in the field typically implies greater influence from sources of error than in a lab environment.

The example calculation above has been performed only for stainless steel, though the formula shown could be applied with any sample. Inverting the EWF stress relationship and deducing a change in stress from two sets of EWF measurements is always possible, though when EWF and stress only show a low correlation, many EWF measurements may be needed, negatively impacting practicality.

#### 4.1.5 Likely mechanisms connecting EWF and stress

With all samples except the ones showing “deviant first tests” a seemingly unconditioned, significant linear relationship between EWF and stress exists. It can be shown that this relationship is unlikely to occur due to the uneven mapping of time on the EWF-stress plane. It can also be demonstrated that the relationship is invertible, be it at the cost of having to take many EWF measurements. What remains to be discussed is why this relationship might arise. This is important for deciding whether this phenomenon is likely to be connected to this particular experimental set-up or if it indicates a relationship than can be exploited in a practical context.

A review of the literature (see section 2.2, page 14) offers several plausible mechanisms, among them the idea that straining a metal crystal will change the EWF because the shape of the primitive unit cell

is altered and the effective potential on the surface changes [9] [11]. The same source makes the prediction that the relationship between EWF and stress should hence be linear. One may discuss how well this is reflected in the experimental data.

Within the current work, all samples were fitted with a simple linear regression. As noted in the previous sub-section, the correlation is typically low. However, this should not necessarily be taken to indicate that a linear regression model is not appropriate. A visual inspection, take the graph for stainless steel (Figure 4.6, page 42) as an example, shows that for most samples<sup>19</sup>, the data points are spread evenly on both sides of the regression line and the width of their spread does not appear to change greatly for the entire range of stress values. Even omitting a more thorough statistical analysis employing residual plots and the comparison of different regression models it may still be appropriate to comment that quadratic regression line, for instance, does not seem to fit better for most experiments. Data from one of the experiments on polished steel, see below, seems to represent an exception. The reasons for this are not clear. A quadratic model would be expected if the EWF was dependent on the work done during the elastic deformation of the metal. In the early stages of the project, estimating calculations were made based on this thought.

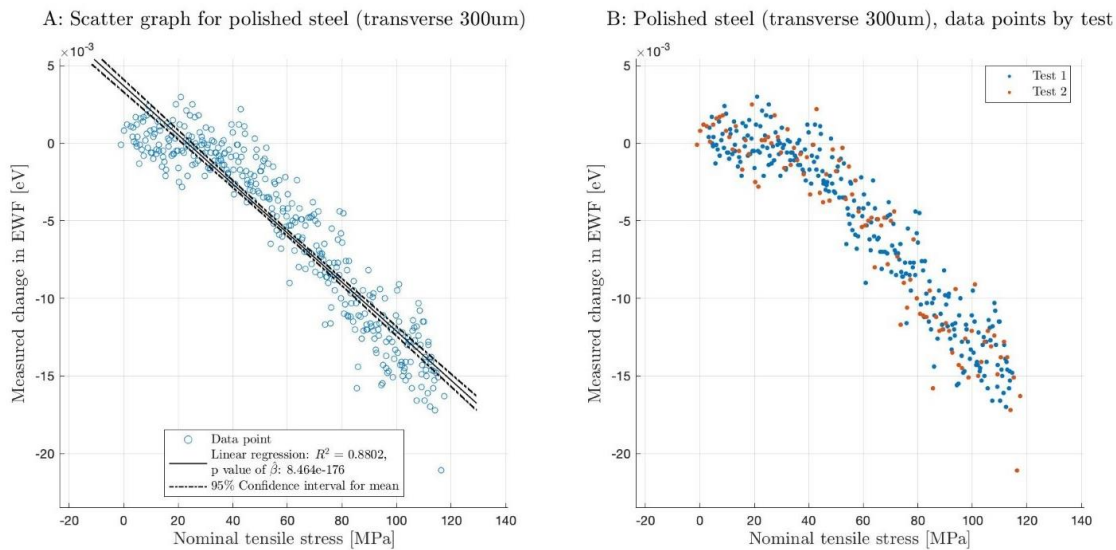


Figure 4.7 Polished steel, strained transversally, initial distance sample-probe 300  $\mu\text{m}$

*This is the only sample that shows a pattern more akin to a quadratic relationship between EWF and stress*

A rational model could also be considered. In an ideal parallel plate capacitor, the capacitance changes with one over the distance between the plates. Indeed, two experiments under suspicion of having been heavily impacted by changes in the sample-probe distance show this pattern: unpainted aluminium at 50

<sup>19</sup> Excluding the ones that portray “deviant first tests”

$\mu\text{m}$  (see Figure 4.8) and  $100\ \mu\text{m}$ . Note that the latter shows “drift”, making it hard to fit any kind of model.

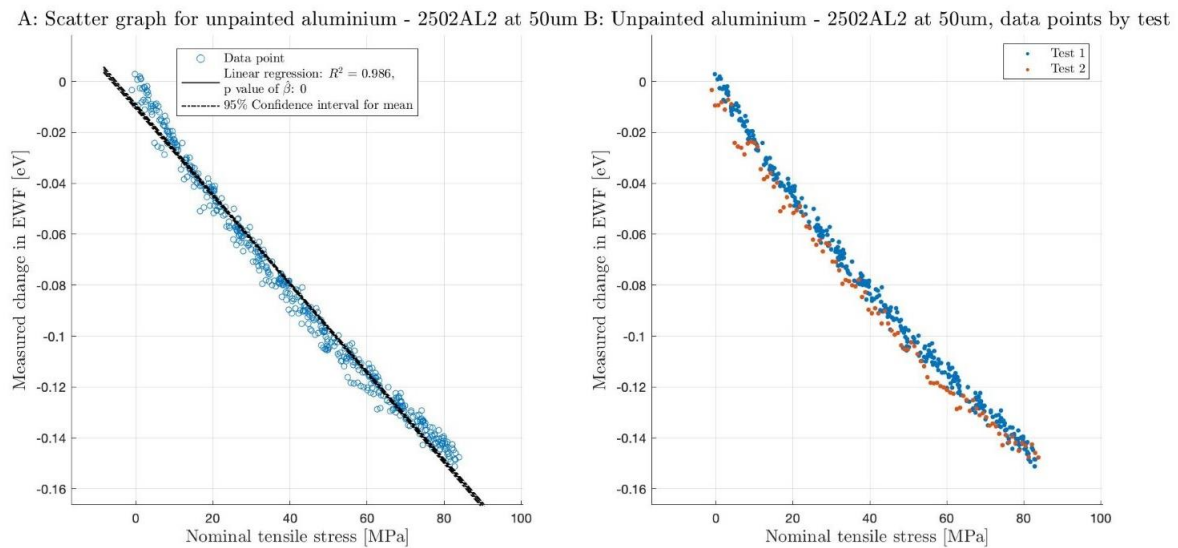


Figure 4.8 Unpainted Al at an initial sample-probe distance of  $50\ \mu\text{m}$ .

*Note the slight curve in the pattern drawn out by the data. Also note the high level of correlation. This experiment has likely been strongly influenced by a changing sample-probe distance.*

Thus, except for the named two cases of unpainted aluminium, the sample of polished steel (Figure 4.7) and those experiments characterised by a “deviant first test”<sup>20</sup> the linear regression model appears appropriate. It is not obvious that another model would be a better choice, the low correlation values seem to stem from the inherent variation in EWF when applied stress is chosen as the explanatory variable. Hence, the predictions made by the model of crystal deformation cannot be said to be inaccurate on a general level, but there are seemingly exceptions to its applicability.

Another model offered by the literature (see section 2.2, page 14) is the one of topography change under elastic deformation. An experiment had been designed based on this model. Polished steel samples were manufactured such that their topographical ridges are oriented in a preferential direction. Regrettably, the results are not of high quality; the day these experiments were performed, the FKP was particularly prone to allowing variations in sample-probe distance influence the readings. It does not seem justified to draw conclusions from the graphs.

This leads over to a discussion of the factor that is perhaps the most influential in mediating the EWF stress relationship in the experiments performed for the current work: Sample-probe distance. To better understand the dynamics of this effect, consider the sample of unpainted aluminium at different distances:  $50\ \mu\text{m}$  (Figure 4.8),  $100\ \mu\text{m}$  (Figure 4.2, page 37),  $250\ \mu\text{m}$  (Figure 4.9) and  $1\ \text{mm}$  (Figure

<sup>20</sup> Painted aluminium 1602AL1 and 2502AL1; Painted steel: 2502ST1; Unpainted steel: 0403ST2 and 1803ST1; Brass 1602BR1 (experiment 1)

4.10). While very close to the sample, the correlation between EWF and stress is impressive. However, as the probe is moved away from the sample, the pattern begins to transform. At 1 mm of distance, what is left may perhaps be called “drift”, something that already began to show at 100 μm of distance. Certainly, the connection between EWF and stress is much less pronounced, and this is not just due to more noise as one might expect from a greater sample-probe distance. The pattern changed fundamentally.

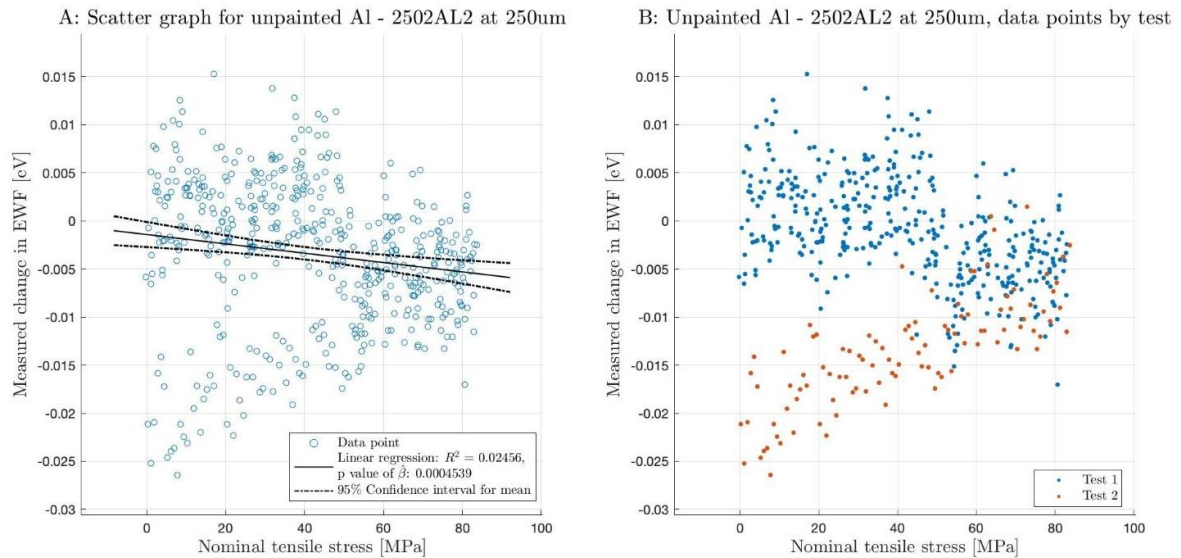


Figure 4.9 Unpainted Al at 250 μm initial distance

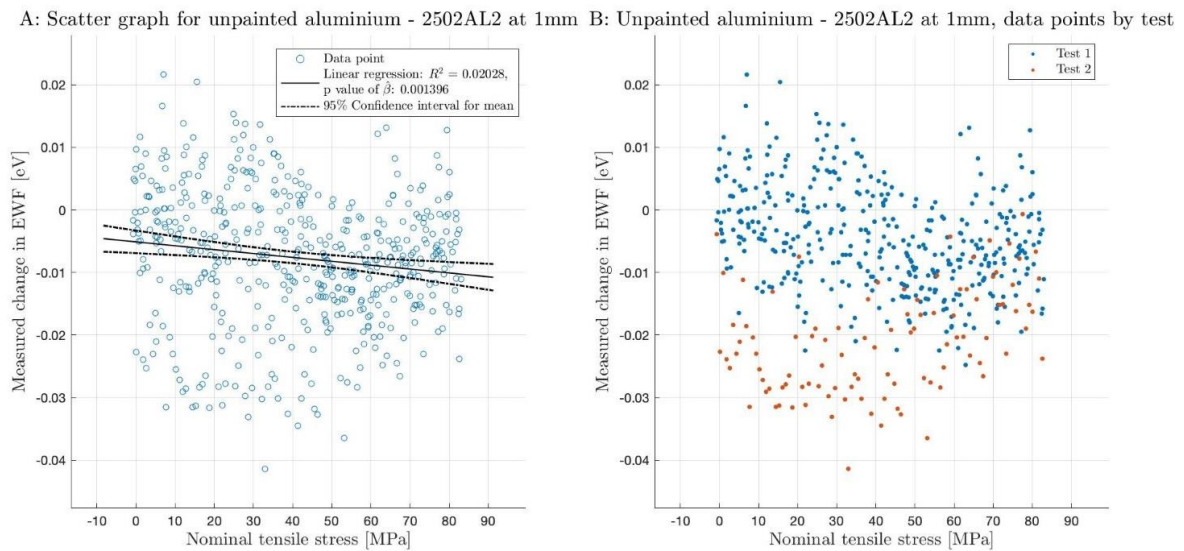


Figure 4.10 Unpainted aluminium at 1 mm initial distance

Not only is it so that the initial sample-probe distance has a great effect on the pattern, particularly while within about 100  $\mu\text{m}$  of the sample, but during this experiment, it was also shown that the sample-probe distance varied during each test. Under load, the probe would be about  $50 \pm 25 \mu\text{m}$  further away from the sample than in the unloaded state. It is this variation of the distance during each test that appears to be responsible for the strong correlation between EWF and stress, when the sample-probe distance is small. Note also that it is unlikely that the transversal contraction of the sample is responsible for this change of distance during each test. A distance change of some 50  $\mu\text{m}$  must have its origins in some shift of the geometry of the testing machine or the rig supporting the probe, but clear answers were not obtainable. The effect showed during some of the experiments but during others it was absent. Once, it would even disappear from one test to the next after simply turning the same sample  $180^\circ$  and reinserting it into the machine. The fact that for experiments portraying “deviant first tests” show no significant linear relationship after the removal of test 1 too shows that distance changes must be of varying pertinence. Otherwise, an unconditional, significant linear relationship would be expected for all experiments

A particularly noteworthy occasion on which the sample-probe distance effect has most likely shown is the day experiments were conducted on stainless steel, painted steel and brass. All three metals showed a non-conditional, linear relationship between EWF and stress with no “drift” (see Figure 4.11, Figure 4.6, page 42, Figure 4.3 page 38). In and of itself these are very promising results and at this stage in the analysis process (see Figure 4.1, flowchart, page 36) these are some of the most interesting sets of data left. However, the fact that three different kinds of metals showed a very similar pattern and one of them, painted steel, had not shown anything akin to it earlier, is perhaps reason enough for the suspicion that the experimental set-up might have been responsible. Indeed, that day, the FKP was closer to the samples than it had been before. Testing the sample-probe distance between tests is something that was only started after the experimental series on unpainted aluminium referred to earlier. For the tests of 25\_03\_ST1, 16\_02\_SST and 16\_02\_BR experiment 2, no data on the sample-probe distance is available and it cannot be stated to what extent sample-probe distance is the factor responsible for these measurements.

It is highly regrettable that these, some of the most expressive results, must be branded with the label of ambiguity. Doing so is inevitable, however, also because another experiment conducted on the same sample of brass found the gradient of the linear regression line to be about 10 times lower. In this second experiment (Figure 4.12), an attempt was made to reduce the influence of distance variations by linking the FKP directly to the sample. This approach, though, was prone to inaccuracies for several reasons (see section 3.8) and cannot be taken to have produced entirely reliable results either. It seems very likely though that the brass sample is susceptible to distance changes. Experiment 3 on this sample, where the distance was measured to have changed by  $50 \pm 25 \mu\text{m}$ , even showed a linear increase of EWF with increasing stress (Figure 4.13). More data would be needed to clarify the situation.

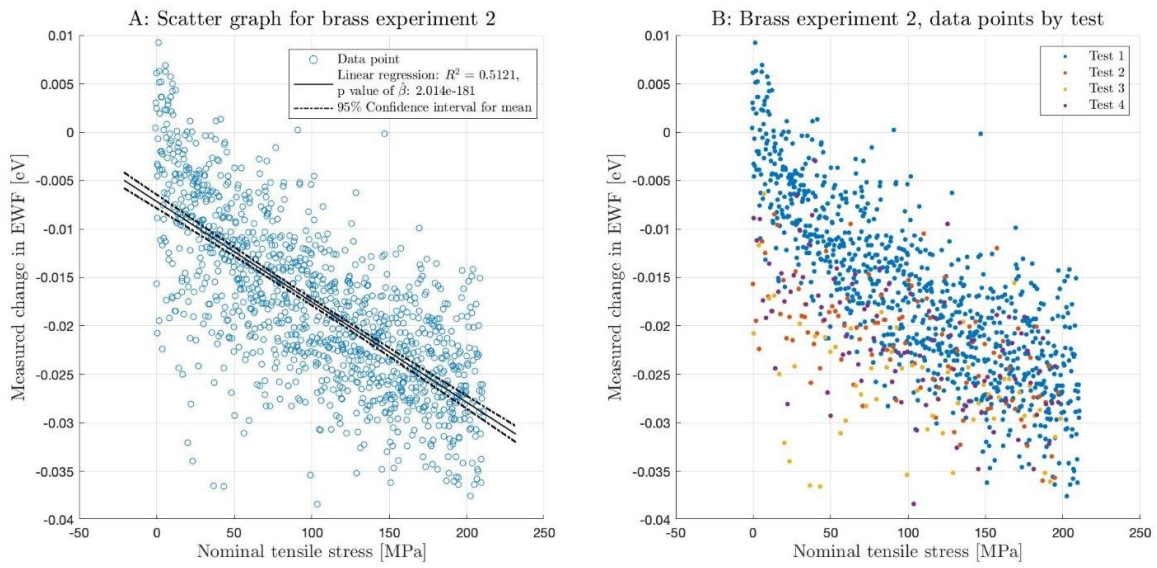


Figure 4.11 Second experiments on brass

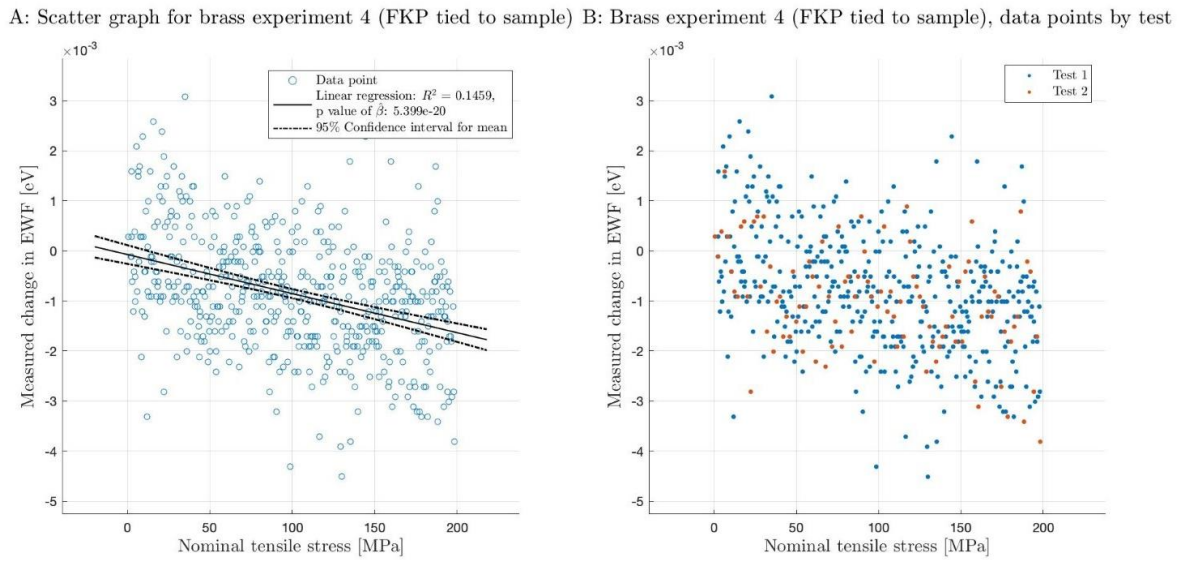


Figure 4.12 Brass, experiment 4. FKP is tied to the sample



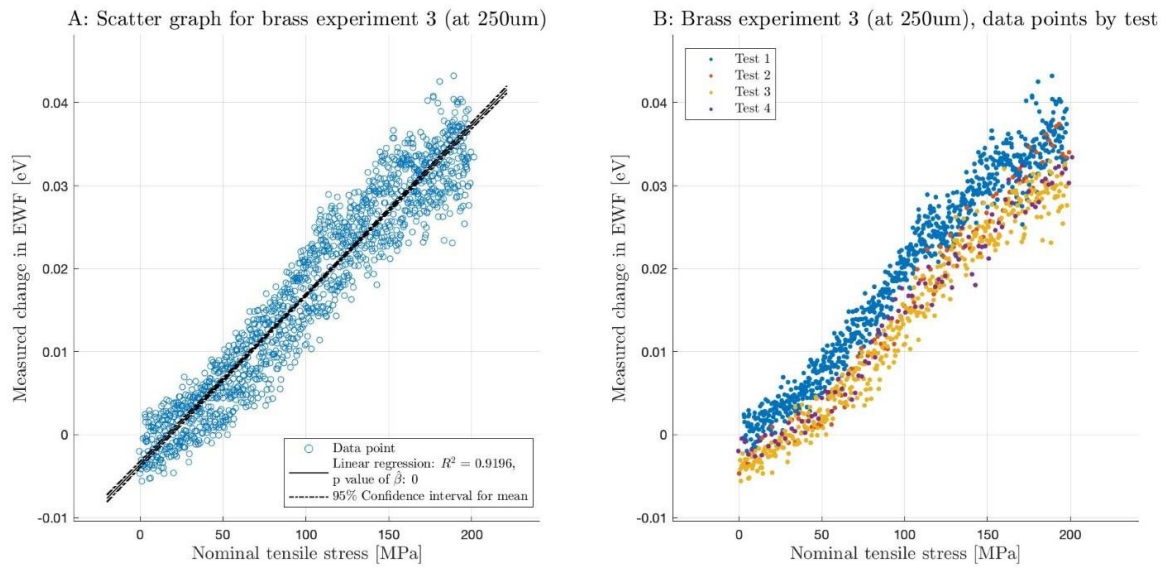


Figure 4.13 Brass, experiment 3. The distance varied by about 50 μm during the test. The result is very dubitable

Due to the great impact sample-probe distance could apparently have on the EWF readings, attempts were made to quantify the magnitude of these influences at different distances. The chapter on methodology has presented the way by which these measurements were made, these are the results:

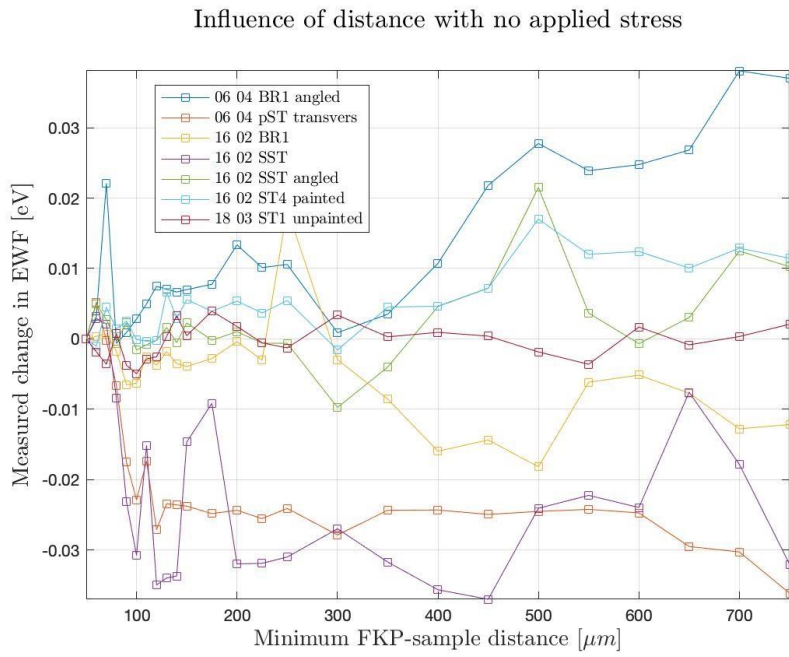


Figure 4.14 Influence of distance; range narrow, overview

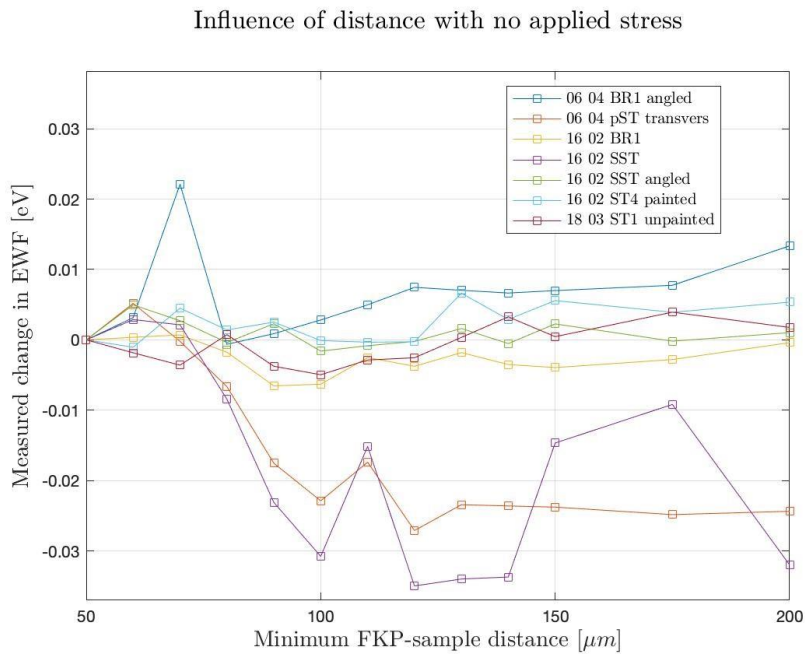


Figure 4.15 Influence of distance; range narrow, detail

Influence of distance with no applied stress

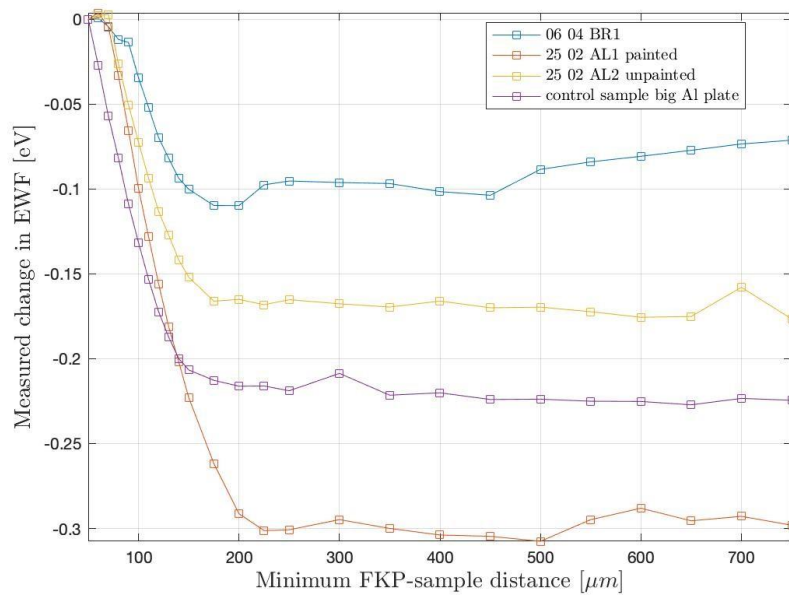


Figure 4.16 Influence of distance; wide range, overview

Influence of distance with no applied stress

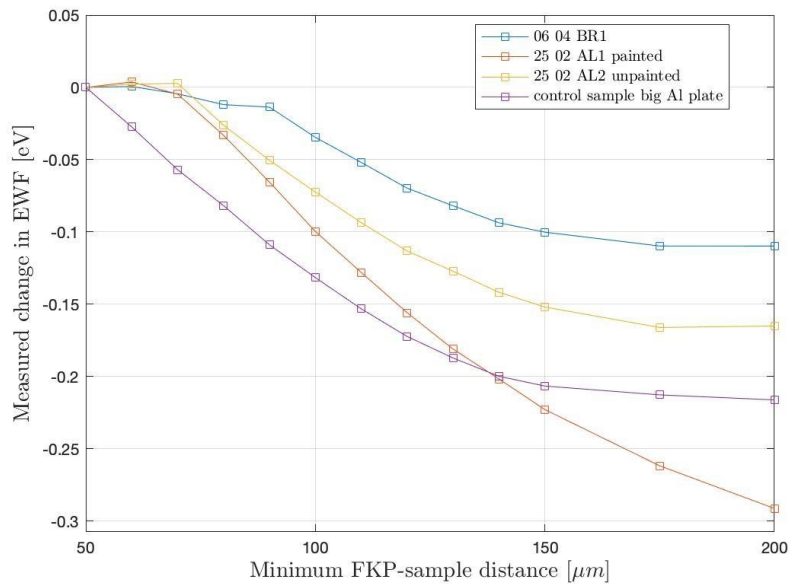


Figure 4.17 Influence of distance; wide range, detail

Several interesting trends can be observed. Note, for instance, that every sample appears to have at least a range where its EWF varies little with varying distance. For the samples in Figure 4.14 this would be between about 100 and 200 μm, except for the sample of unpainted steel, which appears to be most

stable between 0.5 and 0.6 mm. Some samples also show a distinct “levelling-out” effect: polished steel, brass 16\_02\_BR1, painted and unpainted aluminium, and another aluminium plate that was added as an additional sample for reference. Note that the different samples reacting differently to changes in distance is not contrary to the explanation given for the distance effect in section 2.2. Different materials lead to different Volta potentials between probe and sample and hence the displacement current would vary differently with distance. The fact that the graphs for the various samples appear to spread apart at greater distances in Figure 4.14 and to a lesser degree in Figure 4.16, though also note the bigger scale of Figure 4.16, may have to do with the fact that the variance in the EWF measurements can be expected to increase with distance.

The initial idea was to use these results to be able to adapt the sample-probe distance in such a way for each material tested that variations of distance could be expected to have a minimal impact on the results. However, it soon became apparent that the patterns shown above do not relate to the FKP in general, but to the momentary settings on one individual FKP. Since the data was collected with a different FKP than the one used for conducting the experiments and, additionally, the settings on the experimental FKP changed after a service, the data above is of very limited practical use.

Change in sample-probe distance proved to be an elusive and yet impactful effect. Its inconsistent appearance and unquantified dependence on the initial sample-probe distance makes it very hard to tell which sets of experimental data are influenced by it and which are not. The most promising data that would have otherwise been left after the last decision gate (see Figure 4.1, page 36) must now be viewed as ambiguous: all experiments on 1602BR1, 1602SST, and 2503ST1. Potentially, they are explainable by a factor that would not allow the results to be generalised beyond these experiments and hence this evidence cannot be counted on to fulfil the *necessary condition* (subsection 4.1.1, page 34). The sample of unpainted aluminium cannot be taken to pass the last decision gate either, distance effects are strongly visible there. Experiments conducted with the FKP tied to the sample are not what the set-up has been designed for and include a lot of unknown factors, so counting on these would be somewhat deceptive. What remains is the data from two experiments: one with polished steel where, incidentally, no distance change was measured and thus at most 25  $\mu\text{m}$  of distance change in either direction could have occurred. The second is that of a painted aluminium sample that showed an unconditional, linear relationship with a positive slope and only a small tendency to “drift”. Distance effects are not impossible for this case either, but since the initial sample-probe distance was large, the chances are not as high as for most of the samples that have been discussed.

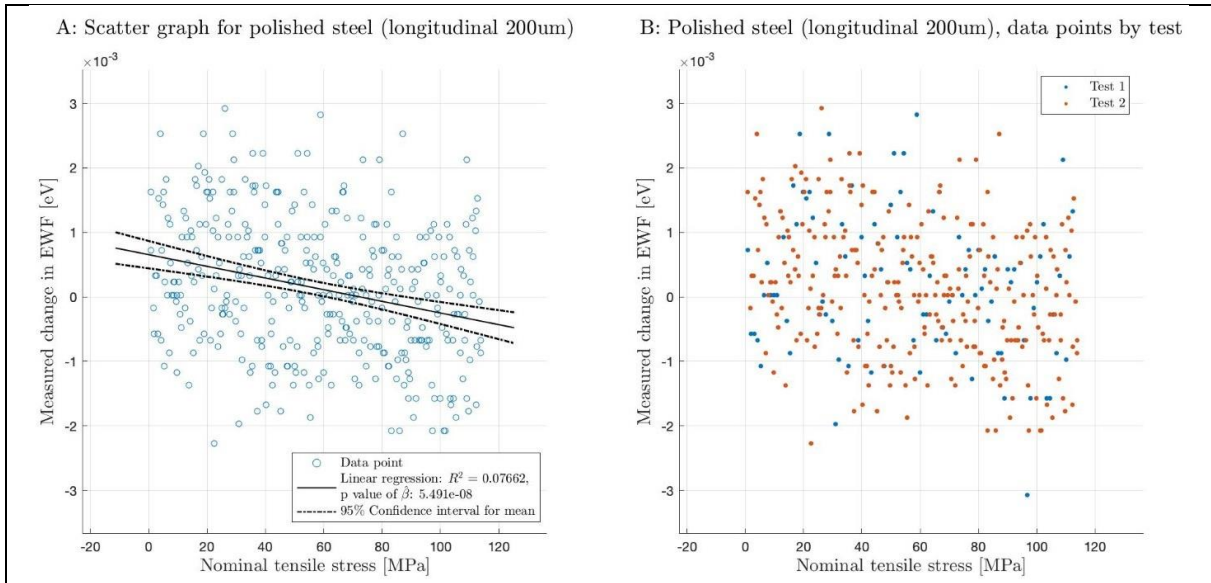


Figure 4.18 Remaining sample: polished steel with 200  $\mu\text{m}$  initial distance

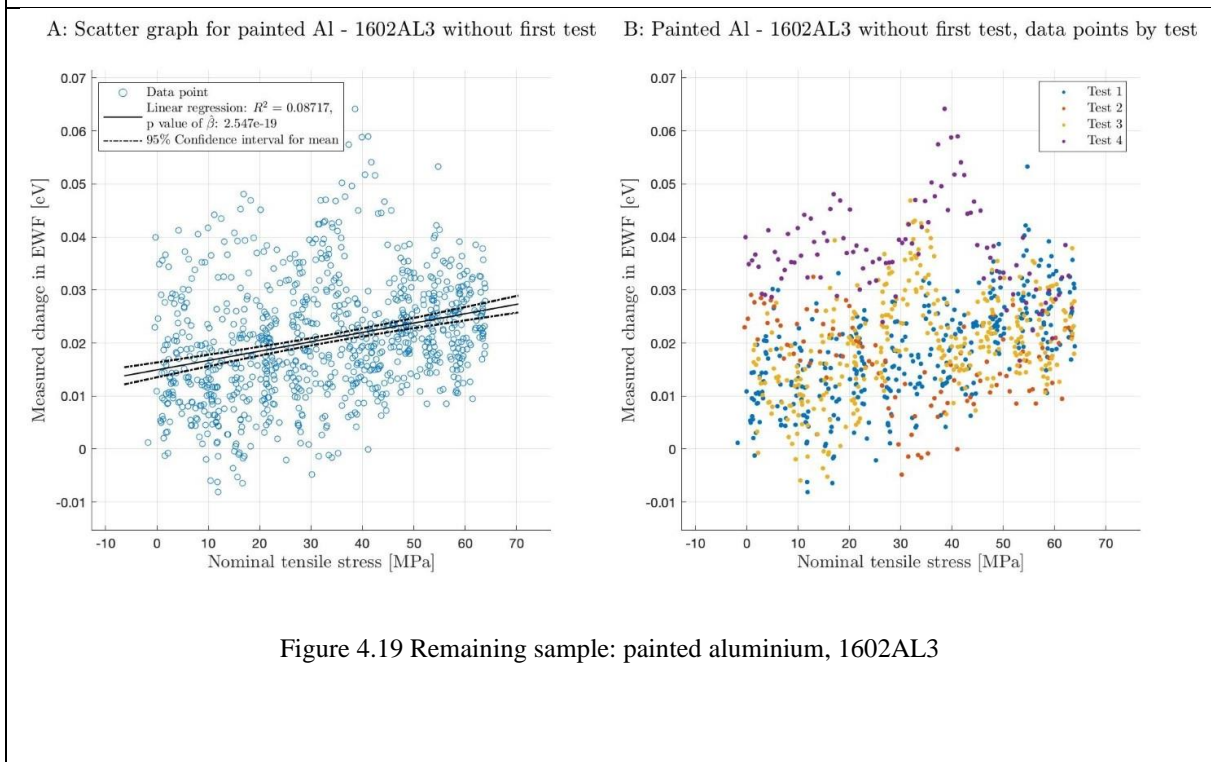


Figure 4.19 Remaining sample: painted aluminium, 1602AL3

As alluded to before, clear conclusions are not what the data inspires. Should any such be drawn with decent confidence, nothing but the zero-hypothesis can be asserted regarding the generalisability of the data. There is also lacking data to make meaningful statements about the extent to which topography changes mediate the relationship between EWF and stress. The predictions based on a model of crystal deformation were not found to be grossly inaccurate, but objections could be made in some cases.

#### **4.1.6 Summary**

The first subsection began by formulating a necessary condition for using the FKP to detect stress: *A significant relationship exists between the EWF and stress while stress is changed and this interconnection of stress and EWF is exploitable in contexts beyond this experiment.* From this, a line of argument was developed that could be applied to every set of experimental data, checking if it might support the fulfilment of the necessary condition. Several patterns began to crystallise in the process. “Drift”, characterised in sub-section 2, is portrayed by sets of data where individual tests within one experiment tend to diverge and time becomes an important factor in the analysis. A method was described to prevent the combination of drift and an uneven distribution of time across the tests of an experiment to masquerade as a genuine connection between EWF and stress. The next pattern, discussed in 4.1.3, was “deviant first tests”. An explanation was offered for the special behaviour of the first test, the rupture of an oxide layer, although not all the observations are explainable by this. Experiments portraying this pattern do not support the fulfilment of the necessary condition since the EWF-stress relationship is not significant without the first test. The question of invertibility was addressed in 4.1.4. It was found that low levels of correlation between EWF and stress can be compensated for in a practical application when more EWF measurements are taken. The increased measurement times may negatively impact practicality. Finally, the nature of the interconnection between EWF and stress was investigated to understand if the results are generalizable. As described in the previous paragraph, the dominant role of sample-probe distance changes effectively prevents confident positive statements about the fulfilment of the necessary condition.

## **4.2 OUTLOOK**

The results above may appear rather sobering. Continuing to investigate the possibility of an FKP-based stress-detection device is certainly still worthwhile and suggestions for further research will be made in the conclusion. Keeping the view on practical contexts, other promising applications could be discussed; several ideas have arisen during the project. The FKP has shown many talents that have not yet been fully exploited.

### **4.2.1 FKP for evaluating corrosion resistance**

The FKP has a strong background in corrosion science and it is with inspiration from that field that the following idea is presented: Using an FKP to quantify the risk of premature corrosion on critical components. Norce is currently involved in experiments concerning this and references to a similar application have been made in the literature [12].

A newly produced metal part will always show areas of varying EWF due to defects introduced by various manufacturing processes. This inhomogeneity can greatly accelerate corrosion [12]. If an FKP with its capability of scanning large areas could be used to monitor the EWF across the surface of newly produced parts, much more accurate predictions about their life span could be made. The quality of galvanisation coatings might also be characterised by an FKP.

#### 4.2.2 FKP for detecting overload

This idea may be novel. It builds on two basic observations. The literature review (see chapter 2.2, page 14) has shown that there is a great change of EWF upon entering the plastic deformation regime of a metal. Within the current work, the pattern of “deviant first tests” could be taken as an indication that the FKP can detect the first time a new maximum load is applied to the sample, be it due to changes in the oxide layer or some other effect. With these capabilities, the FKP could perhaps be developed into a tool for detecting permanent damage to a component due overload.

Suppose a valuable, precisely machined component with accurately defined material properties is to be assembled but right before this can happen, it is dropped inadvertently. The question of whether this component can still be used may be hard to answer and a tool like the FKP may prove to have great utility. Detecting very small amounts of plastic deformation in a component with complex geometry may require many delicate measurements, which could perhaps be replaced by few passes with an FKP. Overload can also occur in operation and in the aerospace industry, where components are often underdimensioned due to weight reasons, evaluating the quality of a part after overload may be very valuable. The FKP’s capability of being able to make measurements despite of layers of paint between the probe and the sample once more greatly facilitates its application.

#### 4.2.3 FKP for early detection of fatigue

Failures due to fatigue may cause great damage and detecting fatigue in its very early stages can be vital for preventing these. The FKP technology may prove to be valuable in this context for several reasons: The EWF changes with the surface interface of a metal [3] and hence also with its topography [13]. It is not at all unlikely that even small cracks on the surface of a metal would produce significant changes in the EWF. Additionally, a kelvin probe can make measurements through a layer of paint and the FKP has been specifically designed to scan large surface areas in comparatively little time. Furthermore, areas of a metal part that show particularly high degrees of work hardening may also present a different EWF, since dislocation density has a great influence on the reading [10].

It is imaginable that the FKP could be used to scan susceptible areas on critical mechanical components. When, during one of the regular inspections, certain characteristic features begin to appear on the EWF map of the surface, a warning can be issued. This way, the operational load on the component can be reduced or it can be replaced long before failure would occur. No mention of a Kelvin probe that was used in this way has been found in the literature that was reviewed for the current work. It may be a novel approach.

The variety of these possible applications showcases that the technology has not yet reached its limits by far. What is challenging in working with EWF, the fact that so much influences it, is also what makes this measure potentially so powerful. It is this kind of work that needs to be done, work in small steps, to someday be able to interpret and technologically exploit effects of changing EWF. Working to overcoming the difficulties posed by research in this field is worth the effort.

## 5. CONCLUSIONS AND FURTHER WORK

In the current work, the potential relationship between the EWF and the tensile stress in various metals was experimentally investigated. Stress was varied within the elastic range and the EWF was measured by an FKP.

The EWF appeared to be linked to the stress in some situations. However, it was found that changes in sample-probe distance occurring during the experiments had a dominant effect on the EWF readings of the FKP. It is not clear from the data whether any connection between EWF and stress exists independent of distance changes. Hence, no affirmative claim can be made regarding the possibility of using the current version of the FKP as a stress-detection device.

Further work evaluating this application of the FKP would profit from:

1. An effective way of controlling the impact of changes in sample-probe distance
2. An investigation of the possible relationship between compression stress and EWF
3. An investigation of the possible relationship between tensile stress in the plastic regime and EWF
4. The comparison of various regression models when analysing the relationship between stress and EWF
5. A more extensive set of sample materials and a greater number of individual samples for each material

Further, the development of an FKP-based stress-measuring tool would also profit greatly from work dedicated to characterising the EWF maps of entire surfaces. It would need to be ascertained how patterns of corrosion, stress, varying topography, etc. manifest on such a map and how they could possibly be differentiated.

Perhaps even more promising might be the evaluation of one of the following applications from the FKP technology:

1. As a device for detecting fatigue in its early stages
2. As a device for detecting and evaluating the damages of mechanical overload
3. As a device for evaluating the corrosion resistance of an individual component



## Referances

- [1] A. Volta, "II. Of the method of rendering very sensible the weakest natural or artificial electricity," *The Royal Society's Philosophical Transactions*, vol. 72, pp. 7-35, 31 December 1782.
- [2] W. Thomson, "Contact Electricity of Metals," in *Mathematical and physical papers*, Cambridge, Cambridge University Press, 1898, pp. 110-147.
- [3] M. Rohwerder, "Scanning Kelvin Probe and Scanning Kelvin Probe Force Microscopy and their application in corrosion science," in *Analytical Methods in Corrosion Science (1st ed.)*, CRC Press, 2005, pp. 605-648.
- [4] INDIKEL, "The FKP Technology," 2019. [Online]. Available: <https://www.indikel.no/the-fkp-technology>. [Accessed 20 May 2022].
- [5] O. Vilitis, M. Rutkis, J. Busenberg and D. Merkulov, "Determination of Contact Potential Difference by the Kelvin Probe (part 1) I. Basic Principles of Measurements," *Latvian Journal of Physics and Technical Sciences*, April 2016.
- [6] S. H. Simon, *The Oxford Solid State Basics*, Oxford: Oxford University Press, 2013.
- [7] C. R. Nave, "Hyperphysics - Fermi level," 2017. [Online]. Available: <http://hyperphysics.phy-astr.gsu.edu/hbase/Solids/Fermi.html>. [Accessed 5 January 2022].
- [8] C. R. Nave, "Hyperphysics - Parallel Plate Capacitor," 2017. [Online]. Available: <http://hyperphysics.phy-astr.gsu.edu/hbase/electric/pplate.html>. [Accessed 29 May 2022].
- [9] A. V. Babich and V. V. Pogosov, "Effect of dielectric coating on the electron work function and the surface stress of a metal," *Surface Science*, vol. 603, no. 16, pp. 2393-2397, August 2009.
- [10] Y. Zhou, L. Q. Lu and W. G. Qin, "Change in the electronic work function under different loading conditions," *Materials Chemistry and Physics*, vol. 118, pp. 12-14, 2009.
- [11] A. Kiejna and V. Pogosov, "Simple theory of elastically deformed metals: Surface energy, stress, and work function," *Physical Review B*, vol. 62, no. 15, pp. 10445-10450, 15 October 2000.
- [12] A. Nazarov and D. Thierry, "Application of Volta potential mapping to determine metal surface defects," *Electrochimica Acta*, vol. 52, no. 27, pp. 7689-7696, 2007.
- [13] R. J. Wang, J. X. Li, Y. J. Su, L. J. Qiao and A. A. Volinsky, "Changes of work function in different deformation stage for 2205 duplex stainless steel by SKPFM," *Procedia Materials Science* 3, vol. 3, pp. 1736-1741, 2014.
- [14] N. F. Casales, A. Nazarov, F. Vucko, R. Pettersson and D. Thierry, "Influence of Mechanical Stress on the Potential Distribution on a 301 LN Stainless Steel Surface," *Journal of The Electrochemical Society*, vol. 162, no. 9, pp. C465-C472, 2015.
- [15] Ø. Kristensen and A. Wikan, *Sannsynlighetsregning og statistikk for høyere utdanning (2. utgave)*, Bergen: Fagbokforlaget, 2019.
- [16] McGraw-Hill Concise Encyclopedia of Physics, "Work function (thermodynamics)," 2002. [Online]. Available: <https://encyclopedia2.thefreedictionary.com/work+functions>. [Accessed 31 March 2022].

- [17] A. H. Sandtorv, *Kjemi for ingeniører*, Oslo: Universitetsforlaget, 2021.
- [18] W. D. J. Callister and D. G. Tethwisch, *Callister's Materials Science and Engineering* (10th ed), John Wiley & Sons (Asia) Pte Ltd, 2015.
- [19] L. A. Jordanger, *Linear regression - summary of a lecture*, 2022.

## List of figures

Figure 2.1 Illustration potential energy .....	4
Figure 2.2 Extracting one electron from an electrostatically neutral sample in a vacuum .....	5
Figure 2.3 Two metals, not yet connected.....	7
Figure 2.4 Two connected metals with dissimilar EWF .....	8
Figure 2.5 Illustration showing skew vacuum condition.....	9
Figure 2.6 Illustration off-nulling method.....	11
Figure 2.7 Variation in EWF of Al; from Zhou et al.....	15
Figure 2.8 Variations in the EWF of Cu; from Zhou et al. ....	15
Figure 2.9 Surface topography along scan line; from Wang et al. ....	18
Figure 2.10 Surface topography, surface potential for stainless steel 9% elongated; from Wang et al. ....	19
Figure 2.11 EWF of Al, plastic region, various strain rates; from Zhou et al. ....	20
Figure 3.1 Three materials tested in the vice. Descending order: Cu, brass, Al.....	24
Figure 3.2 Test set-up with vice, FKP and camera microscope .....	25
Figure 3.3 Test set-up vice from above .....	25
Figure 3.4 Selection of tensile samples .....	28
Figure 3.5 Brass sample in tesing machine; FKP to the left, attached to improved rig .....	29
Figure 3.6 Instron tensile testing machine with inserted sample and mounted FKP.....	29
Figure 3.7 Rig used for distance testing; FKP suspended from computer-controlled frame; sample supported by steel blocks .....	31
Figure 3.8 Close-up FKP and brass sample; starting point for experiment 50 $\mu\text{m}$ initial distance .....	31
Figure 4.1 Overarching line of argument for section 4.1 as flowchart.....	36
Figure 4.2 Graph showing divergence of individual tests .....	37
Figure 4.3 A sample of painted steel, 2503ST1, showing drift where tests still lie close together .....	38
Figure 4.4 Time domain for experiment on 2503ST1 .....	39
Figure 4.5 1602AL1 painted aluminium - example of a "deviant first test" .....	40
Figure 4.6 Scatter graphs for stainless steel showing significant linear relationship, but low correlation .....	42
Figure 4.7 Polished steel, strained transversally, initial distance sample-probe 300 $\mu\text{m}$ .....	44

Figure 4.8 Unpainted Al at an initial sample-probe distance of 50 $\mu\text{m}$ . .....	45
Figure 4.9 Unpainted Al at 250 $\mu\text{m}$ initial distance .....	46
Figure 4.10 Unpainted aluminium at 1 mm initial distance .....	46
Figure 4.11 Second experiments on brass .....	48
Figure 4.12 Brass, experiment 4. FKP is tied to the sample .....	48
Figure 4.13 Brass, experiment 3. The distance varied by about 50 $\mu\text{m}$ during the test. The result is very dubitable .....	49
Figure 4.14 Influence of distance; range narrow, overview .....	50
Figure 4.15 Influence of distance; range narrow, detail .....	50
Figure 4.16 Influence of distance; wide range, overview.....	51
Figure 4.17 Influence of distance; wide range, detail .....	51
Figure 4.18 Remaining sample: polished steel with 200 $\mu\text{m}$ initial distance .....	53
Figure 4.19 Remaining sample: painted aluminium, 1602AL3 .....	53

## Appendix A1: Codes written for data analysis

A brief statement will be given with each piece of code describing its function in the project. The codes themselves include comments should the reader wish to form a detailed picture of their workings.

### CONVERTING FILES FROM FKP

This code was written to convert the .txt files from the FKP into .csv files that could be directly manipulated in Excel. Some unnecessary columns of data were removed along the way.

```
import csv

# change name of target file to parse. You may also need to change the directory
with open("KelvinProbeLog_25032022_145704_BR_second_test.txt", "r") as data_file:
    data_read = csv.reader(data_file, delimiter=" ")

    # change name of csv file that is to be created
    with open ("FKP_log_BR_seciond_test.csv", "w") as output_file:
        data_write = csv.writer(output_file)
        data_write.writerow(["date", "time", "tag", "sample", "reference"])
        for line in data_read:
            data_write.writerow(line[0:5])
```

### CONVERTING FILES FROM INSTRON

The tensile testing machine already produces files in a .csv format. However, it logs 100 data points per second, whereas the FKP only logs one. Hence, what is of interest is only the forces measured at every full second. The very long headers were also removed from the file.

```
import csv

# change name of target file to parse. You may also need to change the directory
with open("Specimen_RawData_2.csv", "r") as data_file:
    data_read = csv.reader(data_file, delimiter=";")

    # change name of csv file that is to be created
    with open ("Force_sample_16_02_BR_1_test_13_05_nr_3.csv", "w") as output_file:
        data_write = csv.writer(output_file)
        for i in range(10):
            next(data_read)
        u=0
        for line in data_read:
            time=str(line[0])
            time_value=time.replace(",",".")
            if float(time_value)>u-0.0001 and float(time_value)<u+0.0001:
                force_content=str(line[1])
                force=float(force_content.replace(",","."))
                takeaway=[force/1000]
                data_write.writerow(takeaway)
                u+=1
```

## DISTANCE EXPERIMENTS

This was the most extensive Python code written for the project. The function is sketched out in chapter 4 of the report. It is subdivided into three functions. The last function calls the two previous ones. Please excuse the small print.

```
import csv

def make_csv_file(FKPinput : str) -> str :
    """Takes raw output file of desktop FKP and turns it into
    readable csv file. Also outputs name of said file"""

    # The .txt file better be in the current directory
    with open(FKPinput, "r") as data_file:
        data_read = csv.reader(data_file, delimiter=" ")

        # The format of the csv file is with commas as decimals and
        # semi-colons to separate the values. That is the format my Excel version is most compatible with.
        # The name for the csv file will be its old name minus the first characters (that indicate date and so on).
        # "FKP" will be put in front of the old name and of course the suffix will be changed
        csv_file_name="FKP"+FKPinput[11:]
        csv_file_name=csv_file_name[:-4]+".csv"
        with open (csv_file_name, "w") as output_file:
            data_write = csv.writer(output_file, delimiter=";")
            data_write.writerow([ "time", "sample raw", "sample average", "reference raw", "reference average"])
            for line in data_read:
                newline=[line[3].replace(".", ":"), line[4], line[5],line[6], line[7]]
                data_write.writerow(newline)

        #output the name of the created csv file so that I can easily use it in the next function
        return csv_file_name

def get_times(name_log_file : str) -> list:
    """Takes log file and turns it into a list of time stams when the wait steps started"""

    times_wait_steps=[]
    with open(name_log_file, "r") as log_file:
        content_log = csv.reader(log_file, delimiter=" ")
        for line in content_log:
            #I am interested in the steps with odd numbers. Those are the waiting steps. The step number is,
            #in this kind of log file the 5th entry, if it is there.
            if line[5].isdigit() and int(line[5])%2==1:
                timestamp=line[1].replace(".",":",2)
                #The seconds are rounded up if the first decimal of a second is more than 5 and rounded down to the
                #next whole second otherwise
                #Check tenth of a second (possible roll-over)
                if int(timestamp[9])>=5:
                    #Check second (possible roll-over to 10seconds)
                    if int(timestamp[7])==9:
                        #Check 10seconds (possible roll-over to minutes)
                        if int(timestamp[6])==5:
                            #Check single minutes (possible roll-over to 10 minutes)
                            if int(timestamp[4])==9:
                                #Check 10 minutes (possible roll-over to single hours)
                                if int(timestamp[3])==5:
                                    #Check hours (possible roll-over to 10 hours)
                                    if int(timestamp[1])==9:
                                        timestamp=str(int(timestamp[0])+1)+"0:00:00"
                                    else:
                                        timestamp=timestamp[0]+str(int(timestamp[1])+1)+":00:00"
                                else:
                                    timestamp=timestamp[0:3]+str(int(timestamp[3])+1)+"0:00"
                            else:
                                timestamp=timestamp[0:4]+str(int(timestamp[4])+1)+":00"
                        else:
                            timestamp=timestamp[0:6]+str(int(timestamp[6])+1)+"0"
                    else:
                        timestamp=timestamp[0:7]+str(int(timestamp[7])+1)
                else:
                    timestamp=timestamp[0:8]
                times_wait_steps.append(timestamp)
    return times_wait_steps
```

```

def make_distance_vs_potential_csv(FKPinput:str, name_log_file:str) -> None:
    """Takes in name of raw .txt file and .log file and creates a finished distance_vs_potential csv list"""

    #Forming distances column (um)
    distance=[]
    for i in range(11):
        distance.append(50+10*i)
    for i in range(1,5):
        distance.append(distance[-1]+25)
    for i in range(1,11):
        distance.append(distance[-1]+50)

    #calling function to make traditional parced .csv file from .txt file
    csv_file_name = make_csv_file(FKPinput)

    #calling function to get time stamps
    timestamps = get_times(name_log_file)

    #reading the csv file created by function "make_csv_file". Make sure the delimiter is what you set it to be in the
    #function "make_csv_file"
    with open(csv_file_name,"r") as FKP_file:
        content_FKP_file = csv.reader(FKP_file, delimiter = ";")
        current_line=next(content_FKP_file)
        average=[]
        #averages of 8 measurements during wait steps
        for time in timestamps:
            running_sum=0
            i=0
            #Check if current line has a time stamp that is still below the time we look for. Too Early variable is
            #initiated as True
            TooEarly=True
            while TooEarly:
                current_line=next(content_FKP_file)
                current_time=current_line[0]
                if int(current_time[:2])>=int(time[:2]):
                    #When we can't tell by the hours already, we need to look at the minutes
                    if int(current_time[3:5])>=int(time[3:5]):
                        #When we can't tell by the minutes already, we need to look at the seconds
                        if int(current_time[6:8])>=int(time[6:8]):
                            #If we're at the right time or later, we do not iterate the line again and end the loop
                            TooEarly=False
                        else:
                            TooEarly=True
                    else:
                        TooEarly=True
                else:
                    TooEarly=True
            #Once you found the line with the right time stamp, iterate once more
            current_line=next(content_FKP_file)
            #Then do the summing and averaging...
            while i < 8:
                running_sum += float(current_line[1].replace(",","."))
                current_line=next(content_FKP_file)
                i+=1
            average.append(running_sum*0.125)

    #making output file
    output_file_name="Distance_vs_potential"+csv_file_name[7:]
    with open(output_file_name, "w") as output_file:
        data_write = csv.writer(output_file, delimiter=";")
        data_write.writerow(["distance (um)", "sample average 8 sec (V)"])
        for i in range(len(average)):
            data_write.writerow([distance[i],average[i]])

```

## MATLAB CODE: GRAPH FOR DISTANCE EXPERIMENTS

This code was used to graph the data from the distance experiments. The Python code above created the .csv files that were the input to this MatLab code. They, together with the code were stored in a folder of their own. This was so that the names and files did not have to be fed into the code manually but that the program could instead look for what was in the folder in which the code was run and access the files itself.

```

%%%%%%%%%   GRAPHING DISTNANCE DATA   %%%%%%%%%

dir_info = dir;
dir_info = struct2cell(dir_info);
number_of_graphs = 7;
figure_title = 'Influence of distance with no applied stress';
save_plots = 1;
x_upper = 200;
%Making the below true overrides the choice for the upper limit of x above
default_axes = 0;

data_name = cell(number_of_graphs,1);
generalfig=figure('Name', figure_title,'NumberTitle', 'off',...
    'Color', 'white');
if default_axes
    x_upper = inf;
end

%Should you add more files to the directory, change number of loops
for i=1:number_of_graphs
    names = dir_info{1,i+3};
    Dist_Pot = readtable(names);

    %Shortening down string of filename to get the name of the current sample
    names = names(30:end);
    names = erase(names,"_distance_50_to_750_steps_01.csv");
    names = erase(names,".csv");
    if strcmp(names(end-2:end),'_01')
        names = names(1:end-3);
    end
    names = strrep(names,'_',' ');
    data_name{i,1} = names;

    %Intersted in change in EWF. All graphs will be braught to common starting
    %point
    pot = zeros(height(Dist_Pot),1);
    for j=1:height(Dist_Pot)
        pot(j) = Dist_Pot{j,2} - Dist_Pot{1,2};
    end
    plot(Dist_Pot.(1),pot,'-s')
    hold on
end

```



```

grid on
legend(data_name,'fontsize',10,'Interpreter','latex','Location','best')
axis([-inf,x_upper,-inf,inf])
title(append(newline,figure_title,newline),'fontsize',16,'FontWeight',...
      'Bold','interpreter','latex')
xlabel('Minimum FKP-sample distance [ $\mu$  m]','...
      'fontsize',14,'interpreter','latex')
ylabel('Measured change in EWF [eV]','fontsize',14,'interpreter','latex')
if save_plots
    saving_name = replace(figure_title,' ','_') + ".jpeg";
    saveas(generalfig,saving_name)
end

```

#### MATLAB CODE: GRAPH FOR ILLUSTRATION IN CHAPTER 4

In chapter 4, the data for the experiment on stainless steel is shown in the time dimension. A dedicated code had to be written for this purpose. The function is simple, taking in data as a .csv file and having the information about the start and stop times of the individual tests given as a matrix.

```

%%%%%% SETTINGS %%%%%

% Sizing figure
generalfig_size = [800,400];
% Marker size
marker_size = 10;
% Title
title_txt = 'Time domain for experiment on 2503ST1';
% Saving plots?
save_plots = true;

% Key times for test. Row by row: Start time first test; end time first
% test; start time second test ...
key_times = [12 32 38; 12 37 31; 12 40 00; 12 41 40; 12 43 07; ...
            12 47 43; 12 48 55; 12 50 35; 12 52 57; 12 57 37; 13 00 14; ...
            13 01 54; 13 03 51; 13 08 29; 13 09 55; 13 11 55; 13 15 48; ...
            13 20 31; 13 22 09; 13 23 49];

```

```
%%%%%%%%%  COMMANDS  %%%%%%%%%%

% Graphing data
data = readtable('FKP_log_ST1_tension.csv');
generalfig = figure('Name', title_txt, 'NumberTitle', 'off', ...
    'Color', 'white');
generalfig.Position(3:4) = generalfig_size;
scatter_1 = scatter(data.(2), data.(4));
hold on
grid on
scatter_1.SizeData = marker_size;
title(append(title_txt,newline), 'fontsize',16, 'FontWeight', 'Bold', ...
    'interpreter', 'latex')
xlabel('Time [hh:mm:ss]', 'fontsize',14, 'interpreter', 'latex')
ylabel('Measured EWF [eV]', 'fontsize',14, 'interpreter', 'latex')

% Graphing out times of tests
number_tests = height(key_times) * 0.5;
key_times_dur = duration(key_times);
for i=1:number_tests
    num_begin = key_times_dur(2*i-1,1) / duration([24 00 00]);
    num_end = key_times_dur(2*i,1) / duration([24 00 00]);
    test = polyshape([num_begin, num_begin, num_end, num_end], ...
        [-0.11, -0.19, -0.19, -0.11]);
    if rem(i,2)
        colour = 'red';
    else
        colour = 'green';
    end
    test_plot = plot(test, 'FaceColor', colour, 'FaceAlpha', 0.2);
    test_plot.LineStyle = 'none';
end

% Save plot
if save_plots
    saving_name = replace(title_txt, ' ', '_') + ".jpeg";
    saveas(generalfig, saving_name)
end
```

## MATLAB CODE: DATA ANALYSIS

This was the most extensive MatLab code written for this project. It completed all the data analysis and created the figures featured in the report. In the first section of the code, settings are made. The most important inputs are the *true* and *false* value on the variables under “output: types”. After the settings section, there is a short commands section calling functions. These functions are, in line with the way MatLab scrips are formatted by default, at the end of the code. All the work is essentially done in the functions. Particularly the graphing function is extensive. Many commands are set into if clauses, since the code was meant to be very flexible, only running certain section when required.

---

```

%%%%%%%%%% SETTINGS AREA %%%%%%%%%%%

%%% INPUT: EXTERNAL FILES %%%

%test_data:
%Force is first column and given in kN. Sample EWF values are second
%column. The third column are the markers. Any entry there will be
%recognized as a marker and displayed for control.
file_test_data='test_25_03_SST_16_02_average_referenced';
%collection sample data:
file_sample_data='general_sample_data_01';

%%% INPUT: NAMES %%%

%sample number in sample data file. Used to locate sample data
sample_number = 1;
%name that is to show on the figure for this sample:
figure_title = 'stainless steel';

%%% OUTPUT: TYPES %%%

%csv output of Stress vs EWF wanted?
sigWF_output = false;
%simple linear regression wanted?
regression_analysis = true;
%should MatLAB make plots?
make_plots = true;
%should it only plot the data points by test and no general scatter and
%regression?
only_scatter_by_test = false;
%If it should make them, should it save them too?
save_plots = false;

%%% OUTPUT: PLOT OPTIONS %%%

%On diagram one:
circle_size=20;
%On diagram two:
point_size=50;
%Size factors first figure
generalfig_size=[1000,450];
%Let the first ... tests show in a different colour in diagram 2, figure 1
numseper=0; %to show all as separate: assign 0. To show no separate ones,
            %assign a negative number. A negative 'numseper' and a true
            %'only_scatter_by_test' are contradictory and and empty
            %figure will be produced
%In case data from the frist tests recive a different colour, they can also
%receive a different size
xtra_sizing_for_sepser=30;

```

---

```
%%%%%%%%%% COMMAND AREA %%%%%%%%%%%

%Read in external files
test_data = readtable(file_test_data);
sample_data = readtable(file_sample_data);

%Call function to make stress-EWF table
sigWF = make_sigWF_table(test_data, sample_data, sample_number);

%Call function to extract marker positions from tables of external files
marks = get_marker_positions(test_data);

%If desired, write output files:
if sigWF_output
    sigWFwrite = "stress_vs_EWF_"+replace(figure_title, ' ', '_')+".xlsx";
    writetable(sigWF, sigWFwrite)
end

%If desired, compute regression model:
if regression_analysis
    [reg_info, reg] = regression_model(sigWF);
else
    reg = 0;
    reg_info = 0;
end

%If desired, call plotting function
if make_plots
    %call plotting function
    create_plots(sigWF, marks, circle_size, point_size, generalfig_size, ..
        numseper, xtra_sizing_for_seper, figure_title, save_plots, reg, ...
        reg_info, only_scatter_by_test);
end
```

```

%%%%%%%%%%%%%% FUNCTION AREA %%%%%%%%%%%%%%%

function [Test_bounds] = get_marker_positions(test_data)
Empty=ismissing(test_data);
rows_with_marker=find(Empty(:,3)==0);

% Check if these markers are right:
fprintf('\n Found these markers:\n\n')
disp(test_data(~Empty(:,3),3))

% This creates a matrix to locate all the data, given the markers in the
% csv file
Test_bounds=[];
number_of_tests=length(rows_with_marker)+1;
for i = 1:number_of_tests
    if i==1
        first_element=1;
    else
        first_element=rows_with_marker(i-1);
    end
    if i==length(rows_with_marker)+1
        last_element=length(Empty(:,3));
    else
        last_element=rows_with_marker(i)-1;
    end
    current_test=[i, first_element, last_element];
    Test_bounds=[Test_bounds;current_test];
end
end

function [output_table] = make_sigWF_table(test_data,sample_data,sample_number)
% takes in sample information and the Force EWF table "test data" to pass

% Find cross-sectional area
where = sample_data.(1) == sample_number;
relevant_table = sample_data(where,:);
Area = relevant_table.width * relevant_table.thickness;
Recip_area = 1/Area;
% calculate stress
elements = height(test_data);
Stress = zeros(elements,1);
for i = 1:elements
    Stress(i) = test_data{i,1} * Recip_area * 1000;
end
%create new table
output_table = table(Stress);
output_table.Sample = test_data.Sample;
output_table.(3) = test_data.(3);
end

```

```

function [] = create_plots(sigWF, marks, circle_size, point_size, generalfig_size, ...
    numsepsr, xtra_sizing_for_sepsr, figure_title, save_plots, reg, reg_info, ...
    only_scatter_by_test)
% creates plots with parameters defined in the settings area.

% interpret function input
number_of_tests = height(marks);
no_second_plot = false;
if numsepsr == 0
    numsepsr = number_of_tests;
elseif numsepsr < 0
    no_second_plot = true;
    generalfig_size(1,1)=generalfig_size(1,1)*0.5;
end
if only_scatter_by_test
    generalfig_size(1,1)=generalfig_size(1,1)*0.5;
end

% create figure
generalfig=figure('Name', figure_title,'NumberTitle', 'off',...
    'Color', 'white');
if or(no_second_plot, only_scatter_by_test)
    tiledlayout(1,1)
else
    tiledlayout(1,2);
end
generalfig.Position(3:4)=generalfig_size;

% TILE 1 (plot 1):
% first check if the tile one should be filled with the general scatter
% plot or regression, or, if it should be showing the scatter by test.
% If it is the general plot and regression, the following segment
% should execute as tile 1
if ~only_scatter_by_test
    nexttile
    scatter_1 = scatter(sigWF.(1), sigWF.(2));
    scatter_1.SizeData = circle_size;
    grid on
    % depending on whether a second plot is needed, there needs to be
    % alphabetical labelling of plots
    if no_second_plot
        title_txt_1 = 'Scatter graph for ' + string(figure_title);
    else
        title_txt_1 = 'A: Scatter graph for ' + string(figure_title);
    end
    end
    title(append(title_txt_1,newline),'fontsize',16,'FontWeight','Bold',...
        'interpreter','latex')
    xlabel('Nominal tensile stress [MPa]','fontsize',14,'interpreter','latex')
    ylabel('Measured change in EWF [eV]','fontsize',14,'interpreter','latex')
    % For axes:
    x_upper = max(sigWF.(1));
    y_upper = max(sigWF.(2));
    y_lower = min(sigWF.(2));
    axis([0-0.2*x_upper, 1.2*x_upper, y_lower-0.1*(y_upper - y_lower), ...
        y_upper+0.1*(y_upper - y_lower)])

```

```

% If a regression line has been computed, all relevant information
% should be displayed here
if ~isa(reg, 'double')
    hold on
    regline = plot(reg_info(:,1),reg_info(:,4),'k');
    conf1 = plot(reg_info(:,1),reg_info(:,2),'k');
    conf2= plot(reg_info(:,1),reg_info(:,3),'k');
    conf1.LineStyle='-.';
    conf1.LineWidth=1;
    conf2.LineStyle='-.';
    conf2.LineWidth=1;
    regline.LineStyle='-.';
    regline.LineWidth=1;
    reg_legend_txt = cell(3,1);
    reg_legend_txt{1} = 'Data point';
    txt_2 = append('Linear regression: ', '$R^{2}$ = ', ...
        string(round(reg.Rsquared.Ordinary,4,'significant')), ...
        ', ', newline, 'p value of $\hat{\beta}$: ', ...
        string(round(reg.Coefficients.pValue(2),4,'significant')));
    reg_legend_txt{2} = txt_2;
    reg_legend_txt{3} = '95\% Confidence interval for mean';
    legend(reg_legend_txt,...
        'fontsize',10,'interpreter', 'latex', 'Location', 'best');
    hold off
end
end

```

```

%TILE 2 (plot 2):
%Check if this next tile (may also serve as tile one in case
%only_scatter_by_test is true), should be formed. (If the numsepser is
%negative, and hence no_second_plot true, it is not needed)
if ~no_second_plot
    nexttile
    legend_txts=cell(numsepser,1);
    for i = 1:numsepser
        scatter_2=scatter(sigWF{marks(i,2):marks(i,3),1},...
            sigWF{marks(i,2):marks(i,3),2},'.');
        scatter_2.SizeData = point_size + extra_sizing_for_sepser;
        legend_txts{i,1} = 'Test '+string(i);
        hold on
    end
    if numsepser ~= number_of_tests
        scatter_2 = scatter(sigWF{marks(numsepser+1,2):marks(number_of_tests,3),1},.
            sigWF{marks(numsepser+1,2):marks(number_of_tests,3),2},'.');
        scatter_2.SizeData = point_size;
        legend_txts{numsepser+1} = 'Consecutive tests';
    end
    legend(legend_txts,'fontsize',10,'interpreter','latex','Location','best');
%Axes
x_upper = max(sigWF.(1));
y_upper = max(sigWF.(2));
y_lower = min(sigWF.(2));
axis([0-0.2*x_upper, 1.2*x_upper, y_lower-0.1*(y_upper - y_lower), ...
    y_upper+0.1*(y_upper - y_lower)])
    hold off
    grid on
    figure_title_capit = append(upper(figure_title(1)),...
        figure_title(2:length(figure_title)));
    %If this is the second plot, 'B' needs to be in the title.
    %Otherwise it does not. This is the first plot if
    %only_scatter_by_test is true

    if only_scatter_by_test
        title_txt_2 = append(figure_title_capit, ', data points by test');
    else
        title_txt_2 = append('B: ', figure_title_capit, ', data points by test');
    end
    title(append(title_txt_2,newline),'fontsize',16,'FontWeight','Bold',...
        'interpreter','latex')
    xlabel('Nominal tensile stress [MPa]','fontsize',14,'interpreter','latex')
    ylabel('Measured change in EWF [eV]','fontsize',14,'interpreter','latex')
end

%Save if desired:
if save_plots
    saving_name = replace(figure_title,' ','_') + ".jpeg";
    saveas(generalfig,saving_name)
end
end

```



```
function [reg_info, reg] = regression_model(sigWF)
% Creates regression model and makes vector to plot as confidence interval
reg = fitlm(sigWF(:,1:2));

% Construct confidence interval for E(Y|X=x)
Sxx = var(sigWF(:,1)) * (reg.NumObservations - 1);
x_upper = max(sigWF(:,1));
x = 0-0.1*x_upper:(1.2*x_upper/100):1.1*x_upper;
% Formula from statistics book (Kristensen & Wikan), page 325.
base = reg.Coefficients.Estimate(1) + reg.Coefficients.Estimate(2) * x;
t = tinv(0.975, reg.DFE);
s = sqrt(reg.SSE/reg.DFE);
n = reg.NumObservations;
x_bar = mean(sigWF(:,1));
margin = t * s * sqrt(1/n + (x - x_bar).^2 ./ Sxx);
margin_upper = base + margin;
margin_lower = base - margin;

% Evaluate regression line at a number of values. More convenient when
% plotting. The output matrix reg_info has four columns with different
% information, as shown below
y_hat = reg.Coefficients.Estimate(2) .* x + reg.Coefficients.Estimate(1);
reg_info = [x.', margin_lower.', margin_upper.', y_hat.'];
end
```

## Appendix A2: Statistical calculation – number of necessary measurements

It is assumed that the FKP makes its EWF measurements with a certain standard deviation,  $\sigma$ , which does not change with stress and can be taken to be equal to the root mean squared error of the regression model.

The average of the EWF measurements in state one,  $\bar{E}_1$ , is normally distributed around the population mean  $\mu_1$  and has the standard deviation  $\frac{\sigma}{\sqrt{n}}$ , where  $n$  is the number of measurements. This is a consequence of the central limit theorem. Corresponding statements can be made about the average of the EWF measurements in state two,  $\bar{E}_2$ .

Consider now the difference between the two averages:

$$\Delta\bar{E} = \bar{E}_1 - \bar{E}_2 \quad (\text{A2.1})$$

The variance can be found.  $\bar{E}_1$  and  $\bar{E}_2$  are independent and  $\text{Var}(\bar{E}_1) = \text{Var}(\bar{E}_2) = \frac{\sigma^2}{n}$

$$\text{Var}(\Delta\bar{E}) = \text{Var}(\bar{E}_1 - \bar{E}_2) = \text{Var}(\bar{E}_1) + \text{Var}(\bar{E}_2) = \frac{2\sigma^2}{n} \quad (\text{A2.2})$$

In the end, a range of stress values should be specified, e.g.  $\pm 25$  MPa, corresponding to a certain range of EWF values through the factor  $\beta$ , within which some percentage of the distribution of  $\Delta\bar{E}$ , e.g. 90%, should lie. That means that  $n$  simply needs to be adapted so that the quantiles of the normal distribution align with the outer edges of the interval that was indicated. If the range of stress is  $\pm a$  and  $z$  is the quantile of the normal distribution that is one minus the given confidence all over two. If 90% of the distribution of  $\Delta\bar{E}$  should lie within the range of  $\pm a$ , then the quantile for 5% would be needed.

$$a\beta = z \sigma \sqrt{\frac{2}{n}} \quad (\text{A2.3})$$

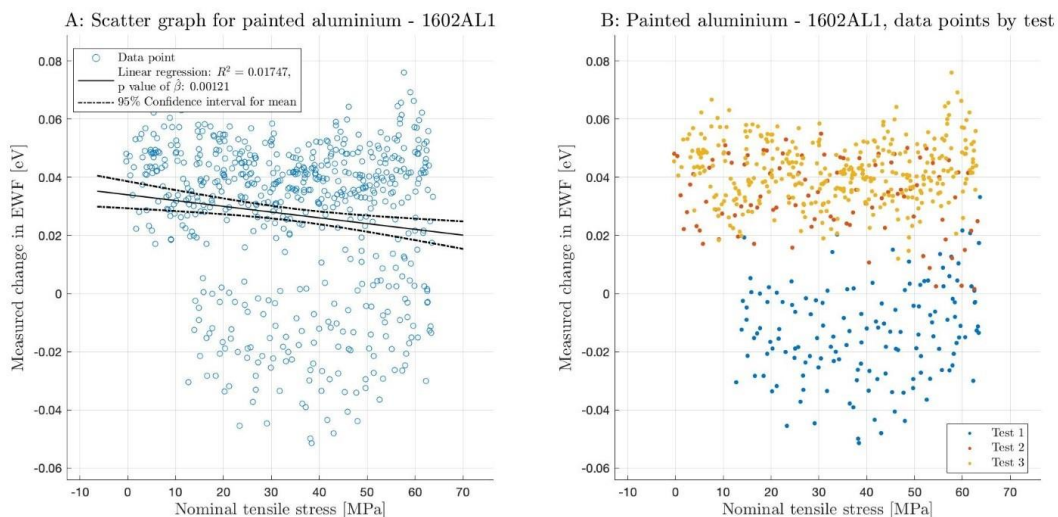
$$n = \frac{2 z^2 \sigma^2}{a^2 \beta^2} \quad (\text{A2.4})$$

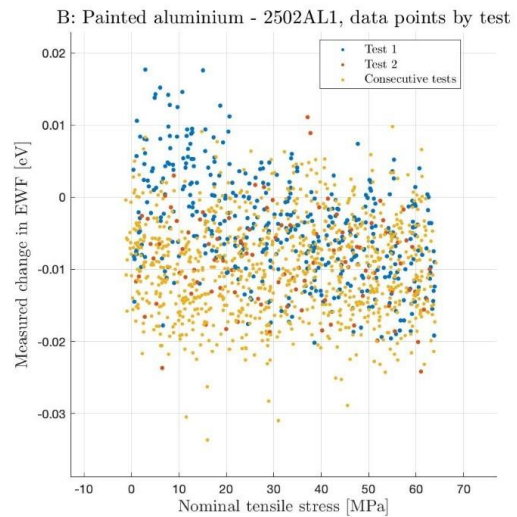
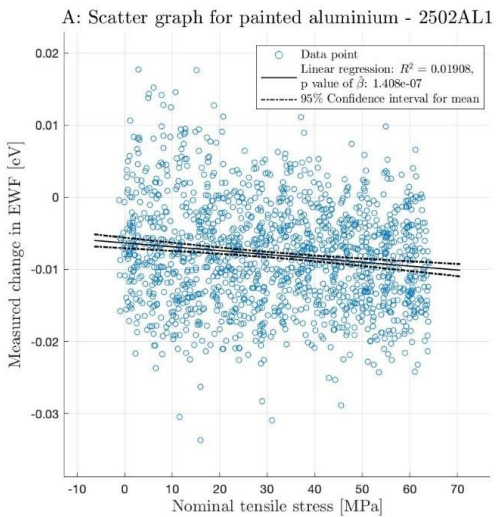
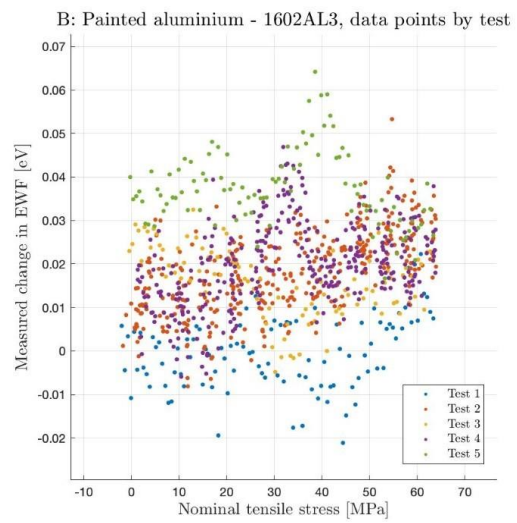
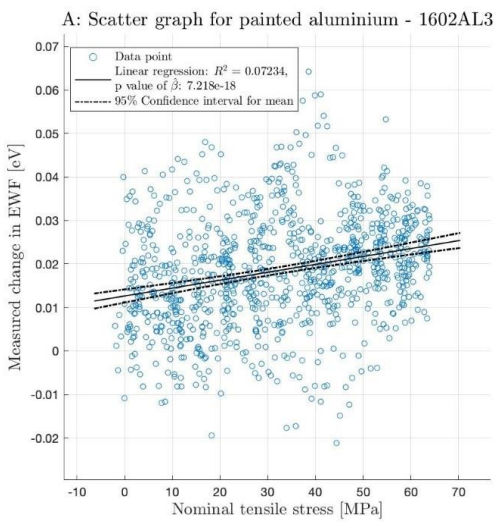
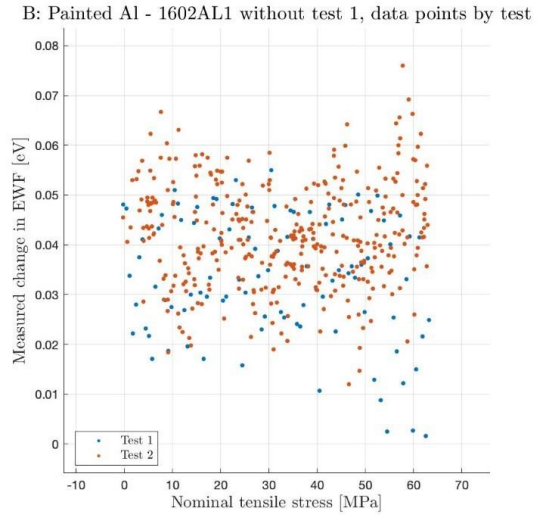
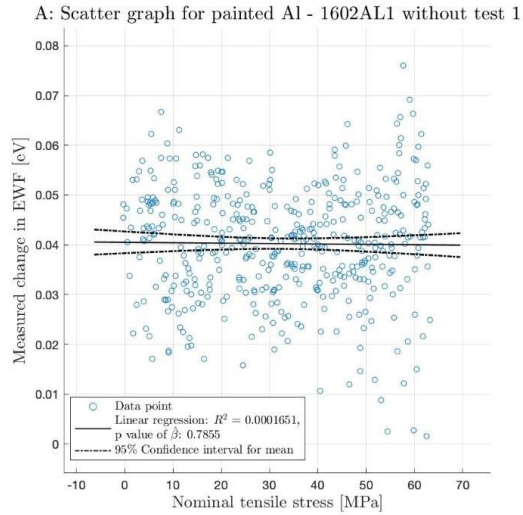
## Appendix A3: Experimental results

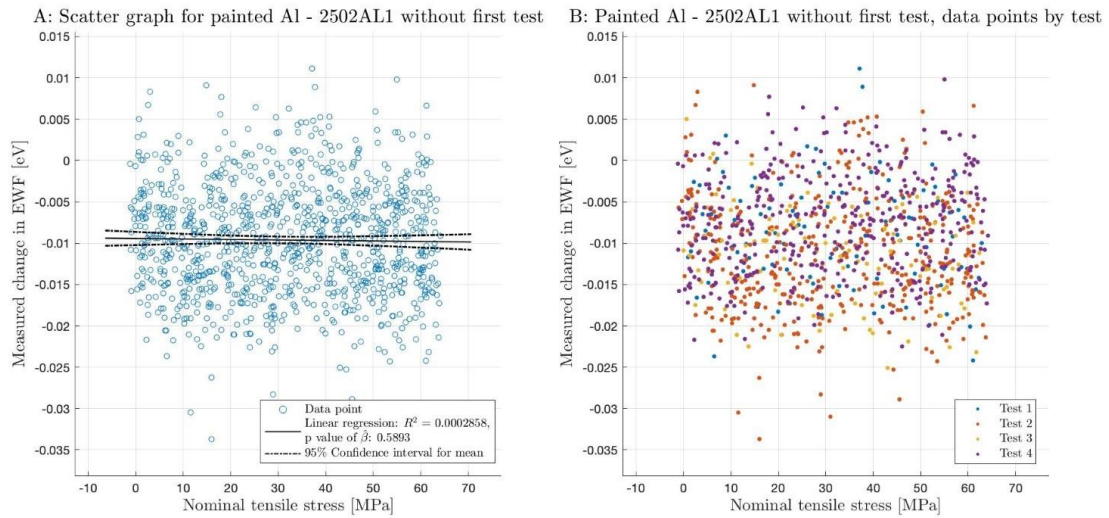
Here, all results from the experiments on the servo-hydraulic testing machine referred to in section four will be presented. First is a table showing the estimated values for BEATA and the mean squared error for the regression models. This will be displayed for the experiments that do not show “deviant first tests” or extreme amounts of drift. With this data, calculations of the kind shown in 4.1.4 can be performed for any experiment. Subsequently, the graphs for all experiments will follow.

NAME OF EXPERIMENT	$\hat{\beta}$	MSE
1602AL3 painted Al	0.00018172	1.4643e-04
1602AL2 unpainted Al	0.00023145	2.2429e-06
2502AL2 unpainted Al at 1 mm	-6.2056e-05	1.1006e-04
2502AL2 unpainted Al at 250 $\mu\text{m}$	-4.8519e-05	5.3990e-05
2502AL2 unpainted Al at 100 $\mu\text{m}$	-0.001047	6.2724e-04
2502AL2 unpainted Al at 50 $\mu\text{m}$	-0.0017404	2.5010e-05
1602BR1 brass experiment 2	-0.00010364	3.7347e-05
1602BR1 brass experiment 3	0.0002041	1.1892e-05
1602BR1 brass experiment 4	-7.8028e-06	1.1604e-06
0604BR1 brass	-1.3472e-05	1.1905e-06
1602SST stainless steel	-2.4106e-05	0.0045
0604pST1 polished steel longitudinal 200 $\mu\text{m}$	-9.0471e-06	1.0331e-06
0604pST1 polished steel transverse 300 $\mu\text{m}$	-0.00015818	3.7874e-06
2503ST1 painted steel	-8.0496e-05	1.1843e-04

### GRAPHS FOR PAINTED ALUMINIUM

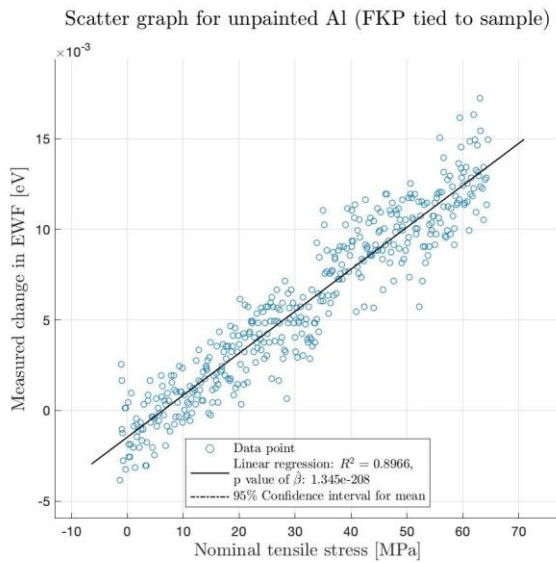






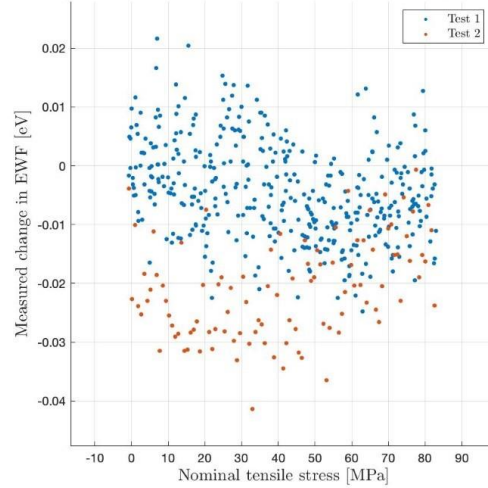
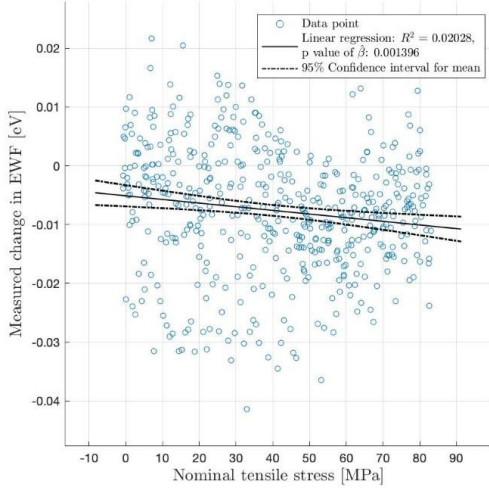
### GRAPHS FOR UNPAINTED ALUMINIUM

This first graph is from a very brief test done on the last day of experiments. It consists of just a single test. The sample is 1602AL2

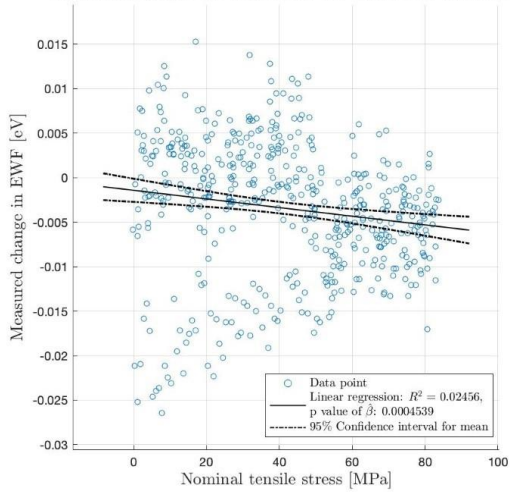


What follows are the graphs for the unpainted aluminium sample that was tested at different initial distances between probe and sample and strong distance effects where present.

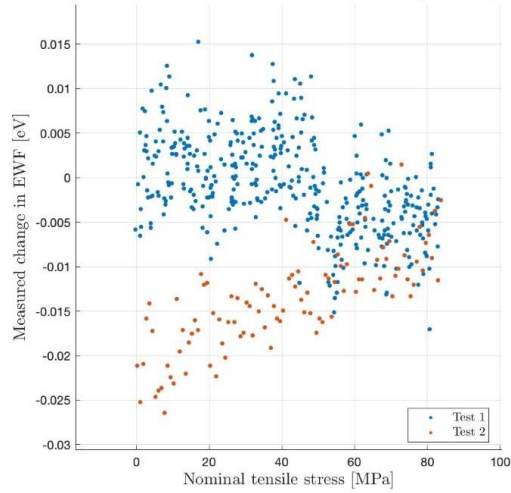
A: Scatter graph for unpainted aluminium - 2502AL2 at 1mm B: Unpainted aluminium - 2502AL2 at 1mm, data points by test



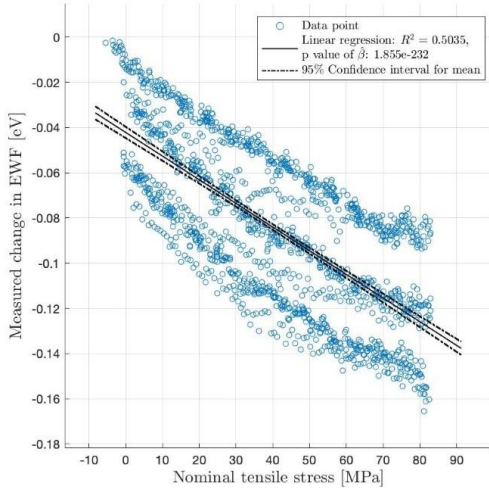
A: Scatter graph for unpainted Al - 2502AL2 at 250um



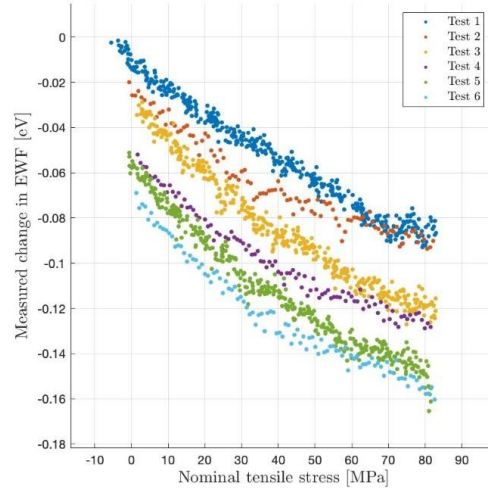
B: Unpainted Al - 2502AL2 at 250um, data points by test



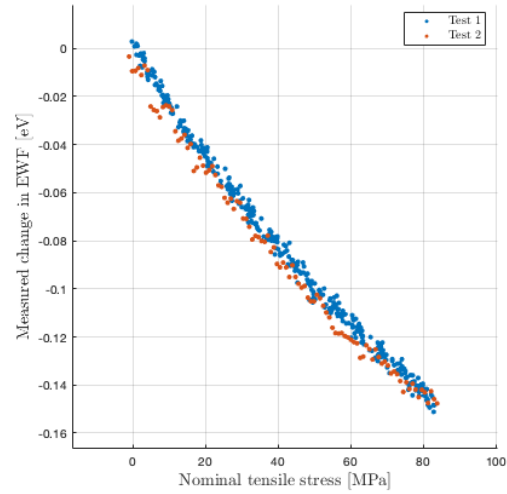
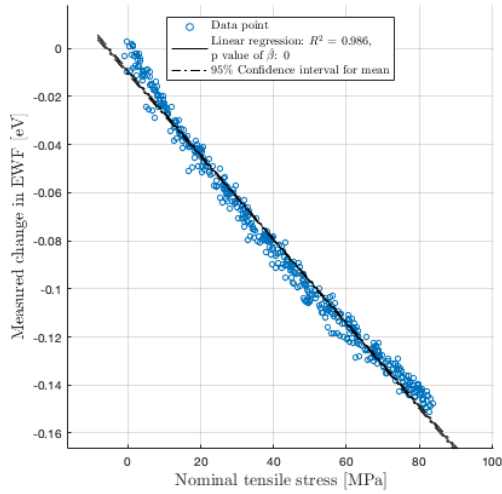
A: Scatter graph for unpainted Al - 2502AL2 at 100um



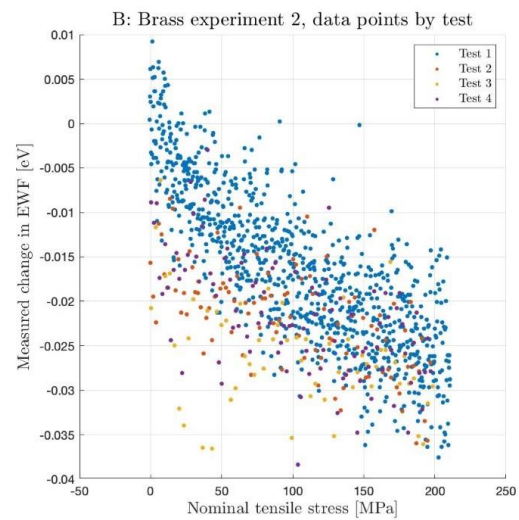
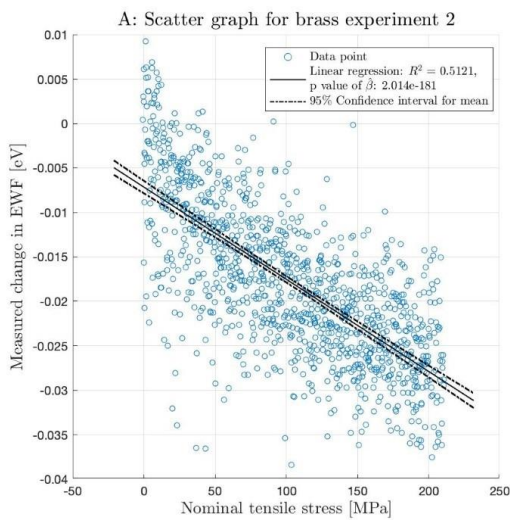
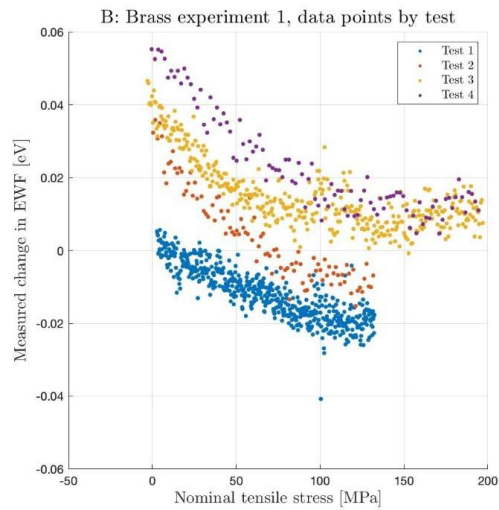
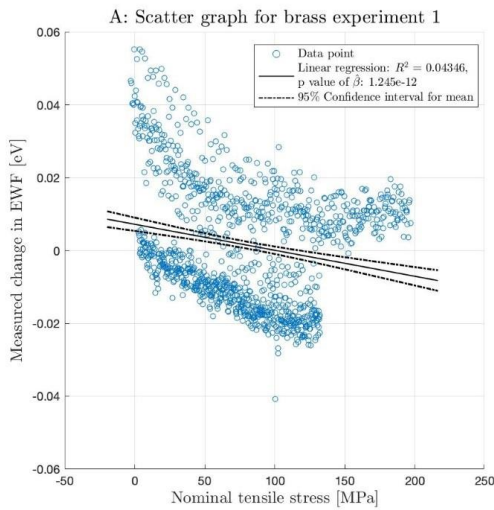
B: Unpainted Al - 2502AL2 at 100um, data points by test

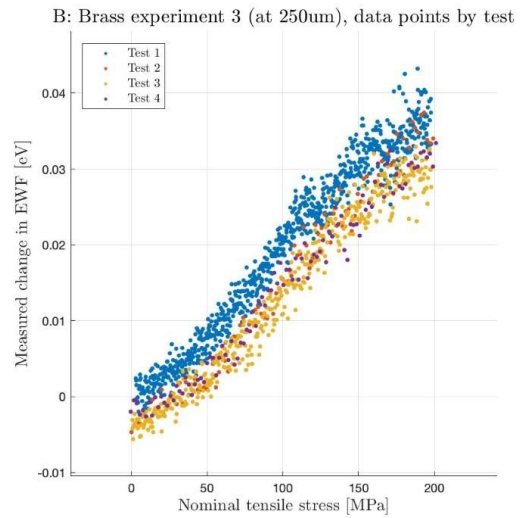
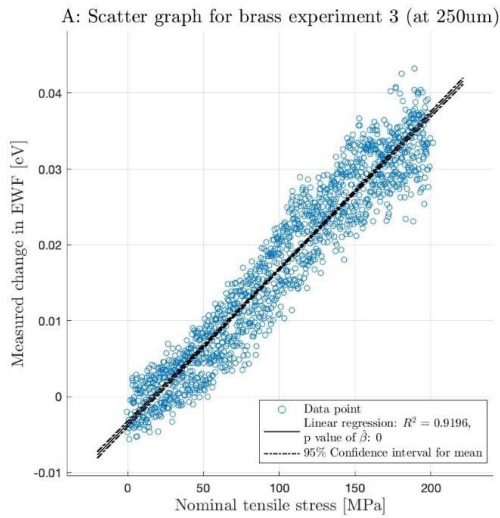


A: Scatter graph for unpainted aluminium - 2502AL2 at 50µm B: Unpainted aluminium - 2502AL2 at 50µm, data points by test

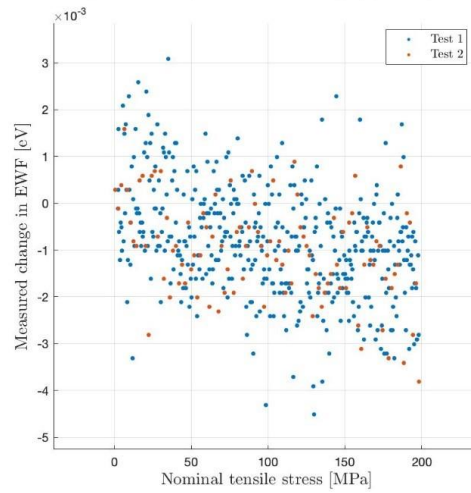
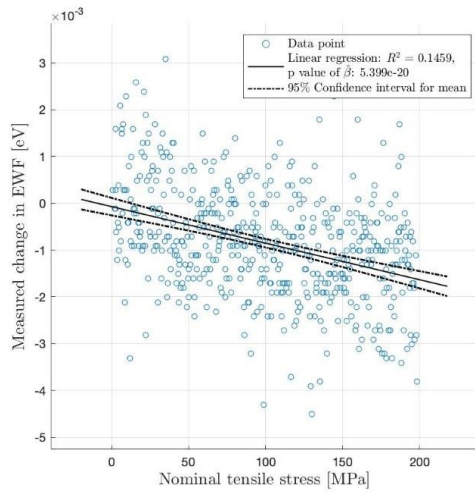


GRAPHS FOR BRASS



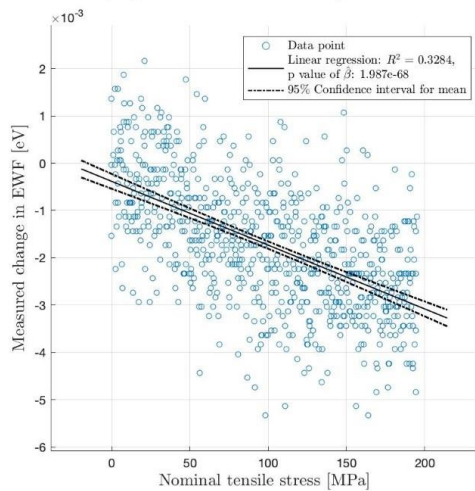


A: Scatter graph for brass experiment 4 (FKP tied to sample) B: Brass experiment 4 (FKP tied to sample), data points by test

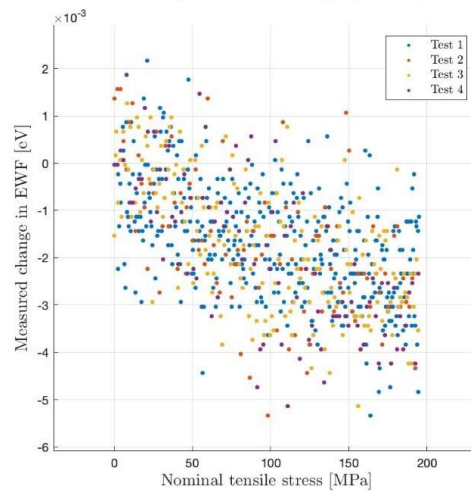


Now follows another brass sample from a different brass alloy.

A: Scatter graph for brass 06-04-BR1 (FKP tied to sample)

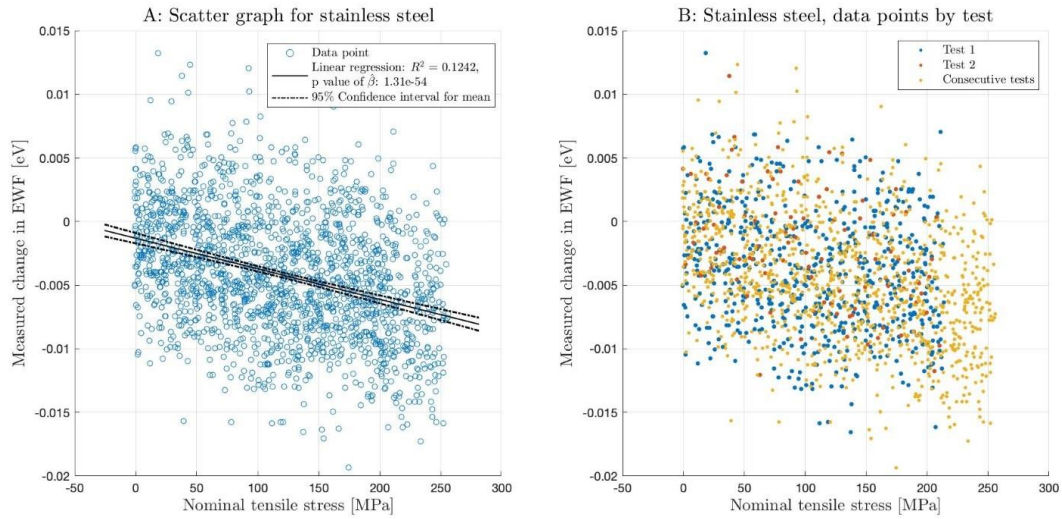


B: Brass 06-04-BR1 (FKP tied to sample), data points by test



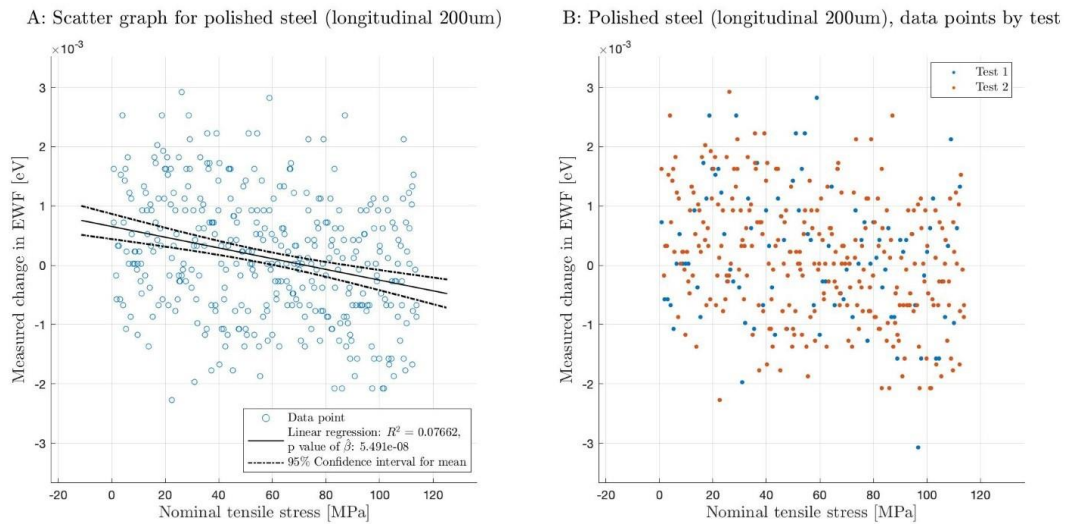


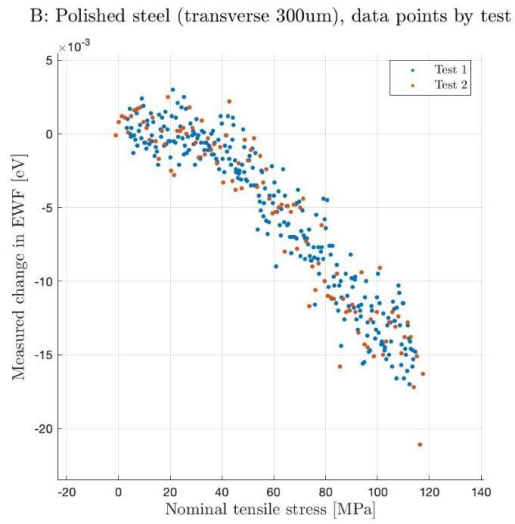
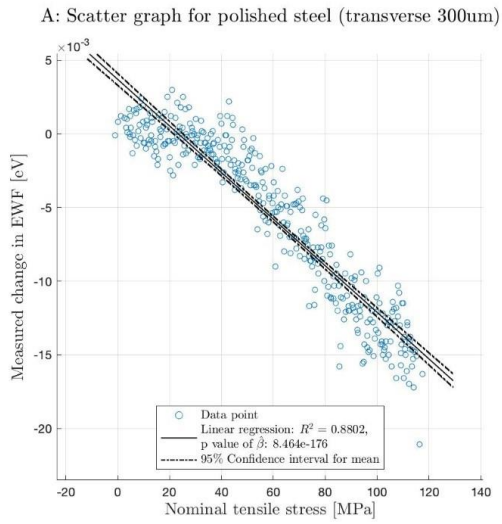
GRAPH FOR STAINLESS STEEL



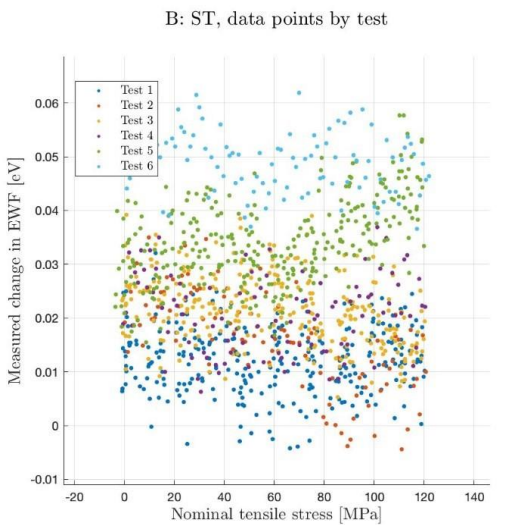
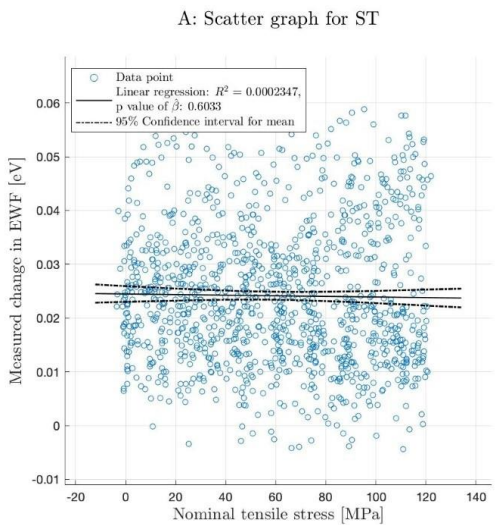
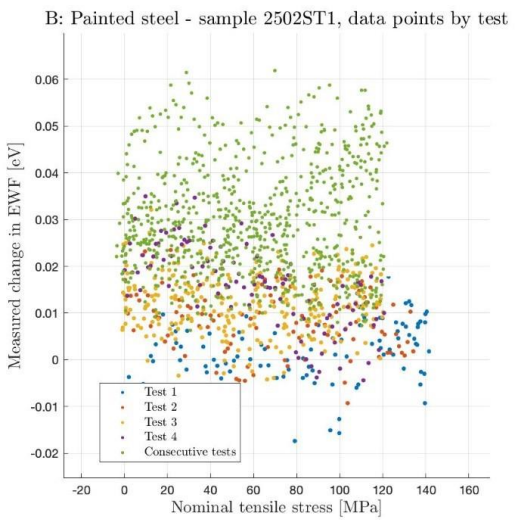
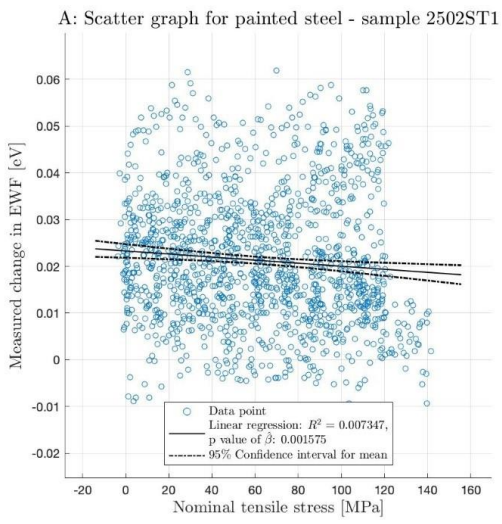
POLISHED STEEL

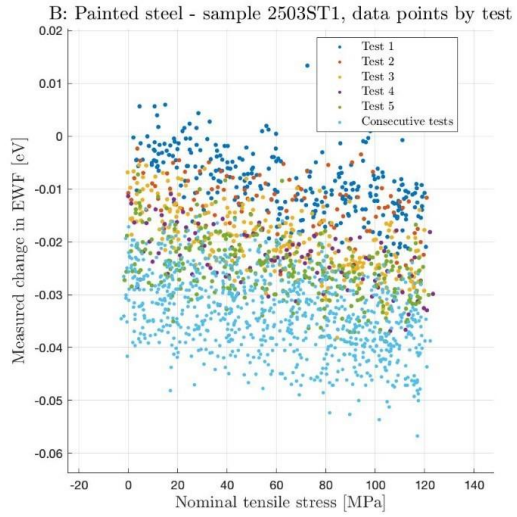
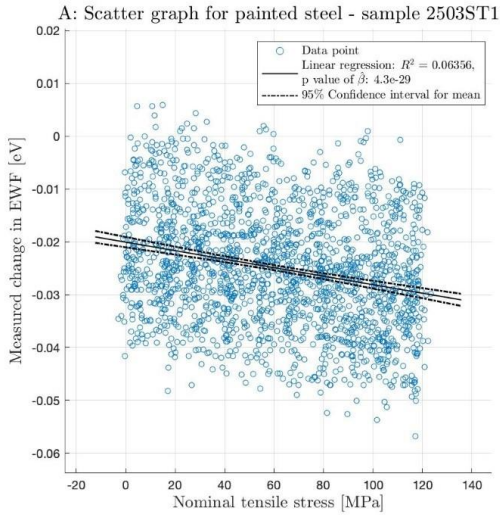
For the polished steel, little change of the distance could be measured during the tests for the longitudinal measurement, but distance changes had a big influence on the transversal measurement, corrupting the data.



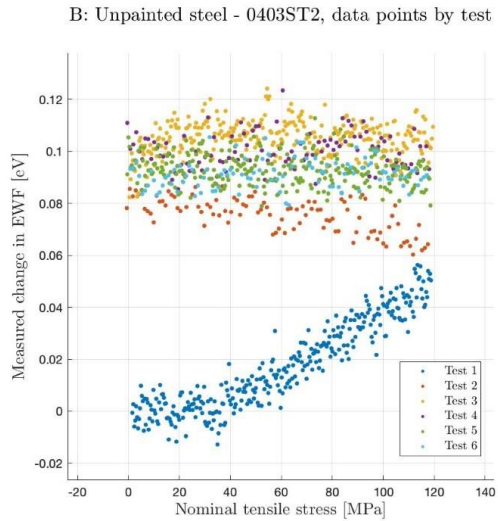
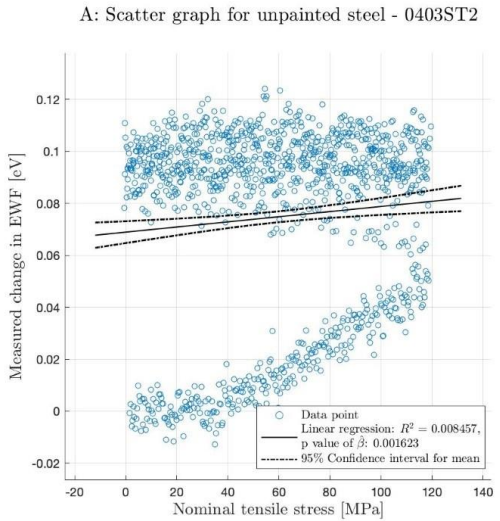


PAINTED STEEL

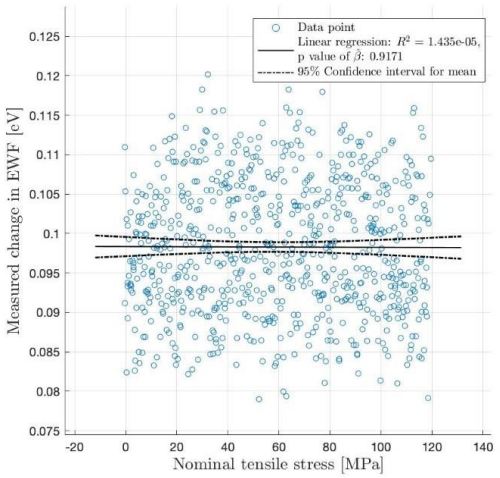




UNPAINTED STEEL



A: Scatter graph for unpainted steel - 0403ST2 no test 1-2



B: Unpainted steel - 0403ST2 no test 1-2, data points by test

